ABSTRACT

Title of dissertation: RADIO RESOURCE MANAGEMENT
IN HETEROGENEOUS CELLULAR NETWORKS

Doohyun Sung, Doctor of Philosophy, 2014

Dissertation directed by: Professor John S. Baras
Department of Electrical and Computer Engineering

Heterogeneous cellular networks (HetNets) have been considered as one of enabling technologies not only to increase the cell coverage and capacity, but to improve the user experience. In this dissertation, we address two research challenges in HetNets: one is the cross-tier interference problem where cell range expansion (CRE) is applied for user offloading in cell association so that pico mobile stations located in expanded range (ER-PMSs), which are connected to macrocells unless CRE is enabled, are severely interfered. The other is the load-aware cell association which tries to overcome the drawback of the received signal strength-based cell association including CRE, i.e., the degradation of network performance by user load imbalance.

In the first part, we present the frequency-domain transmit power reduction scheme for the cross-tier interference mitigation. Inspired by the fact that a macrocell accommodates more users than its underlaid picocells, we focus on minimizing the macrocell's performance degradation while improving the throughput of ER-PMSs by the transmit power reduction. Due to the discreteness of frequency re-

source block scheduling, we also propose a greedy-based heuristic algorithm to solve the binary integer programming problem.

In the following part, we present a different approach for the cross-tier interference mitigation, which is the time-domain transmit power nulling scheme utilizing the almost blank subframes (ABSs) in 3GPP standards. We turn our attention to a network-wide performance enhancement through configuring a certain number of ABSs while improving the performance of ER-PMSs as in the first part. A new scheduling policy for pico mobile stations is proposed and the optimal ER-PMS scheduling onto ABSs/non-ABSs is solved by decomposing the problem into multiple independent problems for pico base stations.

In the last part, we study the load-aware cell association problem. Due to the combinatorial nature of the cell association problem and the cross-tier interference between macrocells and picocells, we propose an online heuristic algorithm where the cell association and the number of ABSs for cross-tier interference mitigation are jointly optimized. Through approximation of the required condition for load balancing and ABS control from the network-wide utility point of view, the proposed online algorithm not only requires simple feedback messages, but also be applicable to any state of cell association/ABSs in HetNets.

RADIO RESOURCE MANAGEMENT IN HETEROGENEOUS CELLULAR NETWORKS

by

Doohyun Sung

Dissertation submitted to the Faculty of the Graduate School of the
University of Maryland, College Park in partial fulfillment
of the requirements for the degree of
Doctor of Philosophy
2014

Advisory Committee:
Professor John S. Baras, Chair/Advisor
Professor Richard J. La
Professor Michael C. Rotkowitz
Professor Ashok Agrawala
Professor Subramanian Raghavan

Dedication

To my parents, my wife Sunah, and our son Daniel

Acknowledgments

I would like to express my sincere gratitude and appreciation to my advisor Dr. John S. Baras for his guidance and encouragement during my graduate research. His ideas and suggestions made my work all the more stimulating. I would also like to thank Dr. Richard J. La, Dr. Michael C. Rotkowitz, Dr. Ashok Agrawala, and Dr. S. Raghavan for serving on my dissertation committee.

I am grateful to my colleagues in HyNet center and SEIL lab for making the lab a great place to work. Special thanks to Shalabh Jain, Tuan (Johnny) Ta, and Anup Menon for numerous discussions. Also, a special thank you to Ms. Kimberly Edwards for her great administrative support.

I owe my deepest thanks to my family who have always stood be me and guided me through my career, and have pulled me through against impossible odds at times.

This dissertation research is based upon work supported by the National Science Foundation (NSF) grants CNS1035655 and CNS1018346, by the AFOSR under MURI grant W911NF-08-1-0238, and by the National Institute of Standards and Technology (NIST) award 70NANB11H148.

Table of Contents

List of Tables

List of Figures

Chapter 1: Introduction

1.1 Heterogeneous Cellular Networks

As smartphones and tablet PCs are widely spread throughout the world, mobile data and video traffic demand has been increasing significantly. According to [1], there are several noticeable trends and forecasts as follows:

- Mobile network trends in 2013
  - Mobile video traffic exceeded 50% of the total mobile traffic in 2013.
  - Mobile network connection speeds more than doubled in 2013 (average downstream speed 1,387 Kbps) than that in 2012 (526 Kbps).
  - A fourth-generation (4G) connection generated 14.5 times more traffic on average than a non-4G connection, although 4G connections represent only 2.9% of mobile connections.
- Mobile network forecasts through 2018
  - Over $\frac{2}{3}$ of the mobile traffic will be video by 2018.
  - The average mobile connection speed will surpass 2 Mbps by 2016.

– The average smartphone will generate 2.7 GB of traffic per month by 2018.

– 4G traffic will be more than 50% of the total mobile traffic by 2018.

As observed from trends and forecasts above, 4G mobile communication systems[1] such as Mobile WiMAX or LTE have started playing an important role in delivering traffic generated from mobile devices. Recent mobile communication standards such as 3GPP LTE-A [2] or IEEE 802.16m [3] have proposed advanced physical layer (PHY) techniques such as carrier aggregation, coordinated MIMO transmission, etc. Adopting those link technologies to the existing cell sites can improve user data rates and system capacity. However, as we are facing situations where the mobile data traffic demand increases relentlessly and the radio link performance approaches theoretical limits [4], an evolved network topology plays an important role for 4G and beyond-4G mobile communication systems.

In traditional cellular networks, macro base stations (MBSs)[2] having similar transmit power levels, antenna patterns, and receiver noise floors are deployed in a well-planned manner so as to maximize the coverage and control the interference between MBSs. Therefore, it requires much more cost and effort to install more

[1]Strictly speaking, 4G communication systems, or IMT-Advanced systems according to ITU-R's definition, include Mobile WiMAX Release 2.0 (also known as IEEE 802.16m) and 3GPP LTE-Advanced. However, we here refer to Mobile WiMAX and LTE as 4G systems since the term *4G* has been widely used by carriers such as Verizon and AT&T.

[2]We will use *base stations* and *cells* interchangeably.

MBSs (MBS densification) in urban areas as the deployment process is complex and iterative. Moreover, it is more difficult to find an appropriate site for those MBSs especially in dense urban area [5, 6].

As a consequence, heterogeneous cellular networks have been emerged as an efficient way to improve spectral efficiency per unit area by utilizing a diverse set of low-powered BSs such as picos, , femtos, relays, and remote radio heads (RRHs). This network structure consists of high-powered (5 W $\sim$ 40 W) macrocells that are regularly deployed in a planned manner and overlaid small cells of those low-powered BSs with transmit power (100 mW $\sim$ 2 W) that are deployed in a relatively unplanned manner. The example of heterogeneous cellular network deployment is illustrated in Figure 1.1.

Those low-powered BSs have unique features. Pico BSs typically cover a small area such as outdoor cafes and indoor offices or shopping malls. They are deployed

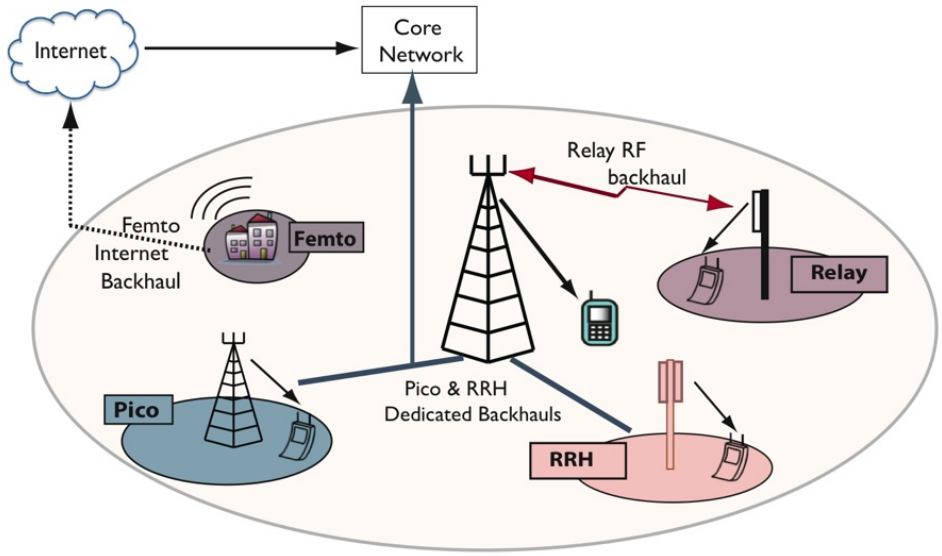

Figure 1.1: Heterogeneous cellular network deployment

(source by `http://www.profheath.org/wp-content/uploads/2011/02/cellularSystems_hetnet-1024x576.jpg`)

by operators and are connected to the operators' core network directly so that interactive signaling exchange with macro BSs are possible for coordination. Femto BSs are deployed in a home or small business. They are connected to the core network via public ISPs such as DSL or cable network. Due to its limited connectivity to the core network, interactive signaling between macro- and femto BSs is harder than that between macro- and pico BSs. In addition, femto BSs control their public users' access by managing a user group. When the access is only allowed to legitimate users, it is called a femtocell is in a closed subscriber group (CSG) mode. An open subscriber group (OSG) mode is the opposite policy in which every user is accessible to a femtocell. Relay BSs, unlike picos and femtos, are connected to super-ordinating macro BSs via wireless backhaul. The installation is rather easier due to its wireless connectivity, however dedicated time- and/or frequency domain resource is necessary for wireless backhaul which could require possible frame structure changes. Remote radio heads (RRHs)[3] are not regular BSs mentioned above, but remote RF circuitry plus analog-to-digital/digital-to-analog converters and up/down converters which are connected to the central BS via optical fibers. They are known to enable distributed antenna systems [7]. Among these low-powered BSs, we are focusing on a heterogeneous network deployment with macro- and pico BSs as pico BSs have no restrictions on interactive signaling with macro BSs and their operation can be totally transparent to macro BSs as well.

[3]There are high-powered RRHs of which transmit power is as strong as that of MBSs.

By deploying low-powered small cells, we can eliminate the coverage holes and further improve the network capacity by spatial cell-splitting within the existing macrocell sites. Since those small cells have physically small sizes and require much less cost than macrocells do, it provides more flexible site acquisition in a much more cost-effective manner.

1.1.1 3GPP Rel-10 LTE-Advanced Systems

In 3GPP LTE-A (Long Term Evolution - Advanced) systems, a method called *cell range expansion* (CRE) has been proposed to further enhance the cell-splitting effect by deploying small cells. Under the CRE-based cell association policy, the associating BS b^* is determined as follows:

$$b^* = \arg\max_{b \in \mathcal{B}} \ (Q_b + \Delta_b), \tag{1.1}$$

where $\mathcal{B}$ is the set of all BSs in the network, Q_b is the received signal strength of the pilot signal from BS b (Reference Signal Received Power (RSRP) in 3GPP standards), and Δ_b is a bias offset. Both Q_b and Δ_b are in a dB-scale. If BS b belongs to overlaid small cells, Δ_b has a positive value (> 0), otherwise Δ_b becomes zero for macrocells. By applying the CRE bias offset, more MSs can be associated with small cells, which results in an improved cell-splitting effect. In Figure 1.2, two cell association cases are illustrated where the cell association is done by the received signal strength and the received signal strength plus the CRE bias offset, respectively.

In addition, a time-domain method for cross-tier interference mitigation from

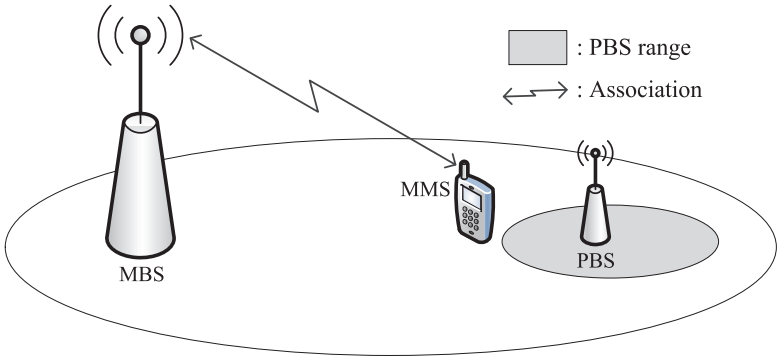

(a) No CRE case

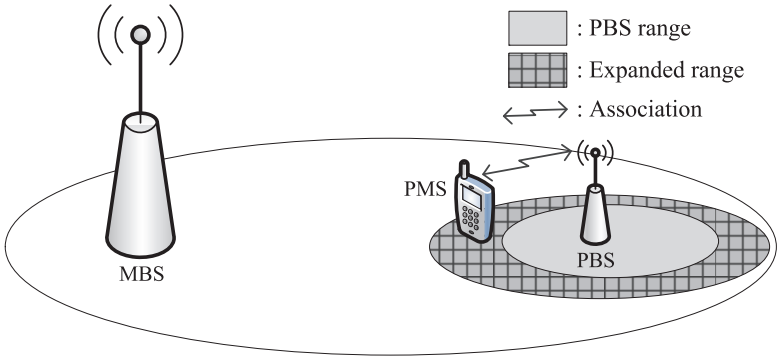

(b) CRE case

Figure 1.2: Cell association w/ and w/o CRE

macrocells to small cells has been proposed, which is called almost blank subframe (ABS). The use of ABSs is also referred to as *enhanced intercell interference coordination* (eICIC). During a certain period of time, or configured ABSs, macrocells don't transmit any control or data signals except for essential signals for system maintenance or backward compatibility such as broadcast system information, synchronization signals, common reference signals, or paging signals. By *nulling (or muting) the transmit power by macrocells*, the cross-tier interference toward small cells can be effectively coordinated. In Figure 1.3, the usage of almost blank sub-

frames is illustrated.

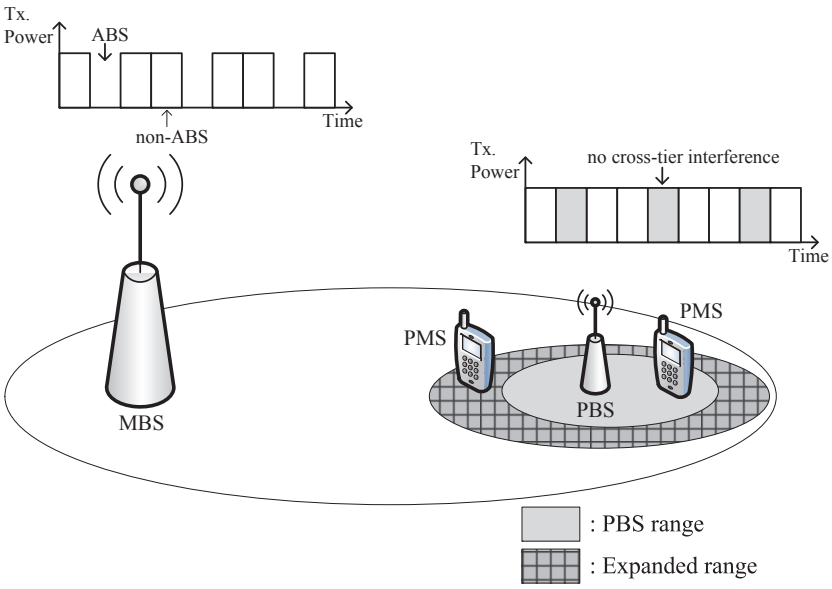

Figure 1.3: ABS configuration

1.2 Problem Statement

In this dissertation, we tackle two research problems in heterogeneous cellular networks, which are the cross-tier interference mitigation and the load-aware cell association.

1.2.1 Downlink Cross-tier Interference Mitigation

Due to the applied CRE bias offset, MSs located in the expanded range are associated with picocells even if they observe the stronger received signal from a macrocell than from associated picocells. Although this CRE operation helps MSs to be offloaded toward picocells from the network point of view, it leads those

pico MSs in the expanded range to suffering a strong cross-tier interference from macrocells because they have originally observed a stronger received signal and the stronger signal has become an interfering signal for them. In Figure 1.4, the cross-tier interference toward a pico MS in the expanded range is illustrated.

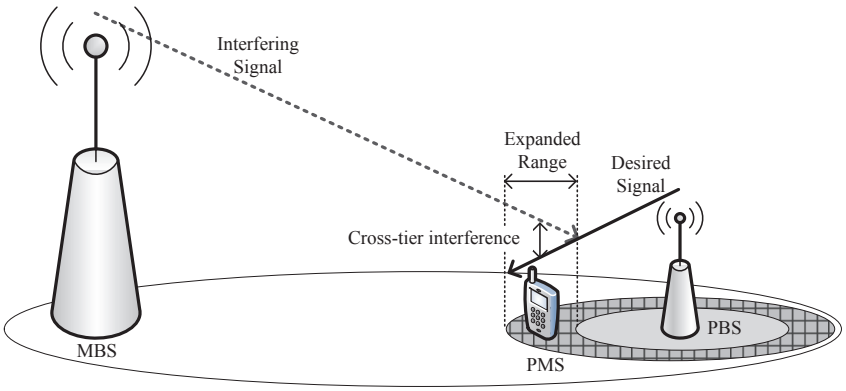

Figure 1.4: Cross-tier interference toward a pico MS in the expanded range

To mitigate this cross-tier interference, macrocells' transmit power control should be necessarily performed. Since the downlink transmit power control at macrocells would result in macro MSs' throughput degradation, it should be carefully determined.

1.2.2 Load-aware Cell Association

Although the CRE-based cell association could bring the user offloading effect (macro MSs toward picocells), the received signal strength-based cell association policy has an absence of MS load balancing throughout BSs. When a large number of MSs are associated with a single BS based on the received signal strength, their achievable throughput could be lower as the available resource per MS is inversely

proportional to the number of associated MSs. Moreover, in heterogeneous cellular networks, offloading MMSs toward picocells without cross-tier interference mitigation becomes limited as offloaded MMSs' achievable throughput would be severely degraded by strong interference from macrocells. As a result, the load-aware cell association should be jointly optimized with cross-tier interference mitigation simultaneously in heterogeneous cellular networks.

1.3 Contributions

The research contributions of this dissertation can be listed as follows:

- Firstly, we present two problem formulations for mitigating downlink cross-tier interference with the CRE-based cell association in heterogeneous cellular networks.
  - In the first problem formulation, the frequency-domain transmit power reduction is studied where the sum of transmit power reduction is minimized in a heterogeneous cellular network with a single macro BS. A heuristic algorithm with much less computational complexity is proposed to solve the integer linear programming (ILP) problem.
  - In the second problem formulation, the time-domain transmit power nulling (i.e., ABS optimization) is studied where the sum of utilities of MSs in the network except for those located in the expanded range is maximized in a heterogeneous cellular network with multiple macro BSs. By formulating the optimization problem, we can find the optimal

number of ABSs that needs to be configured in heterogeneous cellular networks.

- Lastly, we discuss a load-aware cell association problem in conjunction with the use of ABSs for compensating the cross-tier interference in a heterogeneous cellular network with multiple macro BSs. Due to the NP-hardness of the formulated problem, an online heuristic algorithm is proposed where the load balancing and the ABS control are determined based on *the expected throughput*.

1.4 Dissertation Organization

This dissertation is organized as follows:

- Chapter 2 provides brief literature overviews in areas of intercell interference mitigation and load-aware cell association in multi-cellular networks.

- Chapter 3 and 4 discuss the details of resource allocation problems and solutions in the context of cross-tier interference mitigation in downlink heterogeneous cellular networks.

  - In Chapter 3, we discuss a frequency-domain transmit power reduction problem in a heterogeneous cellular network with a single macrocell and multiple overlaid picocells. An optimization problem is formulated to minimize the sum of transmit power reduction at the macrocell subject to the minimum required data rate of pico MSs located in the expanded

range. A heuristic algorithm is proposed to solve the formulated integer linear programming problem. The performance evaluation is performed via system-level simulations in MATLAB.

  - In Chapter 4, we discuss a time-domain transmit power nulling problem (i.e., ABS configuration) in a heterogeneous cellular network with 7 macrocells with multiple overlaid picocells. An optimization problem is formulated to maximize the sum of utilities of all MSs except for pico MSs in the expanded range subject to the minimum required data rate of those pico MSs located in the expanded range. The performance evaluation is performed via numerical simulations using a system-level simulator in MATLAB.

- Chapter 5 discusses the details of the cell association problem and the solution in the context of MS load-balancing in downlink heterogeneous cellular networks. An optimization problem is formulated to maximize the sum of utilities of MSs in the network along with respect to MSs' cell association and ABS control. An online heuristic algorithm is proposed to solve the formulated combinatorial problem (NP-hard). The performance evaluation is performed via numerical simulations using a system-level simulator in MATLAB.

- Chapter 6 concludes the dissertation.

Chapter 2: Background and Related Work

2.1 Resource Allocation in Downlink OFDMA Networks

2.1.1 Homogeneous Networks

Briefly reviewing the resource allocation problem in a single cell case, the *water-filling* [8] algorithm provides a way to optimally allocate the transmit power over resource blocks to maximize the sum rate of a single user under the constraint of the total transmit power. As we consider multiple users in the cell, the optimization problem tends to be combinatorial as binary user scheduling indication onto each resource block needs to be dealt along with the transmit power level. There have been different problem formulations and various approaches to solve them in an efficient way.

Jang *et al.* [9] formulate a sum rate maximization problem subject to the constraint of the total transmit power. Due to the computational complexity of finding an optimal transmit power level by water-filling, authors show that selecting a user with the best channel condition on each resource block by equally distributing the total transmit power over resource blocks provides the marginal performance degradation compared to the jointly optimal transmit power and user scheduling on

each resource block.

Wong *et al.* [10] formulate a total transmit power minimization problem subject to the constraint of achievable data rates. Lagrangian relaxation (LR) is applied to the number of bits to be achieved and the scheduling indicator, and a 2-step algorithm is proposed where a resource block allocation is performed, and then an appropriate number of bits are allocated accordingly.

Kivanc *et al.* [11] formulate a total power minimization problem subject to the constraint of users' minimum required data rate. A greedy algorithm is proposed where users are scheduled onto resource blocks in an order of channel gain after calculating the required number of resource blocks based on the minimum data rate and average SNR.

Rhee *et al.* [12] formulate a max-min optimization problem where the minimum of all users' throughput is maximized for fairness among users. By relaxing the binary scheduling indicator to real values, the original problem becomes convex, and a sub-optimal algorithm is proposed where resource blocks are assigned to users based on the equally distributed transmit power.

Wong *et al.* [13] formulate a rate maximization problem subject to the constraints of total power and proportional fairness among users. Due to non-linearity of proportionality constraints, authors propose an algorithm where the user scheduling is performed in a greedy manner to maximize the total rate based on the proportional fairness. Then, the transmit power level is determined based on water-filling.

In a multi-cell case, the presence of inter-cell interference is a critical challenge, which means allocating more transmit power on a specific resource block from each

cell doesn't guarantee a higher network-wide sum data rate unlike the single cell case, because the higher transmit power from a cell results in the stronger inter-cell interference toward neighboring cell. As a result, the resource allocation for mitigating the inter-cell interference is the key issue in multi-cell networks.

As an extension of a single cell optimization, there have been several work on joint optimization of transmit power level and user scheduling in a presence of inter-cell interference. Koutsopoulos *et al.* [14] formulate a system rate maximization problem with respect to user scheduling, modulation order, and transmit power level subject to the constraint of the total transmit power and minimum required SINR values. To solve the optimization problem, a greedy-based heuristic algorithm is proposed where a user with the largest data rate increment scaled by the ratio of desired and interference powers is selected for each resource block, and transmit power levels of base stations are updated accordingly based on the minimum required SINR values.

Li *et al.* [15] formulate a system rate maximization problem with respect to the user scheduling. Due to the intractable interference by dynamic transmit power control and the presence of adaptive modulation & coding (AMC) technique, the total transmit power is assumed to be equally distributed over resource blocks. To solve the problem, a hierarchical user scheduling algorithm is proposed where the best user assignment is calculated to maximize the sum data rate by utilizing each user's achievable rate with and without a dominant interference in a large scale at a network controller, and the resource block allocation is performed in a small scale at each base station based on the traffic diversity and the fading of wireless channel.

Thanabalasingham *et al.* [16] formulate a total transmit power minimization with respect to the user scheduling and the transmit power level subject to the constraint of minimum required data rates. By relaxing the binary scheduling indicator to be real values and assuming inter-cell interference can be averaged out by frequency hopping, the original multi-cell optimization problem is transformed into multiple single-cell problems which can be solved using a standard Lagrangian technique.

Due to dynamically changing inter-cell interference by transmit power control with frequency reuse 1 (e.g., all base stations can access resource blocks without any restriction) in multi-cell networks, a different approach of inter-cell interference avoidance has been discussed. The main principle is that the scheduling restriction in a frequency domain is applied to neighboring cells so that inter-cell interference can be avoided/mitigated, and the transmit power level is upper-limited to a certain value (normally equally distributed transmit power level). One method is to divide the total system bandwidth into 3 groups each of which has equally distributed transmit power and is exclusively allocated to each cell, which is known as *frequency reuse- 3* illustrated in Figure 2.1(a). Since each cell can only utilize $\frac{1}{3}$ of the system bandwidth in frequency reuse-3, fractional frequency reuse (FFR) schemes are proposed which are *partial frequency reuse (PFR)* and *soft frequency reuse (SFR)*. The PFR scheme [17] is a blend of frequency reuse-1 and reuse-3 as illustrated in Figure 2.1(b). For the cell-center area, reuse-1 is applied with a lower transmit power level, and for the cell-edge area, each cell occupies an orthogonal frequency resource blocks so that inter-cell interference can be effectively avoided.

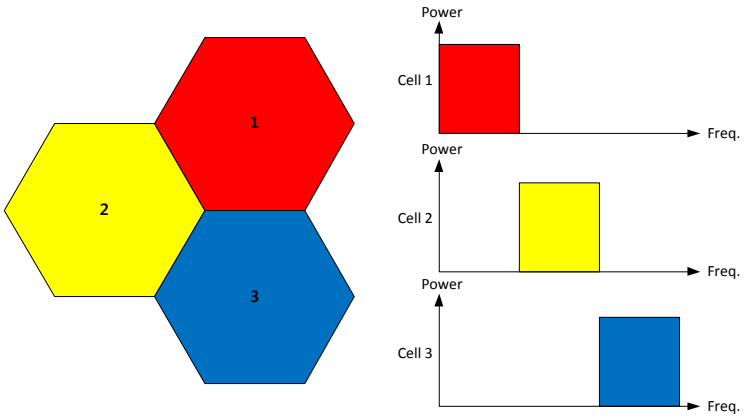

(a) Reuse-3

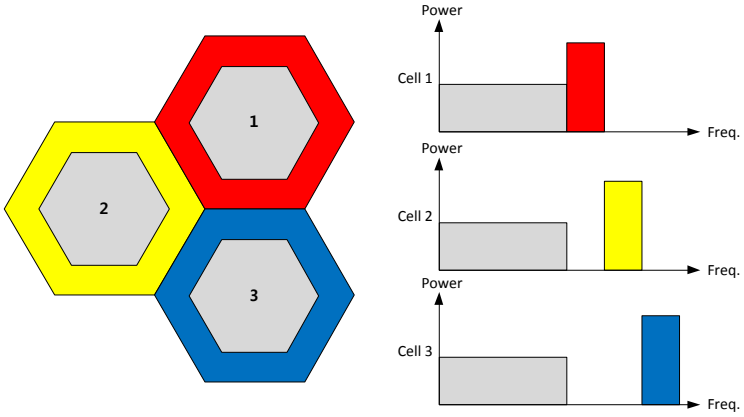

(b) Partial frequency reuse

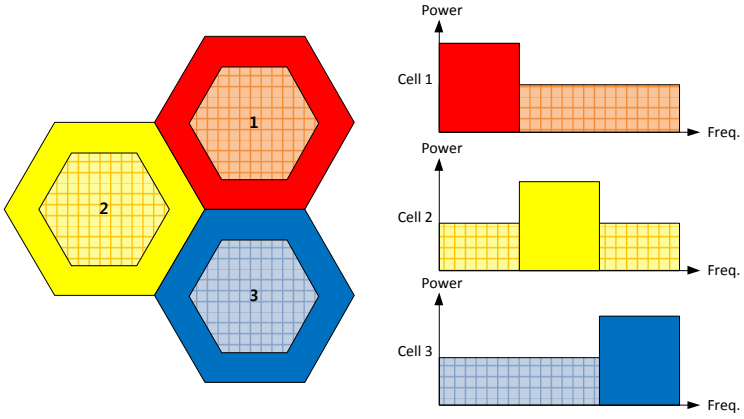

(c) Soft frequency reuse

Figure 2.1: Frequency reuse schemes

The SFR scheme [18] provides more efficient resource utilization than PFR does as it allows each cell utilizes all frequency resource blocks with different transmit power level, illustrated in Figure 2.1(c).

In 3GPP Rel-8 LTE systems [19], *Inter-Cell Interference Coordination (ICIC)* scheme is proposed to mitigate inter-cell interference through signal exchanges between eNodeBs. For the downlink transmissions, a bitmap called the *Relative Narrowband Transmit Power (RNTP)* indicator can be exchanged between eNodeBs over the X2 interface. Each bit of the RNTP indicator corresponds to one resource block in the frequency domain and is used to inform the neighboring eNodeBs if the cell is planning to keep the transmit power for the resource block below a certain upper limit or not. The value of this upper limit, and the period for which the indicator is valid into the future, are configurable. This enables the neighboring cells to take into account the expected level of interference in each resource block when scheduling UEs in their own cells. The reaction of the eNodeB in case of receiving an indication of high transmit power in a resource block in a neighboring cell is not standardized (thus allowing some freedom of implementation for the scheduling algorithm); however, a typical response could be to avoid scheduling cell-edge UEs in such resource blocks. In the definition of the RNTP indicator, the transmit power per antenna port is normalized by the maximum output power of a base station or cell. The reason for this is that a cell with a smaller maximum output power, corresponding to smaller cell size, can create as much interference as a cell with a larger maximum output power corresponding to a larger cell size.

Elayoubi *et al.* [20] [21] develop an analytical model for the collisions for an

arbitrary number of users in the different cells to compare the performance of different frequency reuse schemes: reuse-1, reuse-3, partial frequency reuse, and soft frequency reuse. They calculate the capacity of the system using a Markov model and adaptive modulation & coding under inter-cell interference.

Ali *et al*. [22] propose a two-step hierarchical algorithm to maximize the system data rate. In the first step, resource blocks are assigned to reuse-1 or reuse-3 region for base stations by the network controller such that the achievable system data rate is maximized subject to the constraint of QoS data rates of base stations. Then, in the second step, in each base station the best user is selected for the allocated resource blocks to maximize the sum rate subject to the constraint of each user's minimum required data rate.

Rahman *et al*. [23] [24] [25] discuss an inter-cell interference avoidance scheme with a performance comparison to frequency reuse schemes. A utility maximization problem is formulated where the utility function is a product of the achievable date rate and the demand factor of a user. To solve the optimization problem, a hierarchical algorithm is proposed where in each base station resource restriction request is generated based on users' utility and their dominant interfering base station information, and in the network controller those restriction requests are resolved in an optimal manner to maximize the total utility.

Chang *et al*. [26] utilize the graph framework to support dynamic fractional frequency reuse schemes - partial/soft frequency reuse. As a first step, an interference graph is constructed where users and interference between two users represent vertices and edges, respectively. Then, as a second step, a graph coloring algorithm

is proposed to efficiently allocate resource blocks to users. Any two neighboring users (i.e., vertices connected by an edge) in the graph are assigned with different colors.

2.1.2 Heterogeneous Cellular Networks

Heterogeneous cellular networks can be seen as a subset of multi-cell networks, even if there is only one macrocell assumed in the network due to the presence of multiple low-powered small cells. However, the interference scenarios are quite different from those in homogeneous networks. In femtocell-based heterogeneous cellular networks [27], cross-tier interference mitigation from closed access femtocells to macro users is one of challenges as macro users are unable to hand over those femtocells due to their closed access policy. The other interference scenario is co-tier interference mitigation among femtocells, of which challenge comes from the limited connectivity to the core network. This limitation makes the centralized interference mitigation method unavailable so that distributed methods are discussed. In picocell-based heterogeneous cellular networks, cross-tier interference mitigation from macrocells to pico users (or specifically pico users located in the expanded range). Since these pico users in the expanded range are associated with picocells by the CRE operation even if they observe a stronger received signal strength from macrocells, the interference from macrocells is much stronger than the desired signal from picocells for those pico users.

Firstly, we briefly review some work on interference mitigation in femtocell-

based heterogeneous cellular networks. Su *et al.* [28] discuss a cross-tier interference mitigation in femtocell networks by formulating a problem of minimizing the sum of interference observed by macro users subject to the constraints of all users' minimum required SINR levels and interference levels. Due to the small coverage of femtocells, co-tier interference between femtocells are not considered, and only cross-tier interference between macros and femtos. In their algorithm, macro users feed back the interference power from femtocells to their macrocells, and macrocells update & signal to femtocells the parameters by which femtocells adjust their transmit power accordingly.

Chandrasekhar *et al.* [29] discuss an orthogonal resource allocation to macros and femtos such that the average throughput per frequency and area is maximized. Assuming that the system frequency bandwidth F is divided into two parts - macro part F_c and femto part F_f, the spectrum fraction of macro $\rho = F_c/F$ is used as a key parameter to determine the per-tier area spectral efficiency. Utilizing a stochastic geometry framework, the optimal ρ^* for different femtocell deployment scenarios is calculated.

Ling *et al.* [30] discuss a co-tier interference mitigation in densely-deployed femtocell networks, and a self-organizing algorithm for resource block allocation to users is proposed. In order to minimize its suffered interference, each femtocell independently measures all resource blocks and select resource blocks with the lowest interference.

Kamel *et al.* [31] discuss the optimized ABS operation (offset and ratio) for interfered macro users by closed femtocells. To maximize the network-wide utility

as an objective, in the first stage macro users are divided into two groups - normal macro users and victim macro users, and a bargaining starts between the two groups to partition the resources. In the second stage, a bargaining starts for only victim macro users in a given highly interfering femtocells for the reduction of the blanking rate associated with each highly interfering femtocells.

Lastly, we review work on interference mitigation in picocell-based heterogeneous cellular networks, which is of our main interest. Lopez-Perez *et al.* [32] [33] discuss a macrocell's transmit power reduction for mitigating cross-tier interference toward pico users in the expanded range. Assuming there is a minimum required SINR level for each pico user in the expanded range, the reduced macrocell's transmit power level is determined for resource blocks where those pico users are scheduled. Given the reduced transmit power level on each resource block, a transmit power minimization problem is formulated subject to the constraint of macro users' minimum required QoS data rates, and is solved by utilizing a network simplex algorithm [34].

Li *et al.* [35] discuss an FFR scheme in heterogeneous cellular networks. Given the cell association based on the CRE operation, the transmit power level, FFR band portion, and user scheduling are jointly optimized to maximize the network-wide utility. To solve the optimization problem, a two-loop algorithm is proposed where every combination of FFR band partition and transmit power level is examined with a certain step size in an outer loop, and user scheduling onto two FFR bands is solved using a gradient-descent method in an inner loop.

Pang *et al.* [36] discuss a time-domain macrocells' transmit power nulling, i.e.,

the optimal number of almost blank subframes (ABSs). The network-wide utility (i.e., the sum of users' utilities) maximization problem is formulated to find the optimal number of ABSs. The pico user scheduling policy is based on the pico user categorization into one of two groups - *normal* and *victim*. The pico users in the normal group are only scheduled in non-ABSs, and those in the victim group are only scheduled in ABSs. For every possible value of ABSs, every base station needs to calculate the sum of the associated users' utilities. Unlike macro base stations of which users are only scheduled to non-ABSs, pico base stations need to find the best categorization of their users into two groups and calculate the sum of utilities using a dynamic programming algorithm. Those utility values from base stations are signaled to a central coordinating entity so that the optimal number of ABSs that maximizes the network-wide utility is chosen.

Cierny *et al*. [37] also discuss the optimal number of ABSs in the heterogeneous cellular networks. The minimization problem of the number of ABSs is formulated subject to the constraint of minimum required data rate of pico users in the expanded range. The pico user scheduling policy is that pico users in the expanded range are scheduled in both ABSs and non-ABSs, and regular pico users are only scheduled in non-ABSs. In other words, the ABS resource is exclusively available for pico users in the expanded range and the non-ABS resource is shared by both regular pico users and pico users in the expanded range. The smallest number of ABSs is selected by which all pico users in the expanded range can achieve their minimum required data rate.

2.2 Load-aware Cell Association in Wireless Networks

The user load balancing in wireless networks has gained attention and interest from researchers due to the following aspects: (i) when a large number of users are served by a single cell, each user's expected throughput is severely degraded by a small amount of available resource for them, (ii) the conventional user association policy, where each user is associated with a cell (or BS) from which it observes the strongest received signal strength, can cause the user load imbalance across cells.

2.2.1 Homogeneous Wireless Networks

One approach for load balancing is to change the cell size depending on the user load, so called *cell breathing* technique, which is used in CDMA networks [38] [39] [40] or wireless LANs [41] [42]. The key principle is that the heavily loaded cells shrink their cell size by reducing the transmit power so that users are encouraged to be handed over lightly loaded neighboring cells, or vice versa. Finding the appropriate transmit power level among neighboring cells is the key challenge for cell breathing, and heuristic algorithms are proposed to reduce the computational complexity.

The more common approach in OFDMA-based multi-cell networks such as wireless LANs, LTE networks, or WiMAX networks is to change each individual user's association with a cell in a way to maximize/minimize the objective function. Bu *et al.*discuss a problem formulation of the network-wide utility maximization. Based on the observation in [43] that the proportionally fair allocation of network

resources is equivalent to the optimization of the following objective function:

$$\max \sum_{u \in \mathcal{U}} \sum_{a \in \mathcal{S}_u} \log(\gamma_{ua}), \tag{2.1}$$

where $\mathcal{U}$ is the set of users, $\mathcal{S}_u$ is the set of base stations from which the user u can achieve the average rate $r_{ua} > 0$, and γ_u is the bandwidth allocation to the user u by the network. Assuming that all users have Rayleigh fading channels and the priority, and the feasible rate is linear in SINR, γ_{ua} under a generalized proportional fairness scheduling can be defined as

$$\gamma_{ua} = r_{ua} \frac{G(y_a)}{y_a}, \tag{2.2}$$

where y_a is the number users associated with the base station a and $G(y_a)$ is the multi-user diversity gain which is a function of y_a according to [43] [44]. As a result, from the objective function in (2.1), the following optimization problem is formulated:

$$\max \sum_{u \in \mathcal{U}} \sum_{a \in \mathcal{S}_u} x_{ua} \log \left(r_{ua} \frac{G(y_a)}{y_a} \right) \tag{2.3a}$$

$$\text{s.t.} \quad x_{ua} = \{0, 1\} \quad \forall u \in \mathcal{U} \quad \forall a \in \mathcal{S}_u \tag{2.3b}$$

$$\sum_{a \in \mathcal{S}_u} x_{ua} = 1 \quad \forall u \in \mathcal{U}, \tag{2.3c}$$

$$y_a = \sum_{u \in \mathcal{U}} x_{ua} \quad \forall a \in \mathcal{A}, \tag{2.3d}$$

where $\mathcal{A}$ is the set of base stations. Due to the binary nature of the association indicator x_{ua}, it is proved that the optimization problem in (2.3) is NP-hard, and there is no algorithm that can find the optimal solution in a polynomial time unless $P = NP$. To solve the optimization problem, authors propose 1 offline and 2 online

algorithms. In the offline algorithm, it is shown that the original problem becomes the maximum weighted matching problem for every fixed value y_a. By enumerating all possible y_a configurations, the problem can be solved in a polynomial time. The first online algorithm is a greedy-based heuristic algorithm where each user is associated with the base station such that the objective function improves the most. In the second online algorithm, assuming that the association of at most k users can be changed, all the possible cases for those k users are evaluated and the best association is selected.

Son *et al.*discuss the same objective function (i.e., the network-wide proportional fairness-based utility maximization) as Bu's [45], and they take the inter-cell interference mitigation into account by applying a partial frequency reuse. To solve the optimization problem, they use a notion of *expected throughput* which is the average throughput expected by handing over a user from a serving cell to a target cell. With an assumption of the large number of users associated with each base station and the Euler's approximation to harmonic series, it is proved that a user's handover to another cell improves the network-wide utility (i.e., the net utility is greater than 0). Using this observation, an online heuristic algorithm is proposed where the user with the largest net utility is handed over to the target cell for each iteration.

Berjerano *et al.* [46] discuss an objective function of the network-wide max-min fairness in wireless LANs. In their work, the goal is to maximize the minimal fair share of each user, of which type of fairness is known as max-min fairness. Informally, a bandwidth allocation is max-min fair if there is no way to give more bandwidth to

any user without decreasing the allocation of a user with less or equal bandwidth. Due to the NP-hardness of the problem, they propose an efficient algorithm where a fractional association solution is computed first, and then the integral solution is obtained by a rounding method.

Kim *et al.* [47] discuss a generalized optimal user association policy, which is called α *optimal*. The distributed association decision made at users is proposed where a user located at x simply selects the base station $i(x)$ using the deterministic rule as

$$i(x) = \arg\max_{j \in \mathcal{B}} \; c_j(x) \left(1 - \rho_j^{(k)}\right)^{\alpha}, \tag{2.4}$$

where $c_j(x)$ is the achievable rate of the user at location x with a base station j, $\mathcal{B}$ is the set of base stations, and $\rho_j^{(k)}$ is the user load information of the base station j in k-th iteration. The proposed algorithm supports a family of load-balancing objectives as α ranges from 0 to ∞: rate-optimal ($\alpha = 0$), throughput-optimal ($\alpha > 1$), delay-optimal ($\alpha = 2$), and equalizing BS loads ($\alpha = \infty$).

2.2.2 Heterogeneous Cellular Networks

Due to the presence of overlaid low-powered cells, the key issue of load balancing in heterogeneous cellular networks is how to distribute user load toward those small cells in a macrocell.

As introduced in Section 1.1.1, a modified version of the received signal strength-based cell association, i.e., cell range expansion in 3GPP LTE-A systems, can achieve the user distribution from macrocells to small cells. However, the possible user load

imbalance is still a challenge even if the CRE operation is applied.

Ye *et al.*formulate a network-wide utility maximization problem with respect to the user association. Similar to the work in [45] [48], the following optimization problem is formulated:

$$\max \sum_{i\in\mathcal{U}} \sum_{j\in\mathcal{B}} x_{ij} \log\left(\frac{c_{ij}}{\sum_k x_{kj}}\right) \tag{2.5a}$$

$$\text{s.t.} \quad x_{ij} = \{0,1\} \quad \forall i \in \mathcal{U} \;\; \forall j \in \mathcal{B} \tag{2.5b}$$

$$\sum_{j\in\mathcal{B}} x_{ij} = 1 \quad \forall i \in \mathcal{U}, \tag{2.5c}$$

where $\mathcal{U}$ and $\mathcal{B}$ denote the set of users and base stations, respectively. By relaxing the binary cell association indicator, the optimization problem in (2.5) becomes convex, and using the Lagrangian dual decomposition method, the dual problem of the primal formulation becomes

$$\min_{\mu} \;\; f_x(\mu) + g_K(\mu) \tag{2.6a}$$

$$\text{where} \quad f(\mu) = \begin{cases} \max_x \;\; \sum_i \sum_j x_{ij} \left(\log(c_{ij}) - \mu_j\right) \\ \quad \text{s.t. } x_{ij} = [0,1] \\ \qquad \sum_{j\in\mathcal{B}} x_{ij} = 1 \end{cases} \tag{2.6b}$$

$$g(\mu) = \max_{K\le N_U} \;\; \sum_j K_j \left(\mu_j - \log(K_j)\right), \tag{2.6c}$$

where μ is a Lagrangian multiplier, K_j is the number of associated users in base station j, and N_U is a constraint for the distributed algorithm. From above dual problem, a distributed algorithm is proposed where at the user side, user i at time t determines its associating base station j^* as

$$j^* = \arg\max_j \;\; \log(c_{ij}) - \mu_j(t), \tag{2.7}$$

where μ_j is assumed to be broadcast from base station j, and at the base station side, the new Lagrangian multiplier μ_j is updated based on the number of associated users as

$$\mu_j(t+1) = \mu_j(t) - \delta(t) \cdot \left(K_j(t) - \sum_i x_{ij}(t) \right), \tag{2.8}$$

where $\delta(t) > 0$ is a dynamic step size.

Madan *et al.*discuss the network-wide utility maximization with respect to cell association, user scheduling, and transmit power control. For a fixed transmit power level, the utility maximization problem can be solved using a convex optimization tool, during each iteration a base station evaluates the total utility by solving above optimization problem for different combinations of its transmission power and neighbors' transmission powers. By exchanging the transmit power level information with other neighbors through over-the-air signalling via users, the optimal transmission power level is determined. Similarly, during each iteration, a base station evaluates the total utility in a neighborhood for different associations of a user with its neighbors so that the association is determined in a way that the total utility is maximized.

Corroy *et al.*discuss the network-wide rate maximization with respect to the cell association. For each macrocell area, authors divide the user association into three cases: association with macro, association with pico, and partial association with macro and pico simultaneously. For the partial association case, the optimization problem becomes quasi-convex by relaxing the association indicator, and the bisection method is used to solve the problem. For the reduced computational com-

plexity, a heuristic algorithm is proposed where for each iteration a user with the largest difference in the received signal strength between pico and macro is selected and the best cell association is determined by examining all possible associations.

Yu *et al.* [49] [50] discuss the composite utility maximization in relay-based heterogeneous cellular networks. Their objective is to maximize the system capacity which is expressed as the sum of connected users in the network, and minimize the resource consumed for supporting the connected users, which is expressed as

$$\max \quad -\sum_{i=1}^{N}\sum_{j=1}^{M_r}\sum_{k=1}^{M_c}\Omega_{ijk} + \epsilon\sum_{i=1}^{N}\sum_{j=1}^{M_r}\sum_{k=1}^{M_c}x_{ijk}, \tag{2.9}$$

where N is the number of users, M_r is the number of relay base stations, M_c is the number of macro base stations, Ω_{ijk} is the weighted resource required to support user i, x_{ijk} is the association indicator, and ϵ is a factor to adjust the relative importance between two objectives. For a reduced computational complexity, a heuristic algorithm is proposed where, for each user entering the network, the base station from which the user achieves the lowest weighted resource consumption is chosen. In [51] authors expand above composite utility maximization problem to full/partial frequency reuse cases. Depending on the frequency reuse schemes, the resource consumption for supporting users becomes different. To solve the problem, a gradient descent-based algorithm is proposed.

Li *et al.* [52] discuss a proportional fairness-based utility maximization problem with respect to cell association in relay-based heterogeneous cellular networks. Depending on a user's association with macro or relay, the portions of direct link from macro, forward link from relay, and wireless backhaul link to relay are chang-

ing accordingly. Using the gradient-based scheduling framework, the cell association variable is chosen to maximize the drift of the objective function. The multi-carrier proportional fair scheduling is decomposed into multiple single-carrier scheduling problems.

The tractable framework to analyze SINR in heterogeneous cellular networks has been discussed. Using stochastic geometry, SINR distribution in multi-tier heterogeneous cellular networks is discussed in [53] [54], and Jo *et al*.studies long-term average rate-based flexible cell association with cell range expansion.

Oh *et al*. [55] discuss the cell selection policy based on the expected user data rate with respect to an ABS ratio α. For a given ABS ratio α, macro users can only utilize $(1-\alpha)$ non-ABS resource and pico users can utilize both $(1-\alpha)$ non-ABS resource and α ABS resource. Based on this observation, users determine their serving cells from which they can achieve the highest expected data rate.

Hu *et al*. [56] discuss cell associations in relay-based heterogeneous cellular networks. Assuming the multiple associations in downlink and uplink for every user are available, two association policies for downlink and uplink are proposed. In downlink, users are associated with a base station from which they observe the strongest received signal strength which provides the higher achievable data rates. In uplink, on the other hand, users are associated with the closest base station by which users can minimize the uplink transmit power towards the serving base station.

There have been some work on performance evaluation of unique features in heterogeneous cellular networks. Okino *et al*. [57] evaluate the downlink network

throughput with the various CRE bias values and ABSs. Saleh *et al.* [58] discuss the performance of relay-based heterogeneous cellular networks. By applying different CRE bias values for initial cell association and handover, both downlink and uplink throughput gains by cell-splitting and load balancing are studied.

Chapter 3: Frequency-domain Macrocell Transmit Power Reduction

3.1 Motivation

When the MBS's transmit power needs to be reduced for mitigating cross-tier interference toward pico MSs located in the expanded range (ER-PMSs) who receive a stronger interfering signal than the desired, two issues at the MBS can be raised as follows: i) how much transmit power should be reduced and ii) how many frequency-domain resource blocks (RBs) should be configured with the reduced transmit power.

Although the transmit power nulling in a time-domain (3GPP LTE-A's ABSs) or a frequency-domain [59] can be the most effective way to mitigate the cross-tier interference, the challenging issue here would be MMSs' throughput degradation by transmit power nulling where the achievable throughput of MMSs is zero during those time- and frequency-domain resources. Authors in [60] have introduced a concept of low power transmissions from MBSs during ABSs so that MMSs' throughput can be improved. Due to the coarse granularity of teim-domain subframes, the frequency-domain transmit power reduction could be better for the MBS to control the transmit power in a finer manner.

In addition to the transmit power level, it is also important to determine how many RBs are configured with the reduced transmit power. In [32], a transmit power

reduction scheme at an MBS is proposed, whereby RBs and their trantmit power level at the MBS are determined by ER-PMSs' scheduled RBs and their required signal-to-interference plus noise ratio (SINR) values. For those RBs, the MBS needs to reduced the transmit power so that the scheduled ER-PMSs could achieve the minimum required SINR. Since ER-PMSs' scheduled RBs are not aligned at all, the MBS may need to reduce its transmit power over all RBs in the worst case. This could deteriorate MMSs' throughput significantly.

In this chapter, we propose a coordinated scheduling and power control algorithm for heterogeneous cellular networks where the sum of MBS's reduced transmit power is minimized. To maximize the interference mitigation effect by reducing MBS's transmit power, it is assumed that all ER-PMSs are scheduled onto the same RBs. The reduced transmit power level on each RB is determined by MMSs' minimum required SINR as a QoS requirement. Then, a group of RBs for ER-PMSs is selected to satisfy ER-PMSs' minimum required data rate by solving a binary integer programming problem.

3.2 System Model

The network model considered in this paper is a heterogeneous downlink cellular network consisting of 1 MBS and P PBSs deployed inside the MBS's coverage. Let $\mathcal{U}^m$, $\mathcal{U}_l^p$ and $\mathcal{U}_{ER}^p$ denote the set of MMSs, PMSs in the l^{th} PBS, and all ER-PMSs in picocells, respectively. The corresponding cardinalities are represented as following: $|\mathcal{U}^m| = K^m$, $|\mathcal{U}_l^p| = K_l^p$, and $|\mathcal{U}_{ER}^p| = P$. For the simplicity of explana-

tion, we consider only 1 MBS and each PBS is assumed to have one ER-PMS, i.e., P ER-PMSs in total. The system bandwidth W is divided into N resource blocks and the co-channel deployment is assumed which means both MBS and PBSs are sharing the system bandwidth together. The noise power spectral density is N_0, and the averaged channel gain between a BS and an MS over a resource block including path loss, shadowing, and fast fading is assumed to be acquired *a priori* via channel state information feedback.

The received signal-to-interference plus noise ratio (SINR) of MMS i on RB n can be expressed as

$$\Gamma_{i,n}^{m} = \frac{P_{m,n} h_{i,n}^{m}}{\sum_{l=1}^{P} P_p h_{i,n}^{p_l} + \sigma^2}, \tag{3.1}$$

where $P_{m,n}$ is the allocated transmit power at MBS on RB n ranging from 0 to P_m ($0 \leq P_{m,n} \leq P_m$) where P_m is the transmit power by equally distributing the total transmit power P_m^{tot} over N RBs ($P_m = \frac{P_m^{tot}}{N}$), P_p is the equally distributed power over all N RBs at PBSs ($P_p = \frac{P_p^{tot}}{N}$) where P_p^{tot} is the total transmit power of PBSs, $h_{i,n}^{b}$ is the average channel gain from the BS b ('m' for MBS, 'p_l' for PBS l) to MMS i on RB n including path loss, shadowing, and fast fading, and σ^2 is the power of additive white Gaussian noise ($\sigma^2 = N_0 \cdot \frac{W}{N}$). By restricting $P_{m,n}$ to be upper-bounded by P_m, we prevent additional interference toward PMSs which can be caused by allocating extra transmit power onto some RBs when the transmit power control is applied (i.e., $P_m^{tot} - \sum_{n=1}^{N} P_{m,n} > 0$). It is additionally assumed that PBSs do not perform the transmit power control.

For the SINR of PMS j in PBS l on RB n, we define two forms of SINR

depending on MBS's transmit power level. If the transmit power control is not applied by MBS, i.e., $P_{m,n} = P_m$, the corresponding SINR can be expressed as

$$\Gamma_{j,n}^{p_l} = \frac{P_p h_{j,n}^{p_l}}{P_m h_{j,n}^{m} + \sum_{l'=1,l' \neq l}^{P} P_p h_{j,n}^{p_{l'}} + \sigma^2}, \tag{3.2}$$

and if the transmit power control is applied, i.e., $P_{m,n} < P_m$, the corresponding SINR is expressed as

$$\bar{\Gamma}_{j,n}^{p_l} = \frac{P_p h_{j,n}^{p_l}}{\overline{P}_{m,n} h_{j,n}^{m} + \sum_{l'=1,l' \neq l}^{P} P_p h_{j,n}^{p_{l'}} + \sigma^2}, \tag{3.3}$$

where $\overline{P}_{m,n}$ is the reduced transmit power at MBS on RB n with which $P_{m,n}$ is replaced in order to distinguish the reduced transmit power level.

Using Shannon's equation, two achievable data rates of MS u in BS b on RB n, $R_{u,n}$ and $\overline{R}_{u,n}$, can be calculated based on $\Gamma_{u,n}^{b}$ and $\bar{\Gamma}_{u,n}^{b}$ as

$$R_{u,n} = \frac{W}{N} \log_2(1 + \Gamma_{u,n}^{b}) \tag{3.4}$$

$$\overline{R}_{u,n} = \frac{W}{N} \log_2(1 + \bar{\Gamma}_{u,n}^{b}), \tag{3.5}$$

respectively.

3.3 Problem Formulation

Our main objective is to minimize the impact on MBS by performing transmit power control. When the transmit power is reduced on RB n, the achievable data rate of a scheduled MMS on that RB n is obviously decreased. Therefore, the objective can be expressed as follows:

$$\begin{aligned} & \text{minimize} \quad \sum_{n=1}^{N} (P_m - P_{m,n}) \\ = \; & \text{maximize} \quad \sum_{n=1}^{N} P_{m,n}. \end{aligned} \tag{3.6}$$

Although it is optimal to allocate the maximum available power on every RB, i.e., $P_{m,n} = P_m \quad \forall n$, from MBS's perspective, ER-PMSs' performance would be severely degraded without MBS's transmit power control. Therefore, we need to carefully determine how many RBs should be used for transmit power reduction at MBS and how much power should be reduced for those RBs.

To further develop the optimization problem, we make the following assumptions for the remainder of this chapter:

- Every MMS i has their minimum required SINR level, denoted by $\gamma_{i,req}$.
- Every ER-PMS j has their minimum required data rate, denoted by $R_{j,req}$.
- All ER-PMSs in the network are dedicatedly allocated to the group of RBs together.

Based on the assumptions above, we further discuss the optimization problem in (3.6) in the following sections. The proposed radio resource management scheme can be implemented in three steps:

1) The MBS determines a pair of MMS and the reduced transmit power level on every RB based on MMSs' minimum required SINR level and their channel condition.

2) Then, the MBS selectively chooses a group of RBs by which the sum of MBS transmission power is maximized and all ER-PMSs are guaranteed their minimum required data rates.

3) After determining the group of RBs with their reduced transmit power for coordination, MBS and PBSs perform the user scheduling for unselected RBs.

3.4 Problem Solving

3.4.1 MMS & Transmit Power Determination

Suppose that every MMS i has a minimum required SINR level as a QoS requirement, MBS's transmit power $P_{m,n}$ on RB n needs to satisfy the following:

$$\frac{P_{m,n}h_{i,n}^{m}}{\sum_{l=1}^{P} P_p h_{i,n}^{p_l} + \sigma^2} \geq \gamma_{i,req}, \quad \forall i, \ \forall n \tag{3.7}$$

where $\gamma_{i,req}$ denotes the SINR requirement for the MMS i.

From (3.7), we can calculate the minimum required transmit power level $P'_{i,n}$ for MMS i on RB n which is the lowest power level that the MBS can reduce the transmit power down to as

$$P'_{i,n} = \frac{\sum_{l=1}^{P} P_p h_{i,n}^{p_l} + \sigma^2}{h_{i,n}^{m}} \cdot \gamma_{i,req}, \quad \forall i, \ \forall n. \tag{3.8}$$

For every RB n, totally K^m pairs of MMS and its required transmit power, i.e., $\{i, P'_{i,n}\}$ $\forall i$, can be generated. In order to provide the least cross-tier interference toward ER-PMSs, the MBS selects the MMS i_n^* for RB n which requires the lowest transmit power level as

$$\begin{aligned} i_n^* &= \arg\min_{i \in \mathcal{U}^m} \ P'_{i,n}, \quad \forall n \\ &= \arg\min_{i \in \mathcal{U}^m} \ \left(\frac{\sum_{l=1}^{P} P_p h_{i,n}^{p_l} + \sigma^2}{h_{i,n}^{m}} \cdot \gamma_{i,req} \right), \quad \forall n. \end{aligned} \tag{3.9}$$

In order for MMSs to be selected as the MMS i_n^*, they should experience fairly good channel condition and/or low SINR requirement.

After finding the best MMS i_n^* on every RB n, the reduced transmit power level $\overline{P}_{m,n}$ can be obtained as

$$\overline{P}_{m,n} = P'_{i_n^*,n} = \frac{\sum_{l=1}^{P} P_p h_{i^*,n}^{p_l} + \sigma^2}{h_{k^*,n}^{m}} \cdot \gamma_{i^*,req}, \quad \forall n, \tag{3.10}$$

and the transmit power margin on RB n, denoted by $\tilde{P}_{m,n}$, is defined, which is the transmit power difference between the equal power P_m and the reduced transmit power $\overline{P}_{m,n}$ as

$$\tilde{P}_{m,n} = P_m - \overline{P}_{m,n} \geq 0, \quad \forall n. \tag{3.11}$$

3.4.2 Coordinated RB Selection for ER-PMSs

Based on the reduced transmit power $\overline{P}_{m,n}$ on every RB n obtained through (3.9), (3.10), we then determine how many RBs with reduced transmit power need to be allocated for ER-PMSs.

Let us define the coordinated scheduling indicator $x_{m,n}^c$ which represents whether ER-PMSs are scheduled on RB n with reduced transmit power $\overline{P}_{m,n}$ (=1) or not (=0). Since we assume ER-PMSs are only scheduled on RBs with reduced transmit power together, their achievable data rate can be expressed as

$$\overline{R}_j = \sum_{n=1}^{N} x_{m,n}^c \frac{W}{N} \log_2(1 + \overline{\Gamma}_{j,n}^{p_l(j)}), \quad \forall j \in \mathcal{K}_{ER}^p, \tag{3.12}$$

where $p_l(j)$ is the PBS index that PMS j is associated with.

Using the reduced transmit power in (3.10) and ER-PMSs' achievable data

rate in (3.12), we can develop an optimization problem based on Eq. (3.6) as

$$\min_{\underline{\mathrm{x}}_m^c} \sum_{n=1}^{N} (P_m - \overline{P}_{m,n}) \cdot x_{m,n}^c = \min_{\underline{\mathrm{x}}_m^c} \sum_{n=1}^{N} \tilde{P}_{m,n} \cdot x_{m,n}^c \tag{3.13a}$$

$$\text{s.t.} \sum_{n=1}^{N} \overline{R}_{j,n} \cdot x_{m,n}^c \geq R_{j,req}, \quad j \in \mathcal{K}_{ER}^p, \tag{3.13b}$$

$$x_{m,n}^c \in \{0,1\} \quad \forall n \tag{3.13c}$$

where $\underline{x}_{m,n}^c$ is a coordinated scheduling indicator vector which is expressed as

$$\underline{\mathrm{x}}_m^c = [x_{m,1}^c, x_{m,2}^c, \cdots, x_{m,N}^c]^\top. \tag{3.14}$$

To find an optimal solution $\underline{\mathrm{x}}_m^{c*}$ to the formulated problem above, exact methods such as *Branch-and-Bound* can be considered which utilize linear programming (LP) relaxation where the problem is transformed into a general linear programming by relaxing the integer variables, and branches are generated by integer approximation of the real-number solution. Although those methods prevent us from examining all the possible combinations, they cannot guarantee finding a solution in a polynomial time.

Therefore, to reduce the computational complexity, we propose a max-min greedy algorithm which finds a sub-optimal solution to the optimization problem in (3.6) with a polynomial-time computation. Since every ER-PMS needs to be provided their minimum required data rate, the number of coordinated RBs is determined by how efficiently the coordinated RBs are selected in a way that some ER-PMSs in much worse channel condition achieve their minimum required data rate quickly. Based on this observation, the key idea of the proposed algorithm is to find the ER-PMS which has achieved the lowest data rate with respect to its

minimum required data rate, and then select an RB on which that ER-PMS expects the highest data rate. This procedure enables us to identify those ER-PMSs in much worse channel condition and efficiently select coordinated RBs by utilizing the frequency selectivity.

Let ϕ_j denote the satisfaction ratio of ER-PMS j defined as $\frac{R_{j,ach}}{R_{j,req}}$, where $R_{j,ach}$ is the achieved data rate of ER-PMS j for a given coordinated scheduling indicator vector $\underline{\mathrm{x}}_m^c$ and is expressed as $\sum_{n=1}^{N} \overline{R}_{j,n} \cdot x_{m,n}^c$. In each iteration, ER-PMS j^* is selected of which satisfaction ratio is the lowest among ER-PMSs as

$$j^* = \underset{j \in \mathcal{K}_{ER}^p}{\arg\min}\ \phi_j = \underset{j \in \mathcal{K}_{ER}^p}{\arg\min}\ \frac{R_{j,ach}}{R_{j,req}}. \tag{3.15}$$

For the ER-PMS j^*, the RB $n_{j^*}^*$ is selected on which the ER-PMS j^* can achieve the largest data rate as

$$n_{j^*}^* = \underset{n' \in \mathcal{N}}{\arg\max}\ \overline{R}_{j^*,n'}, \tag{3.16}$$

where $\mathcal{N}$ is the set of RBs which have not been selected for coordinated scheduling defined as $\{n \in \{1, 2, \cdots, N\} : x_{m,n}^c \neq 1\}$. The achieved data rate of every ER-PMS j including j^* is increased by $\overline{R}_{j,n_{j^*}^*}$. This process is iterated until all ER-PMSs meet their minimum required data rate. The detailed procedure is described in Algorithm 3.1. For the infeasible case, we define an additional parameter R_{min} which denotes a minimum threshold of ER-PMSs' data rate for which it is decided whether RB n is allocated for the coordinated scheduling or not.

Proposition 3.1. The computational complexity of Algorithm 3.1 is $O(PN \log PN)$.

Proof: Assuming $\overline{R}_{j,n}$'s of every ER-PMS j are sorted as part of initialization, the complexity of the sorting process for ER-PMS j is $O(N \log N)$. For each iteration,

Algorithm 3.1 Max-min Greedy RB Allocation

1: Initialization: $x^c_{m,n} = 0 \ \ \forall n$, $R_{j,ach} = 0 \ \ \forall j$, $\mathcal{N} = \{1, 2, \cdots, N\}$.

2: **if** $\sum_{n=1}^{N} \overline{R}_{j,n} \geq R_{j,req} \quad \forall j$ {feasible case} **then**

3: **while** $\min_{j \in \mathcal{K}^p_{ER}} \ \frac{R_{j,ach}}{R_{j,req}} < 1$ **do**

4: Find the least satisfied ER-PMS j^*:

$$j^* = \arg\min_{j \in \mathcal{K}^p_{ER}} \ \frac{R_{j,ach}}{R_{j,req}}$$

5: Find the best RB index $n^*_{j^*}$ for ER-PMS j^*:

$$n^*_{j^*} = \arg\max_{n' \in \mathcal{N}} \ \overline{R}_{j^*,n'}$$

6: Update the coordinated scheduling indicator and the RB set:

$$x^c_{m,n^*_{j^*}} = 1, \quad \mathcal{N} = \mathcal{N} \setminus \{n^*_{j^*}\}$$

7: Update the achieved data rate of all ER-PMSs:

$$R_{j,ach} = R_{j,ach} + \overline{R}_{j,n^*_{j^*}} \quad \forall j \in \mathcal{K}^p_{ER}$$

8: **end while**

9: **else** {infeasible case}

10: Allocate a set of RBs $\mathcal{N}'$ to ER-PMSs

$$\mathcal{N}' = \{n \in \{1, 2, \cdots, N\} \mid \overline{R}_{j,n} > R_{min} \ \ \forall j \in \mathcal{K}^p_{ER}\}$$

11: **end if**

ER-PMSs are sorted in an increasing order of the satisfaction ratio, which requires the complexity of $O(P \log P)$. Therefore, the total computational complexity of the

algorithm becomes

$$O(P \cdot N \log N + N \cdot P \log P) = O(PN \log PN), \tag{3.17}$$

where the worst case searching is assumed, i.e., totally N subframes are examined.

Remark: When the number of PBSs P is much smaller than that of RBs N ($P \ll N$), the computational complexity can be approximated as $O(N \log N)$.

3.4.3 Resource Allocation for Unselected RBs

After determining the group of coordinated RBs, for the unselected RBs (i.e., $x^c_{m,n} = 0$), the MBS recovers the transmit power to the original equal power P_m. Therefore, the transmit power on every RB n can be expressed as

$$P_{m,n} = \begin{cases} P_m & \text{if } x^c_{m,n} = 0 \\ \overline{P}_{m,n} & \text{if } x^c_{m,n} = 1. \end{cases} \tag{3.18}$$

For those unselected RBs, the MBS performs any scheduling policy such as MAX C/I, proportional fairness, or round robin. At PBSs, R-PMSs are scheduled on those unselected RBs based on any scheduling policy as discussed in the MBS case.

3.5 Performance Evaluation

In this section, the performance of the proposed scheme is evaluated through system level simulations. The system level simulator has been developed based on the LTE downlink system level simulator in [61].

For simulations, a heterogeneous network topology is generated with 1 MBS and 2 or 4 outdoor PBSs which are randomly distributed within MBS's coverage.

The MBS and each PBS are equipped with a sector and an omnidirectional antenna, respectively. As a co-channel deployment, the system bandwidth is fully accessed by both MBS and PBSs with equally distributed power unless coordinated scheduling and power control is applied. The detailed simulation parameters are described in Table 3.1 most of which are adopted from 3GPP standard documents [62–64].

To evaluate the performance, we compare the following schemes:

- *No Transmit Power Control (NTPC)*: No transmit power control is applied for cross-tier interference coordination, where the transmit power on each RB at the MBS is P_m.

- *Transmit Power Control (TPC-x)*: Transmit power control is applied for cross-tier interference coordination, where the transmit power on each RB at the MBS is reduced by $-x$ dB (i.e., $P_{m,n} = P_m \cdot 10^{-x/10}$). We simulate *TPC-3* where the MBS's transmit power is a half of that in NTPC, i.e., $P_{m,n} = P_m \cdot 10^{-3/10} = \frac{1}{2}P_m$.

- *Coordinated Scheduling & Power Control (CSPC)*: The proposed scheme is applied.

Before discussing the performance of above schemes, in Table 3.2 the performance of the proposed heuristic algorithm is compared to the branch-and-bound (B&B) method. The performance metrics are the number of RBs and the sum of transmit power to be reduced for coordination. The overall performance degradation of the proposed scheme shows less than 2% in both the number of RBs and the sum of transmit power to be reduced, except for a few cases such as "2 picos,

Table 3.1: System Level Simulation Parameters

Simulation Parameter	***Value***
Simulation time	3000 subframes (3000 ms)
Number of simulations per scenario	300
Carrier frequency	2.0 GHz
System bandwidth	10 MHz
Antenna configuration	SISO
Channel model	Typical Urban (TU)
Inter-site distance	750 m
Noise power spectral density	-174 dBm/Hz
Scheduling algorithm	Proportional fairness
Traffic model	Full buffer
Number of macrocells	1
Macrocell transmit power	40 W (46 dBm)
Macrocell path loss model	$128.1 + 37.6\log_{10} R$ (R in km)
Macrocell shadowing model	Log normal fading with std. 10 dB
Macrocell antenna gain	15 dBi
Number of MMSs	30
Min. required SINR of MMSs	5 dB
Picocell transmit power	1 W (30 dBm)
Picocell path loss model	$140.7 + 36.7\log_{10} R$ (R in km)
Picocell shadowing model	Log normal fading with std. 6 dB
Picocell antenna gain	5 dBi
Number of PMSs per picocell	10 (9 R-PMSs + 1 ER-PMS)
Min. distance between MBS and PBS	75 m
Min. distance between PBS and PBS	50 m
Number of picocells per macrocell	2 / 4
Min. required data rate of ER-PMSs	0.4 / 0.6 Mbps
CRE bias offset	8 / 16 dB

Table 3.2: Comparison between optimal and proposed schemes

Case	***Metric***	***B&B***	***Proposed***	***Difference***
2 picos, 8 dB, 0.4 Mbps	No. of RBs	1.163	1.169	0.006 (+0.50%)
	Power (W)	0.892	0.905	0.013 (+1.45%)
2 picos, 8 dB, 0.6 Mbps	No. of RBs	1.640	1.673	0.033 (+2.01%)
	Power (W)	1.239	1.295	0.056 (+4.51%)
2 picos, 16 dB, 0.4 Mbps	No. of RBs	1.884	1.904	0.020 (+1.07%)
	Power (W)	1.453	1.474	0.021 (+1.47%)
2 picos, 16 dB, 0.6 Mbps	No. of RBs	2.756	2.769	0.013 (+0.48%)
	Power (W)	2.117	2.143	0.026 (+1.21%)
4 picos, 8 dB, 0.4 Mbps	No. of RBs	1.322	1.348	0.026 (+2.02%)
	Power (W)	1.012	1.044	0.032 (+3.18%)
4 picos, 8 dB, 0.6 Mbps	No. of RBs	2.020	2.073	0.053 (+2.62%)
	Power (W)	1.535	1.604	0.069 (+4.50%)
4 picos, 16 dB, 0.4 Mbps	No. of RBs	2.232	2.274	0.042 (+1.89%)
	Power (W)	1.722	1.760	0.038 (+2.22%)
4 picos, 16 dB, 0.6 Mbps	No. of RBs	3.243	3.261	0.018 (+0.56%)
	Power (W)	2.498	2.522	0.024 (+0.99%)

8 dB, 0.6 Mbps", "4 picos, 8 dB, 0.4 Mbps", and "4 picos, 8 dB, 0.6 Mbps". From these three exceptional cases, it is noted that the proposed scheme may require 1 or more RBs than the branch-and-bound method so that the performance gap can be larger. The proposed scheme, however, shows a good trade-off between the worst-case computational complexity and the slight performance degradation.

For performance comparison of three schemes (NTPC, TPC-3, and CSPC), we first discuss ER-PMSs' data rates. The CDFs of ER-PMSs' data rates are shown in Figure 3.1 (2 picocell case) and Figure 3.2 (4 picocell case). Based on these results, the detailed performance analysis will be performed.

Table 3.3: Comparison of ER-PMSs' data rate (bps/Hz)

Case	***Metric***	***NTPC***	***TPC-3***	***CSPC 0.4 Mbps*** *(0.042 bps/Hz)*	***CSPC 0.6 Mbps*** *(0.063 bps/Hz)*
2 picos, 8 dB	Average	0.0506	0.0726	0.0608	0.0805
	Edge	0.0166	0.0272	0.0351	0.0287
2 picos, 16 dB	Average	0.0295	0.0428	0.0648	0.0940
	Edge	0.0044	0.0071	0.0256	0.0285
4 picos, 8 dB	Average	0.0488	0.0717	0.0683	0.0951
	Edge	0.0164	0.0303	0.0351	0.0289
4 picos, 16 dB	Average	0.0301	0.0438	0.0812	0.1147
	Edge	0.0045	0.0074	0.0256	0.0397

The average and edge (5%-tile) data rates of ER-PMSs are listed in Table 3.3. As the CRE bias offset increases from 8 dB to 16 dB, for NTPC and TPC-3 schemes, it is noted that about -40% average data rate degradation and about -70% edge data rate degradation are observed because ER-PMSs would experience a stronger cross-tier interference from the macrocell. The proposed CSPC scheme, on the other hand, shows about -10% or less edge data rate degradation even if CSPC requires much less transmit power reduction (about 3 W or less) than TPC-3 does (20 W). In case of average data rates in CSPC, it is noted that the average data rates are improved as the CRE bias offset increases and/or more picocells are deployed due to the fact that more RBs are allocated to satisfy all ER-PMSs' minimum required data rate which results in higher ER-PMSs' average data rate. The distribution of ER-PMSs' data rate can be found in Figure 3.1 (2 picocell case) and Figure 3.2 (4 picocell case).

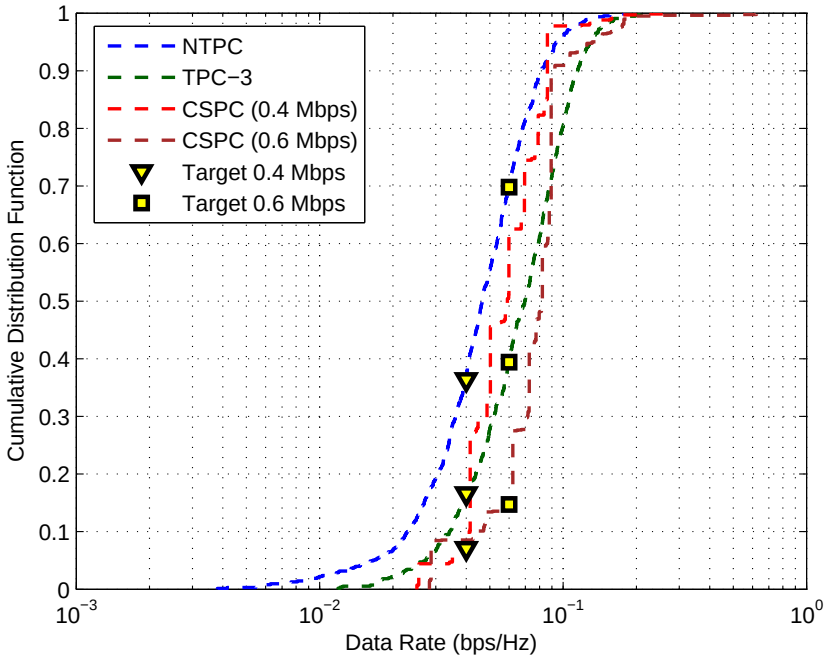

(a) 8 dB CRE bias

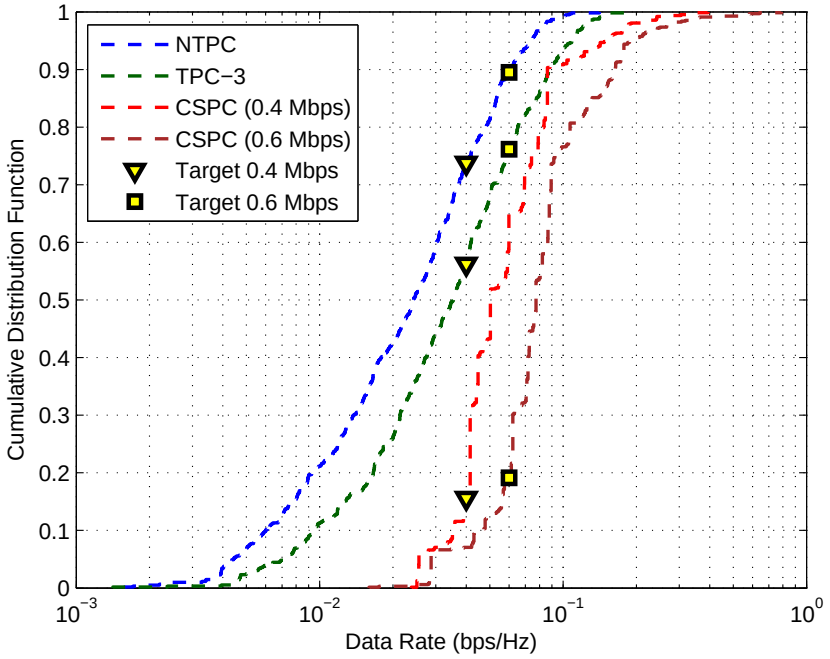

(b) 16 dB CRE bias

Figure 3.1: CDFs of ER-PMSs' data rates (2 picocell case)

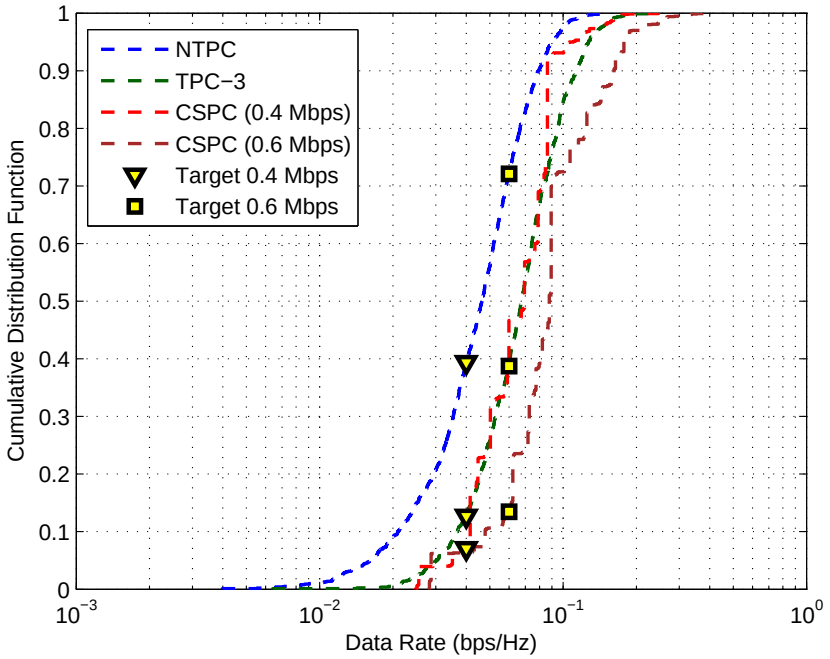

(a) 8 dB CRE bias

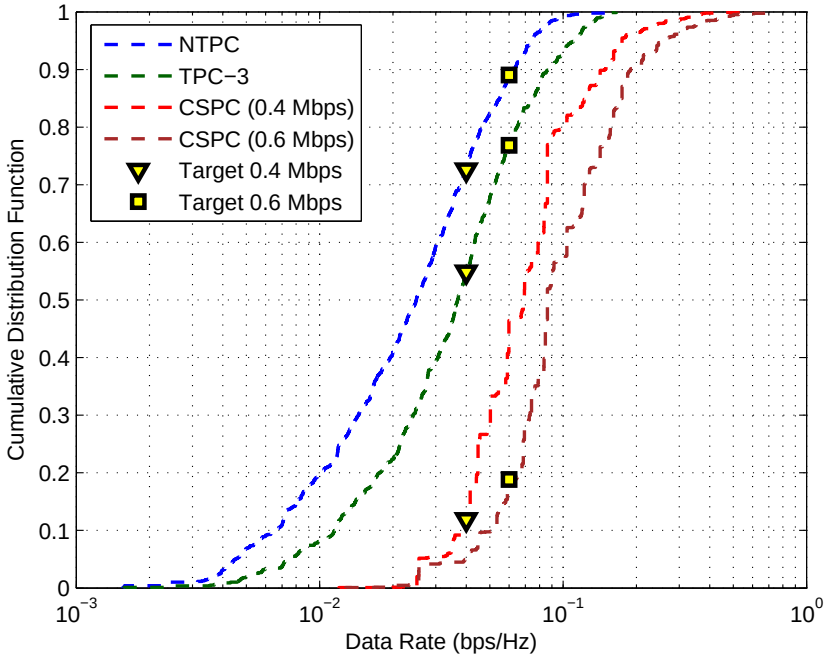

(b) 16 dB CRE bias

Figure 3.2: CDFs of ER-PMSs' data rates (4 picocell case)

It is noted from ER-PMSs' edge data rate with CSPC in Table 3.3 that the minimum required data rate cannot be achieved even though CSPC is applied. This is because for some simulations the optimization problem becomes infeasible as discussed in Algorithm 3.1 where a set of RBs needs to be allocated to ER-PMSs based on R_{min} because some ER-PMSs cannot achieve their minimum required data rate due to the bad channel condition. In our simulations, the threshold R_{min} for every RB is set to be zero whereby RB n is used for the coordinated scheduling if every ER-PMS can achieve a positive data rate on that RB n. The underlying reason for this is that ER-PMSs in the worse channel condition tend to report channel quality indicator (CQI) 0 to PBSs which means the channel quality is too bad to support the lowest modulation and coding scheme. Therefore, we need to choose a set of RBs on which ER-PMSs can achieve the data rate to prevent the unnecessary RB allocation to them. In Table 3.4, the percentage of ER-PMSs which are not provided their minimum required data rate is listed. For NTPC, the percentage of ER-PMSs whose data rate is below the minimum required value ranges from 35% to 90%. Even though TPC-3 is applied, about 80% of ER-PMSs cannot reach the minimum required data rate in the cases of 16 dB and 0.6 Mbps. On the contrary, CSPC shows only less than 20% of ER-PMSs are not guaranteed their minimum required data rate.

Secondly, we discuss data rates of PMSs (i.e., all PMSs including ER-PMSs). The CDFs of PMSs' data rates are shown in Figure 3.3 (2 picocell case) and Figure 3.4 (4 picocell case). Based on these results, the detailed performance analysis will be performed.

Table 3.4: Percentage of ER-PMSs below the minimum required data rate

Case	***NTPC***	***TPC-3***	***CSPC***
2 picos, 8 dB, 0.4 Mbps	36.4%	16.6%	7.1%
0.6 Mbps	69.7%	39.4%	14.7%
2 picos, 16 dB, 0.4 Mbps	73.7%	56.2%	15.6%
0.6 Mbps	89.5%	76.1%	19.1%
4 picos, 8 dB, 0.4 Mbps	39.4%	12.7%	7.0%
0.6 Mbps	72.1%	38.7%	13.4%
4 picos, 16 dB, 0.4 Mbps	72.6%	54.8%	11.9%
0.6 Mbps	89.0%	76.8%	18.9%

Table 3.5: Comparison of PMSs' data rate (bps/Hz)

Case	***Metric***	***NTPC***	***TPC-3***	***CSPC 0.4 Mbps***	***CSPC 0.6 Mbps***
2 picos, 8 dB	Average	0.1876	0.2198	0.1945	0.1920
	Edge	0.0404	0.0585	0.0502	0.0568
2 picos, 16 dB	Average	0.1819	0.2174	0.1814	0.1865
	Edge	0.0227	0.0346	0.0447	0.0492
4 picos, 8 dB	Average	0.1813	0.2131	0.1863	0.1837
	Edge	0.0405	0.0589	0.0498	0.0542
4 picos, 16 dB	Average	0.1755	0.2138	0.1827	0.1795
	Edge	0.0235	0.0361	0.0447	0.0453

The average and edge (5%-tile) data rates of PMSs are listed in Table 3.5. Compared to NTPC, the proposed CSPC scheme shows about $3\% \sim 5\%$ performance improvement in the average rate, and in the edge rate the CSPC scheme shows about 25% and 80% performance improvements for 8 dB and 16 dB CRE bias offset, respectively. Compared to TPC-3, the proposed CSPC scheme shows about -15% degradation in the average rate for all cases due to the fact that TPC-3 reduces

about 8 times more transmit power than CSPC at the MBS. In the edge rate, TPC-3 shows about 10% $\sim$ 20% higher performance for the 8 dB CRE bias offset case, however it shows about -30% performance degradation compared to CSPC despite the large amount of reduced transmit power.

Lastly, we discuss data rates of MMSs of which CDFs are shown in Figure 3.5 (2 picocell case) and Figure 3.4 (4 picocell case). Based on these results, the detailed performance analysis will be performed.

Table 3.6: Comparison of MMSs' data rate (bps/Hz)

Case	***Metric***	***NTPC***	***TPC-3***	***CSPC 0.4 Mbps***	***CSPC 0.6 Mbps***
2 picos, 8 dB	Average	0.0943	0.0759	0.0924	0.0912
	Edge	0.0410	0.0287	0.0376	0.0381
2 picos, 16 dB	Average	0.0953	0.0770	0.0927	0.0902
	Edge	0.0392	0.0297	0.0367	0.0352
4 picos, 8 dB	Average	0.0927	0.0737	0.0885	0.0866
	Edge	0.0395	0.0290	0.0364	0.0357
4 picos, 16 dB	Average	0.0939	0.0755	0.0908	0.0875
	Edge	0.0393	0.0290	0.0374	0.0352

The average and edge (5%-tile) data rates of MMSs are listed in Table 3.6. Due to the large amount of transmit power reduction at the MBS (20 W out of 40 W), TPC-3 shows about -30% performance degradation in both average and edge rates compared to NTPC. In the CSPC case, about -10% performance degradation is shown in both average and edge rates compared to NTPC.

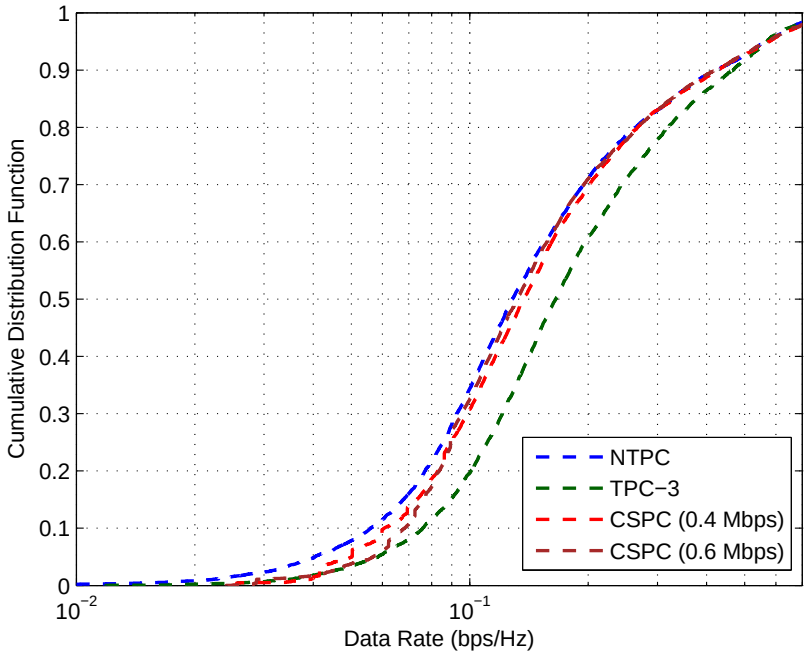

(a) 8 dB CRE bias

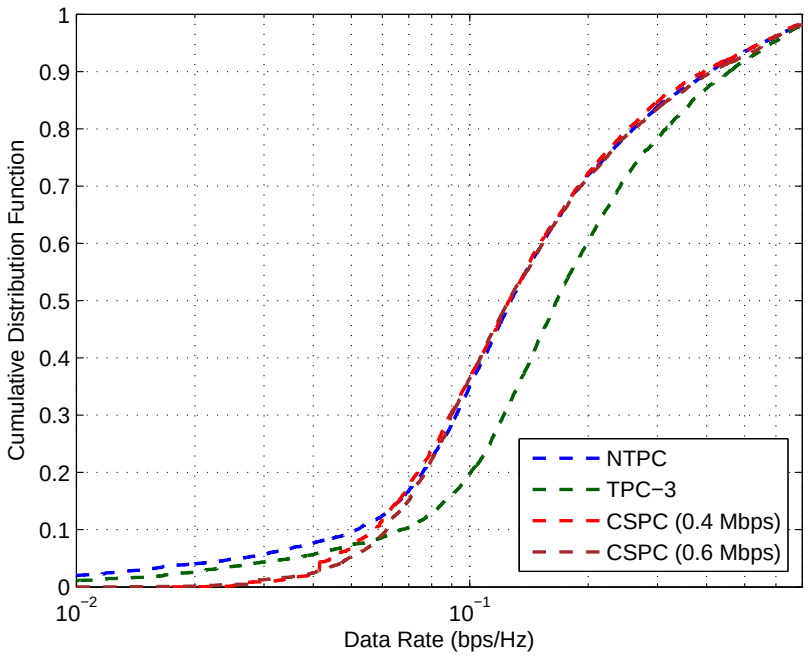

(b) 16 dB CRE bias

Figure 3.3: CDFs of PMSs' data rates (2 picocell case)

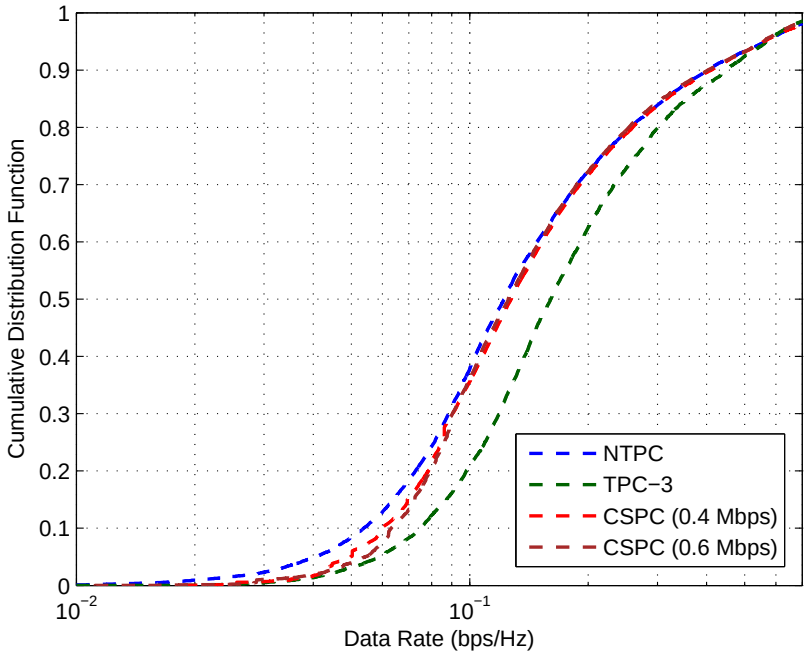

(a) 8 dB CRE bias

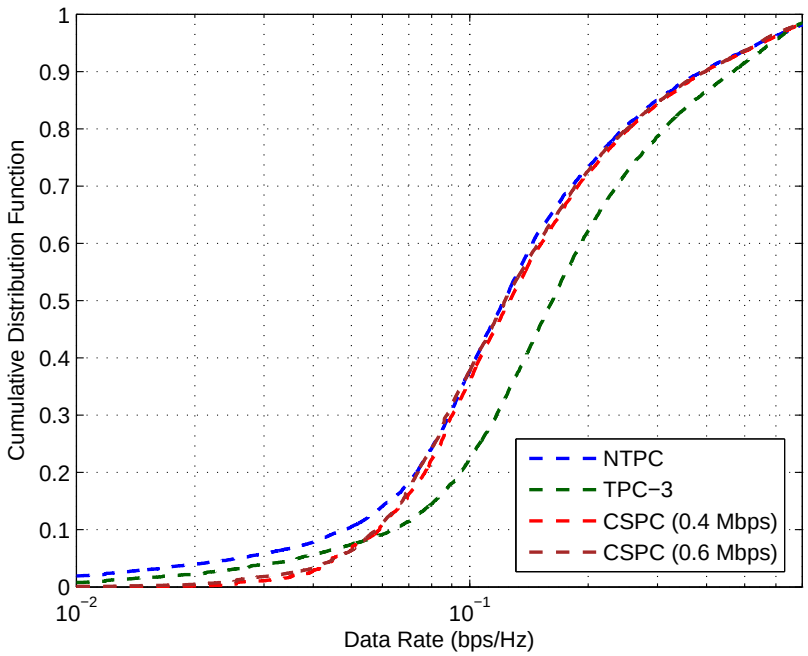

(b) 16 dB CRE bias

Figure 3.4: CDFs of PMSs' data rates (4 picocell case)

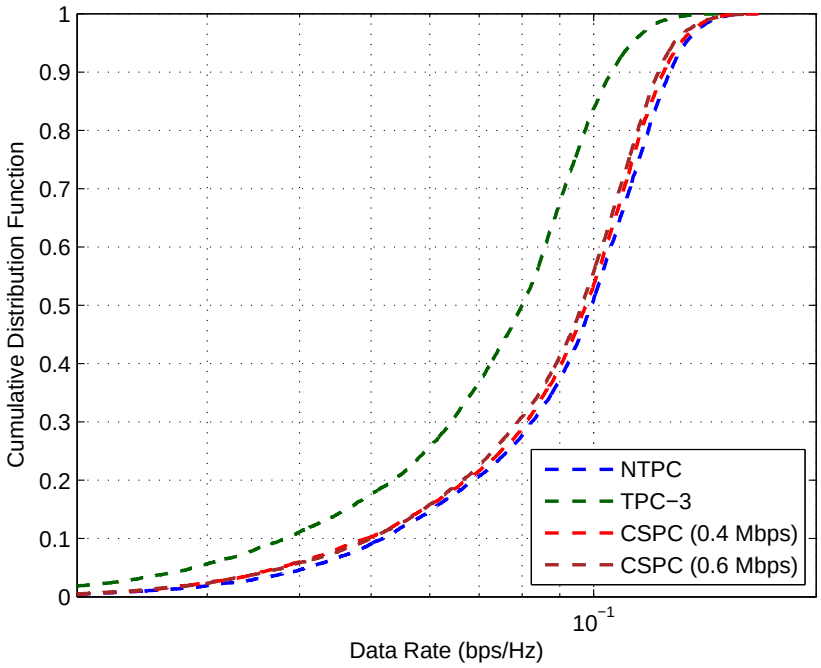

(a) 8 dB CRE bias

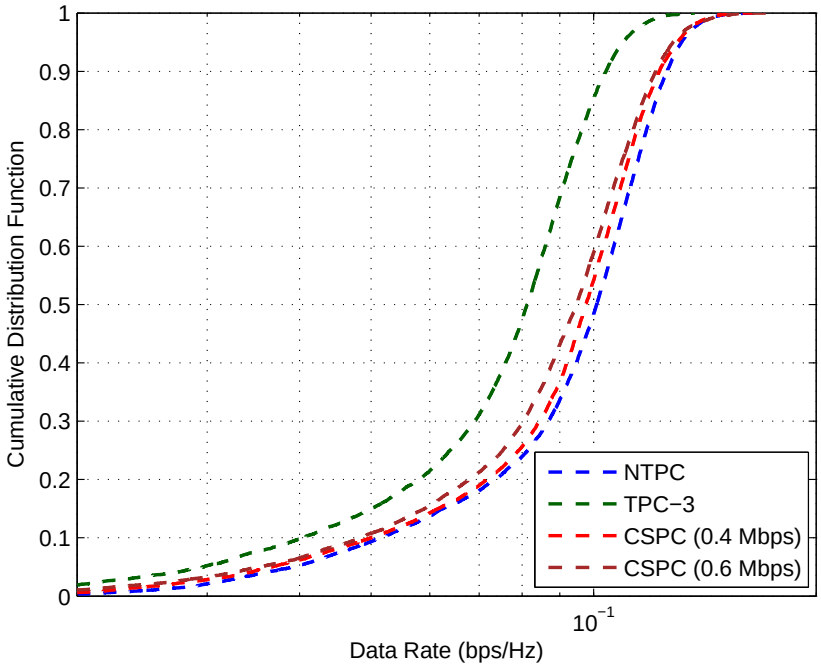

(b) 16 dB CRE bias

Figure 3.5: CDFs of MMSs' data rates (2 picocell case)

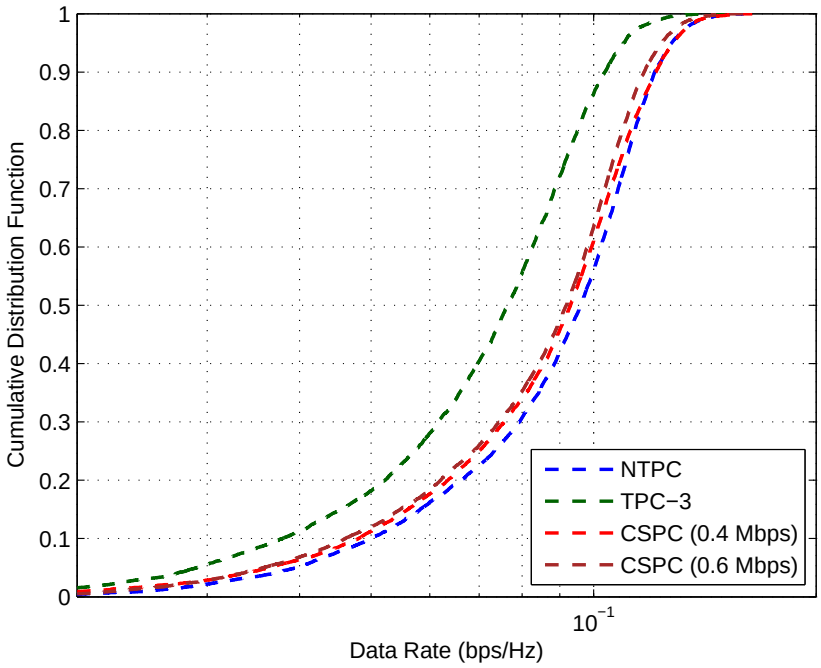

(a) 8 dB CRE bias

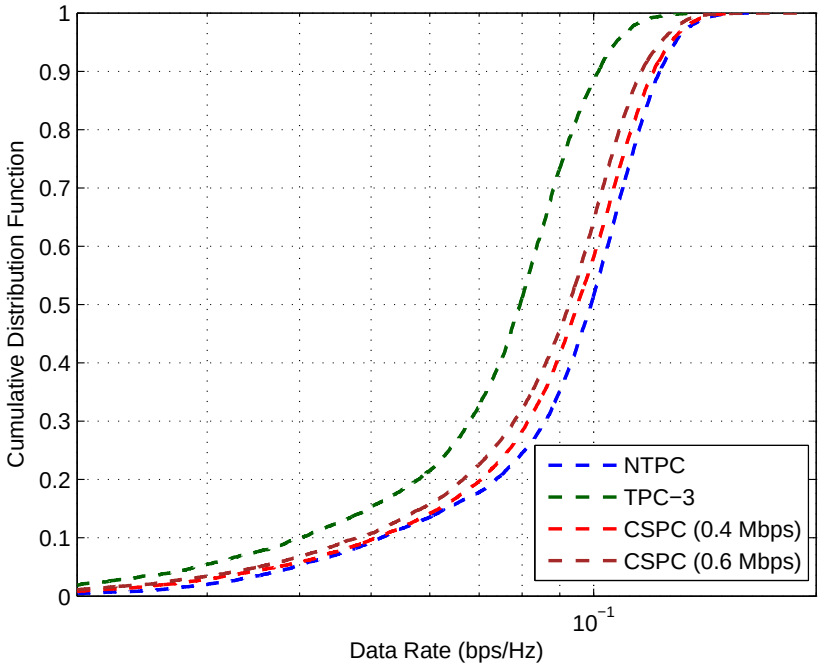

(b) 16 dB CRE bias

Figure 3.6: CDFs of MMSs' data rates (4 picocell case)

3.6 Summary and Future Work

In this chapter, we have discussed a frequency-domain transmit power reduction scheme for downlink cross-tier interference mitigation in heterogeneous cellular networks. By determining MBS's transmit power based on MMSs' required SINR and scheduling ER-PMSs onto the same group of RBs, we can minimize the possible throughput degradation of MMSs. To solve a binary integer programming problem, we propose a heuristic algorithm of which the worst case computational complexity is $O(PN \log PN)$ with marginal performance degradation compared to the optimal solution. Through system-level simulations, we have shown that the proposed coordinated scheduling and power control algorithm can provide the minimum required data rate to ER-PMSs with much less transmit power reduction than other schemes.

As future work, the following research items can be further studied.

- *Algorithm expansion to the multiple ER-PMSs in a picocell*
  - Based on an algorithm for a single ER-PMS per picocell in Algorithm 3.1, we can expand it to the case of multiple ER-PMSs per picocell. When one ER-PMS with the lowest satisfaction ratio is selected per picocell, then the RB selection can be done via Algorithm 3.1 for the single ER-PMS case.
- *Comparison with the RB-level transmit power nulling*
  - Due to the nature of discreteness of RBs, the RB-level transmit power nulling may require less RBs than the proposed algorithm which would

result in less MMSs' performance degradation.

Chapter 4: Time-domain Macrocell Transmit Power Nulling

4.1 Motivation

The time-domain macrocell transmit power nulling, which can be referred to as almost blank subframes based on 3GPP's terminology, can provide zero cross-tier interference from MBSs toward PMSs in a synchronous ABS operation mode in which all MBSs share the same ABS configuration parameters such as periodicity, start offset, and duration. Since an asynchronous ABS operation which allows different ABS configurations among MBSs is less effective for cross-tier interference mitigation as discussed in [36], only synchronous ABS operations are considered in this work.

The challenging issues arise here are how many ABSs should be configured for the network and how PMSs are scheduled onto ABS and non-ABS resources. For MMSs, their achievable throughput decreases as the number of ABSs increases because they can be only scheduled in non-ABSs.

There have been some work to find the optimal number of ABSs by formulating an optimization problem along with the PMS scheduling policy. In [36], the network-wide utility (the sum of MSs' utilities) maximization problem is formulated to find the optimal number of ABSs. The PMS scheduling policy is based on the PMS

categorization into one of two groups - *normal* and *victim*. The PMSs in the normal group are only scheduled in non-ABSs, and those in the victim group are only scheduled in ABSs. For every possible value of ABSs, every BS needs to calculate the sum of the associated MSs' utilities. Unlike MBSs of which MMSs are only scheduled to non-ABSs, PBSs need to find the best categorization of their PMSs into two groups and calculate the sum of utilities using a dynamic programming algorithm. Those utility values from BSs are signaled to a central coordinating entity so that the optimal number of ABSs that maximizes the network-wide utility is chosen. In [37], the minimization problem of the number of ABSs is formulated subject to ER-PMSs' minimum required data rate. The PMS scheduling policy is that ER-PMSs are scheduled in both ABSs and non-ABSs, and R-PMSs are only scheduled in non-ABSs. In other words, the ABS resource is exclusively available for ER-PMSs and the non-ABS resource is shared by both R-PMSs and ER-PMSs. The smallest number of ABSs is selected by which all ER-PMSs can achieve their minimum required data rate.

From the previous work, we could make two arguments. First, we believe that the configured ABSs should be allocated with higher priority to ER-PMSs in order to compensate their achievable rate degradation as in [37], because ER-PMSs are forced to be associated with PBSs by CRE operation even if they observe the stronger received signal strength from MBSs, and suffer from more severe cross-tier interference than R-PMSs do. Second, the optimal number of ABSs needs to be determined from a network point of view because the decision impacts multiple BSs in the network. As discussed in [36], the network-wide utility could be a good

objective function.

As a result, in this chapter, we formulate a utility maximization problem wherein the sum of the utilities of MMSs and R-PMSs is maximized with respect to the number of ABSs and PMS scheduling in ABSs and non-ABSs under the constraint of ER-PMSs' minimum required data rate. Unlike the MMS case where MMSs can be only scheduled in non-ABSs, the PMS scheduling is more complicated as there are four possible ways of scheduling R-PMSs and ER-PMSs onto ABSs and non-ABSs. Therefore, we first present a flexible PMS scheduling policy in which all four possible cases are incorporated, and the data rates of R-PMSs and ER-PMSs are derived based on the scheduling policy. To solve the optimization problem, we first propose an algorithm by which for a given number of ABSs each PBS maximizes the sum of utilities of their R-PMSs, and then the optimal number of ABSs can be found for which the total utility (MMSs and R-PMSs) is maximized.

4.2 System Model

The network model considered in this chapter is a heterogeneous downlink cellular network consisting of mutlipel MBSs and overlaid PBSs within those MBSs' coverage. Let us denote by $\mathcal{B}$ the set of BSs in the network, which is further classified into two disjoint subsets - MBS subset $\mathcal{B}_m$ and PBS subset $\mathcal{B}_p$. We denote by $\mathcal{U}_b$ the MS set of BS b, and if the BS is pico ($b \in \mathcal{B}_p$), the MS set is further divided into two subsets based on CRE bias as the R-PMS subset $\mathcal{U}_b^R$ and the ER-PMS subset $\mathcal{U}_b^{ER}$.

The average received signal-to-interference plus noise ratio (SINR) Γ_{bu} on non-ABSs and $\bar{\Gamma}_{bu}$ in ABSs at MS u from associated BS b are expressed respectively as

$$\begin{aligned} \Gamma_{ub} &= \frac{P_b h_{ub}}{\sum_{b' \in \mathcal{B}, b' \neq b} P_{b'} h_{ub'} + \sigma^2} \\ \bar{\Gamma}_{ub} &= \frac{P_b h_{ub}}{\sum_{b' \in \mathcal{B}^p, b' \neq b} P_{b'} h_{ub'} + \sigma^2} \end{aligned} \qquad \forall b \in \mathcal{B}\ \forall u \in \mathcal{U}_b, \tag{4.1}$$

where P_b is the transmit power of BS b, h_{ub} is the average channel gain of a link between MS u and BS b, and σ^2 is the power of additive white Gaussian noise. As mentioned earlier, we assume the synchronized ABS configuration among MBSs, therefore, there is no interference term from MBSs in ABSs. From the SINR expressions, we can derive the achievable link rates over the system bandwidth W using Shannon's equation as

$$\begin{aligned} c_{ub} &= W \log_2(1 + \Gamma_{ub}) \\ \bar{c}_{ub} &= W \log_2(1 + \bar{\Gamma}_{ub}) \end{aligned} \qquad \forall b \in \mathcal{B},\ \forall u \in \mathcal{U}_b. \tag{4.2}$$

Due to the transmit power nulling in MBSs, $\bar{\Gamma}_{ub}$ is zero for any MMS $u \in \mathcal{U}_b$ ($b \in \mathcal{B}_m$), therefore, $\bar{c}_{ub}$ becomes also zero:

$$P_b = 0 \ \rightarrow\ \bar{\Gamma}_{ub} = 0\ \ \&\ \ \bar{c}_{ub} = 0 \quad \forall b \in \mathcal{B}_m\ \ \forall u \in \mathcal{U}_b. \tag{4.3}$$

For the sake of flexible ABS resource management, the following MS scheduling policy will be assumed for our work.

- MMSs are only scheduled in non-ABSs.
- R-PMSs are scheduled in non-ABSs as a baseline. Exceptionally R-PMSs can be scheduled in ABSs only when the configured ABSs are large enough to support ER-PMSs so that the extra ABS resource is available for R-PMSs.

- ER-PMSs are scheduled in ABSs until their minimum required data rate is achieved. If the configured ABSs are not enough, then additional non-ABS resource is reserved for them.

4.3 Problem Formulation

With the MS scheduling policy introduced in the previous section, our objective is to maximize the aggregated utility of MMSs and R-PMSs while the minimum required data rate of ER-PMSs is satisfied. In this work, ER-PMSs are not included in the objective function to exclude any possible case where prioritized ER-PMSs could dominate the aggregated utility of all MSs. As a result, we can formulate an optimization problem as follows:

$$\max_{\alpha,\underline{\beta},\underline{\gamma}} \; U(\alpha,\underline{\beta},\underline{\gamma}) = \max_{\alpha,\underline{\beta},\underline{\gamma}} \; U_m(\alpha) + U_p^R(\alpha,\underline{\beta},\underline{\gamma}) \tag{4.4a}$$

$$\text{s.t. } \alpha \in \left\{0, \frac{1}{T}, \cdots, \frac{T-2}{T}, \frac{T-1}{T}\right\} \tag{4.4b}$$

$$r_{nj}(\alpha,\beta_{nj},\gamma_{nj}) \geq R_{nj} \qquad \forall j \in \mathcal{B}_p,\ \forall n \in \mathcal{U}_j^{ER} \tag{4.4c}$$

$$0 \leq \beta_{nj} \leq 1, \quad 0 \leq \gamma_{nj} \leq 1 \qquad \forall j \in \mathcal{B}_p,\ \forall n \in \mathcal{U}_j^{ER} \tag{4.4d}$$

$$\sum\nolimits_{n\in\mathcal{U}_j^{ER}} \beta_{nj} \leq 1,\ \sum\nolimits_{n\in\mathcal{U}_j^{ER}} \gamma_{nj} \leq 1 \qquad \forall j \in \mathcal{B}_p \tag{4.4e}$$

$$\left(1 - \sum\nolimits_{n'\in\mathcal{U}_j^{ER}} \beta_{n'j}\right) \gamma_{nj} = 0 \qquad \forall j \in \mathcal{B}_p,\ \forall n \in \mathcal{U}_j^{ER} \tag{4.4f}$$

where α is the normalized ABS ratio, R_{nj} is the minimum required data rate of ER-PMS n in PBS j, β_{nj} and γ_{nj} denote the normalized portion of resource allocated to ER-PMS n in PBS j in ABSs and on non-ABSs, respectively. $\underline{\beta}_j$, $\underline{\gamma}_j$, $\underline{\beta}$ and $\underline{\gamma}$ are

vectors of β_{nj}'s and γ_{nj}'s represented as follows:

$$\underline{\beta}_j = \left[\beta_{1j}, \beta_{2j}, \cdots, \beta_{|\mathcal{U}_j^{ER}|j}\right]^\top \quad \forall j \in \mathcal{B}_p \tag{4.5}$$

$$\underline{\gamma}_j = \left[\gamma_{1j}, \gamma_{2j}, \cdots, \gamma_{|\mathcal{U}_j^{ER}|j}\right]^\top \quad \forall j \in \mathcal{B}_p \tag{4.6}$$

$$\underline{\beta} = \left[\underline{\beta}_1^\top, \underline{\beta}_2^\top, \cdots, \underline{\beta}_{|\mathcal{B}_p|-1}^\top, \underline{\beta}_{|\mathcal{B}_p|}^\top\right]^\top \tag{4.7}$$

$$\underline{\gamma} = \left[\underline{\gamma}_1^\top, \underline{\gamma}_2^\top, \cdots, \underline{\gamma}_{|\mathcal{B}_p|-1}^\top, \underline{\gamma}_{|\mathcal{B}_p|}^\top\right]^\top. \tag{4.8}$$

The constraint in (4.4f) indicates that the non-ABS resource can be allocated to ER-PMSs only if the ABS resource is used up.

$U_m(\alpha)$ represents the aggregated utility of MMSs with ABS ratio α, which is derived as

$$U_m(\alpha) = \sum_{i \in \mathcal{B}_m} U_i(\alpha) = \sum_{i \in \mathcal{B}_m} \sum_{k \in \mathcal{U}_i} \log\left((1-\alpha) r_{ki}\right), \tag{4.9}$$

where the logarithmic utility function $\log(r)$ is used which is one of increasing, strictly concave, and continuously differential utility functions. r_{ki} is the average rate on non-ABSs that MMS k in MBS i could achieve under round-robin scheduling, which is expressed as $r_{ki} = c_{ki}/K_i$, where K_i is the number of MMSs in MBS i. The utility $U_m(\alpha)$ is a strictly decreasing function of α in which the portion of non-ABS resource $(1-\alpha)$ for MMSs decreases as α increases.

$U_p^R(\alpha, \underline{\beta}_j, \underline{\gamma}_j)$ represents the aggregated utility of R-PMSs with ABS ratio α and normalized ER-PMS resource allocation $\underline{\beta}_j$ in ABSs and $\underline{\gamma}_j$ in non-ABSs, which is derived as

$$\begin{aligned} U_p^R(\alpha, \underline{\beta}, \underline{\gamma}) &= \sum_{j \in \mathcal{B}_p} U_j^R(\alpha, \underline{\beta}_j, \underline{\gamma}_j) \\ &= \sum_{j \in \mathcal{B}_p} \sum_{l \in \mathcal{U}_j^R} \log\left(\alpha(1-\beta_j)\bar{r}_{lj} + (1-\alpha)(1-\gamma_j) r_{lj}\right) \end{aligned} \tag{4.10}$$

where β_j and γ_j denote the sum of β_{nj}'s ($= \sum_{n \in \mathcal{U}_j^{ER}} \beta_{nj}$) and γ_{nj}'s ($= \sum_{n \in \mathcal{U}_j^{ER}} \gamma_{nj}$), respectively, and $\bar{r}_{lj}$ is the average rate in ABSs that R-PMS l in PBS j could achieve under round-robin scheduling, which is expressed as $\bar{r}_{lj} = \bar{c}_{lj}/K_j$, where K_j is the number of R-PMSs in PBS j. Depending on ER-PMS allocation (β_j and γ_j), the available resource for R-PMSs in PBS j is determined accordingly.

$r_{nj}(\alpha, \beta_{nj}, \gamma_{nj})$ represents the data rate of ER-PMS n in PBS j with ABS ratio α, and allocated resource portion β_{nj} in ABSs and γ_{nj} in non-ABSs. $r_{nj}(\alpha, \beta_{nj}, \gamma_{nj})$ can be derived as

$$r_{nj}(\alpha, \beta_{nj}, \gamma_{nj}) = \alpha \beta_{nj} \bar{c}_{nj} + (1 - \alpha) \gamma_{nj} c_{nj}. \tag{4.11}$$

4.4 Problem Solving

From the formulated optimization problem in (4.4), we can observe that, for a fixed ABS ratio $\alpha' \in \left\{0, \frac{1}{T}, \cdots, \frac{T-1}{T}\right\}$, the optimization problem in (4.4) can be transformed into multiple independent optimization problems for PBSs where each PBS tries to maximize the available resource for R-PMSs by configuring ER-PMSs' resource allocation $\underline{\beta}$ and $\underline{\gamma}$ in (4.10) with constraints of (4.4c), (4.4d), (4.4e), and (4.4f). Since ER-PMSs are scheduled in ABSs with a higher priority than R-PMSs until they achieve their minimum required rates, we can categorize the PBS set $\mathcal{B}_p$ into two disjoint subsets $\mathcal{B}_p^+(\alpha')$ and $\mathcal{B}_p^-(\alpha')$ depending on whether the given ABS ratio α' is enough to support ER-PMSs or not.

In order to discuss the above two subsets in detail, let us first define δ_{nj} which is the amount of ABS resource for ER-PMS n in PBS j to achieve its minimum

required data rate R_{nj}, and is expressed as

$$\delta_{nj} = \frac{R_{nj}}{\bar{c}_{nj}} \qquad \forall j \in \mathcal{B}_p \;\; \forall n \in \mathcal{U}_j^{ER}. \tag{4.12}$$

Then PBS j would need the ABS resource δ_j in total as

$$\delta_j = \sum_{n \in \mathcal{U}_j^{ER}} \delta_{nj} \qquad \forall j \in \mathcal{B}_p. \tag{4.13}$$

With δ_j's and α', we can define $\mathcal{B}_p^+(\alpha')$ and $\mathcal{B}_p^-(\alpha')$ as

$$\begin{aligned} \mathcal{B}_p^+(\alpha') &= \{j \in \mathcal{B}_p : \alpha' - \delta_j \geq 0\} \\ \mathcal{B}_p^-(\alpha') &= \{j \in \mathcal{B}_p : \alpha' - \delta_j < 0\}. \end{aligned} \tag{4.14}$$

For PBS $j \in \mathcal{B}_p^+(\alpha')$, α' is large enough to satisfy ER-PMSs' minimum required data rate, so that we can derive the optimal $\underline{\beta}_j^*(\alpha')$ and $\underline{\gamma}_j^*(\alpha')$ as

$$\begin{aligned} \underline{\beta}_j^*(\alpha') &= \left[\frac{\delta_{1j}}{\alpha'}, \frac{\delta_{2j}}{\alpha'}, \cdots, \frac{\delta_{|\mathcal{U}_j^{ER}|j}}{\alpha'}\right] \\ \underline{\gamma}_j^*(\alpha') &= [0, 0, \cdots, 0, 0], \end{aligned} \tag{4.15}$$

respectively. Therefore, $U_j^R(\alpha', \underline{\beta}_j^*, \underline{\gamma}_j^*)$ can be represented as

$$U_j^R(\alpha', \underline{\beta}_j^*(\alpha'), \underline{\gamma}_j^*(\alpha')) = \sum_{l \in \mathcal{U}_j^R} \log\left((\alpha' - \delta_j)\bar{r}_{lj} + (1 - \alpha')r_{lj}\right) \qquad \forall j \in \mathcal{B}_p^+(\alpha'), \tag{4.16}$$

where it is observed that the additional ABS resource $(\alpha' - \delta_j)$ is allocated to R-PMSs, which will improve the utility as α' increases since $\bar{r}_{lj} > r_{lj}$ for all l.

For PBS $j \in \mathcal{B}_p^-(\alpha')$, α' is not enough so that one or more ER-PMSs cannot reach their minimum required data rate even if the entire α' is allocated to ER-PMSs, i.e., $\sum_{n \in \mathcal{U}_j^{ER}} \beta_{nj} = 1$. Let $\bar{\delta}_{nj}$ denote the amount of additional non-ABS resource needed for ER-PMS n in PBS j to achieve its minimum required data

rate. From (4.4c) and (4.11), we can derive the condition for ER-PMSs' minimum required data rate as

$$\bar{\delta}_{nj} = (1-\alpha')\gamma_{nj} \geq \frac{R_{nj} - \alpha'\beta_{nj}\bar{c}_{nj}}{c_{nj}} \qquad \forall n \in \mathcal{U}_j^{ER}, \tag{4.17}$$

and the corresponding $U_j^R(\alpha', \underline{\beta}_j, \underline{\gamma}_j)$ becomes

$$U_j^R(\alpha', \underline{\beta}_j, \underline{\gamma}_j) = \sum_{l \in \mathcal{U}_j^R} \log\left(\left(1-\alpha'-\bar{\delta}_j\right) r_{lj}\right) \qquad \forall j \in \mathcal{B}_p^-(\alpha'), \tag{4.18}$$

where $\bar{\delta}_j$ is the sum of additional non-ABS resource for ER-PMSs in PBS j ($= \sum_{n \in \mathcal{U}_j^{ER}} \bar{\delta}_{nj}$). Therefore, the maximization of $U_j^R(\alpha', \underline{\beta}_j, \underline{\gamma}_j)$ for PBS $j \in \mathcal{B}_p^-(\alpha')$ can be transformed into the minimization of δ_j with respect to $\underline{\beta}_j$ with the equality condition in (4.17) as

$$\max_{\underline{\beta}_j, \underline{\gamma}_j} U_j^R(\alpha', \underline{\beta}_j, \underline{\gamma}_j) = \min_{\underline{\beta}_j} \bar{\delta}_j = \min_{\underline{\beta}_j} \sum_{n \in \mathcal{U}_j^{ER}} \bar{\delta}_{nj}$$

$$= \min_{\underline{\beta}_j} \sum_{n \in \mathcal{U}_j^{ER}} \frac{R_{nj} - \alpha'\beta_{nj}\bar{c}_{nj}}{c_{nj}} = \max_{\underline{\beta}_j} \sum_{n \in \mathcal{U}_j^{ER}} a_{nj}\beta_{nj} \tag{4.19a}$$

$$\text{s.t.} \sum_{n \in \mathcal{U}_j^{ER}} \beta_{nj} = 1, \quad 0 \leq \beta_{nj} \leq 1 \quad \forall n \in \mathcal{U}_j^{ER} \tag{4.19b}$$

$$\sum_{n \in \mathcal{U}_j^{ER}} \frac{R_{nj} - \alpha'\beta_{nj}\bar{c}_{nj}}{c_{nj}} \leq (1-\alpha') \tag{4.19c}$$

where a_{nj} is the ratio between $\bar{c}_{nj}$ and c_{nj} ($= \bar{c}_{nj}/c_{nj}$). This problem can be seen as a weighted-sum maximization where ER-PMSs are listed in the decreasing order of a_{nj}'s, and the ABS resource α' is allocated to ER-PMSs from the top of the list to the bottom until ER-PMSs reach their minimum required data rate or the ABS resource is used up. Algorithm 4.1 shows how this operation is performed. By Algorithm 4.1, ER-PMSs in PBS j are categorized into one of three disjoint subsets,

$\mathcal{U}_j^{ER,f}(\alpha')$, $\mathcal{U}_j^{ER,p}(\alpha')$, and $\mathcal{U}_j^{ER,n}(\alpha')$, and have the corresponding $\beta_{nj}^*(\alpha')$'s as

$$\beta_{nj}^*(\alpha') = \begin{cases} \dfrac{R_{nj}}{\alpha' \bar{c}_{nj}} & \text{if } n \in \mathcal{U}_j^{ER,f}(\alpha') \\ 1 - \dfrac{1}{\alpha'} \sum_{n' \in \mathcal{U}_j^{ER,f}} \dfrac{R_{n'j}}{\bar{c}_{n'j}} & \text{if } n \in \mathcal{U}_j^{ER,p}(\alpha') \\ 0 & \text{if } n \in \mathcal{U}_j^{ER,n}(\alpha'), \end{cases} \tag{4.20}$$

respectively, where the superscripts f, p, and n indicate whether the ABS resource α' is allocated to ER-PMSs in those subsets with respect to the minimum required data rate *fully*, *partially*, and *not at all*, respectively. Since the algorithm allocates the ABS resource to a single ER-PMS in each iteration, the number of ER-PMSs in $\mathcal{U}_j^{ER,p}(\alpha')$ is always either 0 or 1. After finding an optimal $\beta_{nj}^*(\alpha')$, the corresponding $\gamma_{nj}^*(\alpha')$ and $\bar{\delta}_{nj}^*(\alpha')$ can be obtained as

$$\begin{aligned} \gamma_{nj}^*(\alpha') &= \frac{R_{nj} - \alpha' \beta_{nj}^*(\alpha') \bar{c}_{nj}}{(1-\alpha') c_{nj}} \\ \bar{\delta}_{nj}^*(\alpha') &= \frac{R_{nj} - \alpha' \beta_{nj}^*(\alpha') \bar{c}_{nj}}{c_{nj}} \end{aligned} \quad \forall n \in \mathcal{U}_j^{ER}, \tag{4.21}$$

respectively. For any ABS ratio $\alpha' \in \left\{0, \frac{1}{T}, \cdots, \frac{T-2}{T}, \frac{T-1}{T}\right\}$, therefore, the maximum utility $U_j^R(\alpha', \underline{\beta}_j^*(\alpha'), \underline{\gamma}_j^*(\alpha))$ of PBS j is derived as

$$U_j^R(\alpha', \underline{\beta}_j^*(\alpha'), \underline{\gamma}_j^*(\alpha')) = \begin{cases} \sum_{l \in \mathcal{U}_j^R} \log\left((\alpha' - \delta_j)\bar{r}_{lj} + (1-\alpha') r_{lj}\right) & \text{if } \alpha' \geq \delta_j \\ \sum_{l \in \mathcal{U}_j^R} \log\left(\left(1 - \alpha' - \bar{\delta}_j^*(\alpha')\right) r_{lj}\right) & \text{if } \alpha' < \delta_j, \end{cases} \tag{4.22}$$

where $\bar{\delta}_j^*(\alpha')$ is calculated as $\sum_{n \in \mathcal{U}_j^{ER}} \bar{\delta}_{nj}^*(\alpha')$. It is noted that the utility in (4.22) is a monotonically increasing function with respect to α'.

Based on Eq. (4.9) and (4.22), each BS can calculate the maximum utility for every $\alpha \in \left\{0, \frac{1}{T}, \cdots, \frac{T-2}{T}, \frac{T-1}{T}\right\}$. Suppose there exists a central coordinating

Algorithm 4.1 Optimal allocation $\underline{\beta}_j^*(\alpha')$ for PBS $j \in \mathcal{B}_p^-(\alpha')$

Initialization $\quad p = \alpha'; \;\; \mathcal{P} = \mathcal{U}_j^{ER}; \;\; \beta_{nj} = 0 \;\; \forall n \in \mathcal{U}_j^{ER}$

while $p > 0$ **do**

Find an ER-PMS n^* with the largest a_{nj}

$$n^* = \arg\max_{n \in \mathcal{P}} \; a_{nj} = \arg\max_{n \in \mathcal{P}} \; \frac{\bar{c}_{nj}}{c_{nj}}$$

if p is sufficient for ER-PMS n^* $\left(p \geq \frac{R_{nj^*}}{\bar{c}_{nj^*}}\right)$ **then**

Update $\beta_{nj^*}^*(\alpha')$, p, and $\mathcal{P}$

$$\beta_{n^*j}^*(\alpha') = \frac{R_{n^*j}}{\alpha' \bar{c}_{n^*j}}, \quad p = p - \frac{R_{n^*j}}{\bar{c}_{n^*j}}, \quad \mathcal{P} = \mathcal{P} - \{n^*\}$$

else

Update $\beta_{n^*j}^*(\alpha')$ and p

$$\beta_{n^*j}^*(\alpha') = \frac{p}{\alpha'}, \quad p = 0$$

end if

end while

entity which could be an MBS or other network controller. The BSs need to report their utility values to the entity so that the optimal ABS ratio α^* can be obtained which maximizes the aggregated utility of MMSs and R-PMSs. According to 3GPP specifications, the periodicity T of ABS operation is set to be 40 subframes, therefore each report message from BSs would contain 40 utility values, which could incur signaling overhead depending on the ABS coordination frequency or the backhaul condition. To further reduce the report size, the central coordinating entity could specify the range of α values. As shown in Figure 4.1 and Figure 4.1, the proposed

scheme provides a relatively small difference ($10 \sim 15$ subframes, or $\frac{1}{4} \sim \frac{1}{3}$ in ABS ratio) between the maximum and minimum of α^*, so the report message size can be reduced by about 30%.

4.5 Performance Evaluation

In this section, we demonstrate the performance of the proposed scheme through simulations. The heterogeneous network deployment is constructed as follows. The macro-tier consists of 7 MBSs each of which is three-sectorized (i.e., 21 macrocells), and outdoor omni-directional picocells are uniformly distributed in each macrocell's coverage. To obtain two achievable link rates c_{ub} and $\bar{c}_{ub}$, instead of using Shannon's formula, we calculate the bit rates based on channel quality indicators (CQIs) fed back from MSs in the system level simulator developed based on the LTE downlink system level simulator in [61]. The detailed parameters are described in Table 4.1, most of which are adopted from 3GPP's system level simulation parameters in [62], [63], [64].

For the performance evaluation, the following schemes are compared through numerical simulations.

- *Proposed scheme*: ER-PMSs in a PBS are prioritized for ABS resource until they are provided their minimum required data rate. If ABS resource is not sufficient, non-ABS resource is reserved. If ABS resource is sufficient, the extra ABS resource is allocated to R-PMSs.

- *ER-PMSs to ABSs only (EtA)*: ER-PMSs and R-PMSs are exclusively sched-

Table 4.1: Simulation Parameters

Simulation Parameter	***Value***
Number of simulations per scenario	400
Carrier frequency	2.0 GHz
System bandwidth	10 MHz
Antenna configuration	SISO
Channel model	Typical Urban (TU)
Inter-site distance	750 m
Noise power spectral density	-174 dBm/Hz
ABS periodicity (T)	40 subframes
Number of macrocells	21 (7 three-sectorized MBSs)
Macrocell transmit power	40 W (46 dBm)
Macrocell path loss model	$128.1 + 37.6\log_{10} R$ (R in km)
Macrocell shadowing model	Log normal fading with std. 10 dB
Macrocell antenna gain	15 dBi
Number of MMSs per sector	30
Picocell transmit power	1 W (30 dBm)
Picocell path loss model	$140.7 + 36.7\log_{10} R$ (R in km)
Picocell shadowing model	Log normal fading with std. 6 dB
Picocell antenna gain	5 dBi
Number of PMSs per picocell	10 (7 R-PMSs and 3 ER-PMSs)
Min. distance MBS-PBS	75 m
Min. distance PBS-PBS	50 m
Number of picocells per macrocell	2 / 4
CRE bias offset	8 / 16 dB
Minimum required data rate for ER-PMSs	0.2 / 0.4 Mbps

uled in ABSs and non-ABSs, respectively, in a round-robin manner.

- *ER-PMSs to ABSs & non-ABSs (EtA_nA)*: ABSs are exclusively scheduled to

ER-PMSs, and non-ABSs are scheduled to both ER-PMSs and R-PMSs, in a round-robin manner for both cases.

In case of EtA and EtA_nA schemes, the optimal α^* is determined as the minimum value of $\alpha \in \left\{0, \frac{1}{T}, \cdots, \frac{T-2}{T}, \frac{T-1}{T}\right\}$ for which all ER-PMSs achieve their minimum required data rate. We compare the performance of the above three schemes for two ER-PMSs' minimum required data rates, 0.2 Mbps and 0.4 Mbps.

Table 4.2: Average ABS Ratio α^*

Case	**Prop.**	**EtA**	**EtA_nA**
2 picos, 8 dB, 0.2 Mbps	0.12	0.13	0.05
2 picos, 16 dB, 0.2 Mbps	0.13	0.17	0.08
4 picos, 8 dB, 0.2 Mbps	0.27	0.18	0.08
4 picos, 16 dB, 0.2 Mbps	0.28	0.22	0.11
2 picos, 8 dB, 0.4 Mbps	0.15	0.25	0.18
2 picos, 16 dB, 0.4 Mbps	0.16	0.32	0.25
4 picos, 8 dB, 0.4 Mbps	0.31	0.37	0.28
4 picos, 16 dB, 0.4 Mbps	0.32	0.43	0.36

Firstly, we discuss the network-wide performance with respect to the ABS ratio α. In Table 4.2, the average ABS ratio α^* is listed. When the CRE bias increases from 8 dB to 16 dB, the proposed scheme requires only about 5% more ABS resource, whereas EtA and EtA_nA require about 50% more ABS resource which results in the performance degradation of both MMSs and R-PMSs. Similarly, when the minimum required data rate increases from 0.2 Mbps to 0.4 Mbps, the proposed scheme requires only about 20% more ABS resource, whereas EtA and EtA_nA require about 70% $\sim$ 80% more. This is caused by the round-robin scheduling

among ER-PMSs which would require much more ABS resource to satisfy the ER-PMS in the worst channel condition. When the number of picocells increases from 2 to 4, the ABS ratio of the proposed scheme requires about 100% more ABS resource, whereas than EtA and EtA_nA require about 50% more. Even though the proposed scheme uses more ABS resource, it should be noted that for each picocell the extra ABS resource ($\alpha^* - \delta_j$) is distributed to R-PMSs so that the total utility of MMSs+R-PMSs would be improved due to doubled R-PMSs in the network.

In Figure 4.1 and Figure 4.2, the CDFs of optimal ABS ratio α^* are shown. Noticeably, it is observed that EtA and EtA_nA require about two times more ABS resource than the proposed scheme does in 90%-ile or above. About 50% or more ABS resource should be allocated to ER-PMSs for EtA and EtA_nA, and it causes a significant performance degradation for MMSs and R-PMSs which can be allocated only to non-ABSs.

In Table 4.3, the mean of the average utility per MS is listed. For the MMSs+R-PMSs case, the proposed scheme shows about 2% and 5% performance gain over EtA and EtA_nA for 0.2 Mbps and 0.4 Mbps cases, respectively. For the all MSs case (MMSs+R-PMSs+ER-PMSs), the proposed scheme shows about -1% lower utility value as the average utility of ER-PMSs is lower than that of MMSs+R-PMSs, i.e., 9.95 for 0.2 Mbps and 10.64 for 0.4 Mbps. However, EtA and EtA_nA show about 3% higher utility value which indicates ER-PMSs achieve much higher data rate than MMSs and R-PMSs. Noticeably, for the 0.4 Mbps case, the proposed scheme shows about 2% higher utility than EtA and EtA_nA.

In Figure 4.3 and Figure 4.4, the CDFs of the average utility per MS (MMSs+R-

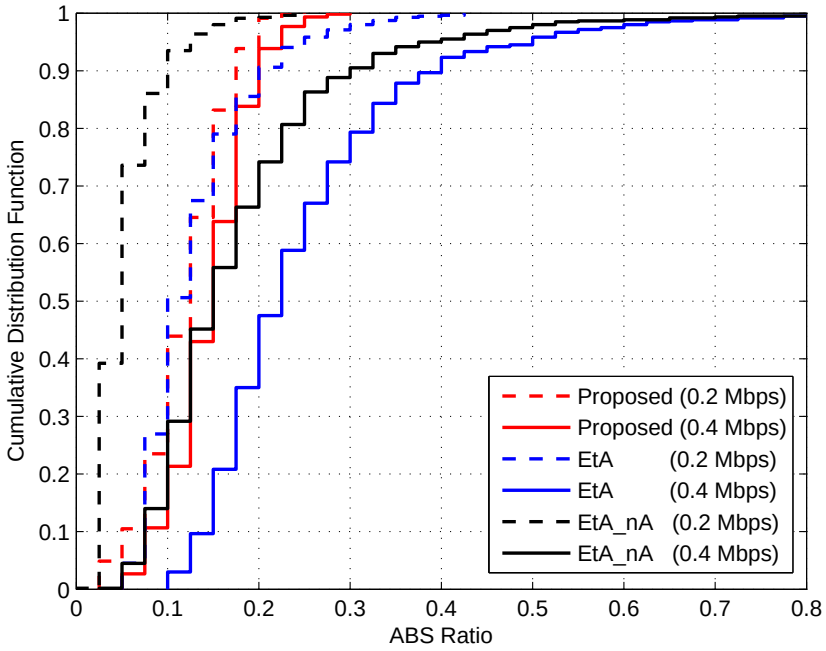

(a) 2 picocells, 8 dB CRE bias

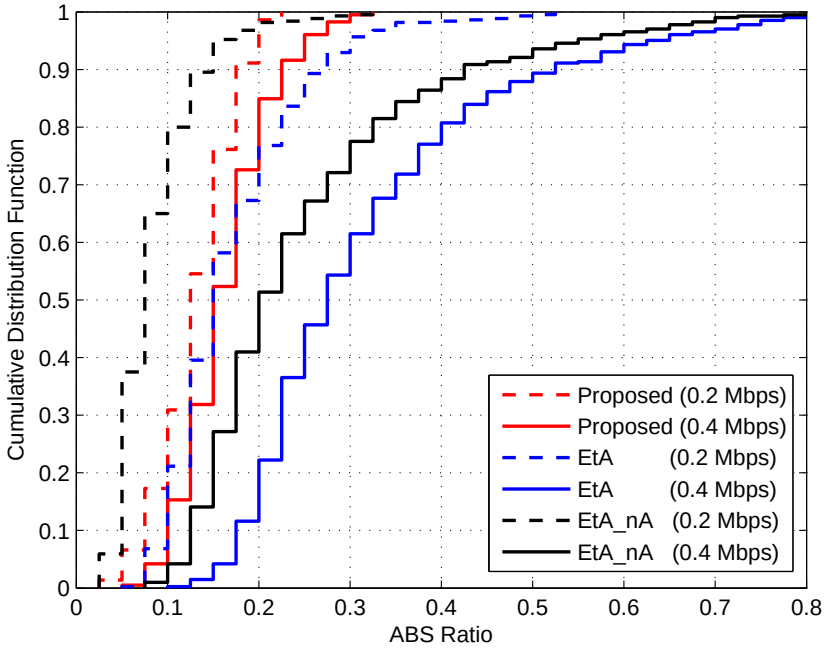

(b) 2 picocells,16 dB CRE bias

Figure 4.1: CDFs of optimal ABS ratio α^* (2 picocells)

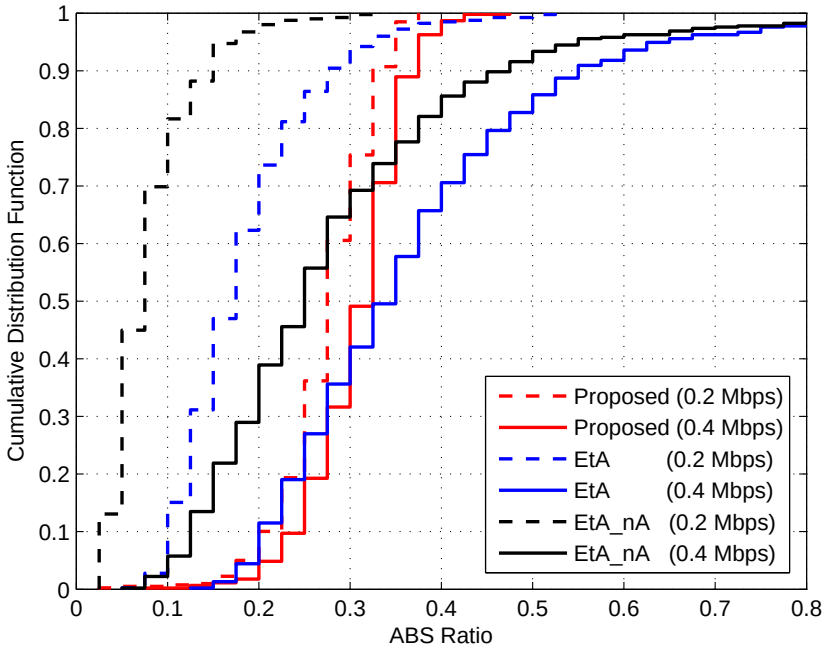

(a) 8 dB CRE bias

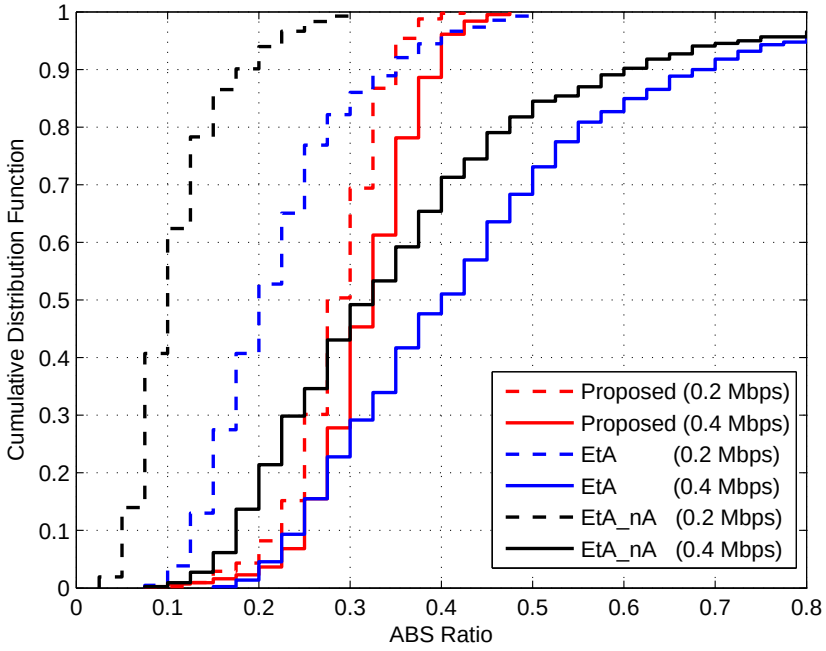

(b) 16 dB CRE bias

Figure 4.2: CDFs of optimal ABS ratio α^* (4 picocells)

Table 4.3: Mean of Average Utility Per MS

MS Type	Case	Prop.	EtA	EtA_nA
MMSs+R-PMSs	2 picos, 8 dB, 0.2 Mbps	13.43	13.28	13.25
	2 picos, 16 dB, 0.2 Mbps	13.42	13.24	13.23
	4 picos, 8 dB, 0.2 Mbps	13.66	13.38	13.33
	4 picos, 16 dB, 0.2 Mbps	13.65	13.35	13.31
	2 picos, 8 dB, 0.4 Mbps	13.38	13.10	13.08
	2 picos, 16 dB, 0.4 Mbps	13.37	13.01	13.00
	4 picos, 8 dB, 0.4 Mbps	13.60	13.06	13.02
	4 picos, 16 dB, 0.4 Mbps	13.58	12.95	12.92
All MSs	2 picos, 8 dB, 0.2 Mbps	13.28	13.35	13.28
	2 picos, 16 dB, 0.2 Mbps	13.28	13.32	13.26
	4 picos, 8 dB, 0.2 Mbps	13.42	13.49	13.38
	4 picos, 16 dB, 0.2 Mbps	13.42	13.46	13.36
	2 picos, 8 dB, 0.4 Mbps	13.33	13.28	13.24
	2 picos, 16 dB, 0.4 Mbps	13.33	13.20	13.17
	4 picos, 8 dB, 0.4 Mbps	13.49	13.34	13.28
	4 picos, 16 dB, 0.4 Mbps	13.48	13.25	13.20

PMSs) are shown. Comparing the 5%-ile average utility values, we can observe about -3% $\sim$ -2% degradation for the 0.2 Mbps case and about -10% $\sim$ -7% degradation for the 0.4 Mbps case, which is much larger gap than the mean value in Table 4.3.

Lastly, we discuss the performance from the MS point of view through Table 4.4 and Figure 4.5 through Figure 4.8. In Table 4.4, the mean and edge (5%-ile) data rates of MSs are compared.

Focusing first on data rates of MMSs+R-PMSs, the mean rate of the proposed scheme shows about 20% $\sim$ 120% performance gain over EtA and EtA_nA. As the minimum required data rate and/or the number of picocells increases, the

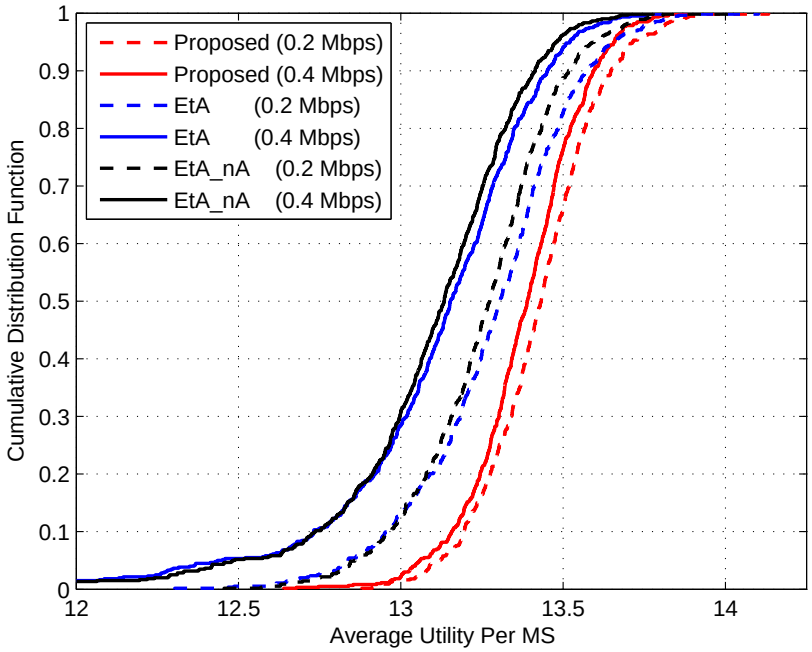

(a) 8 dB CRE bias

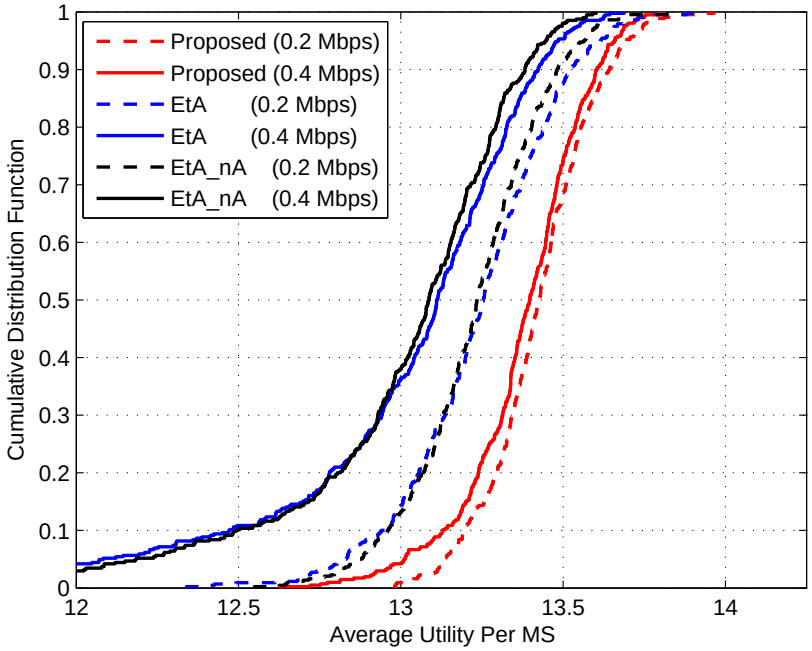

(b) 16 dB CRE bias

Figure 4.3: CDFs of average utility per MS (MMSs+R-PMSs, 2 picocells)

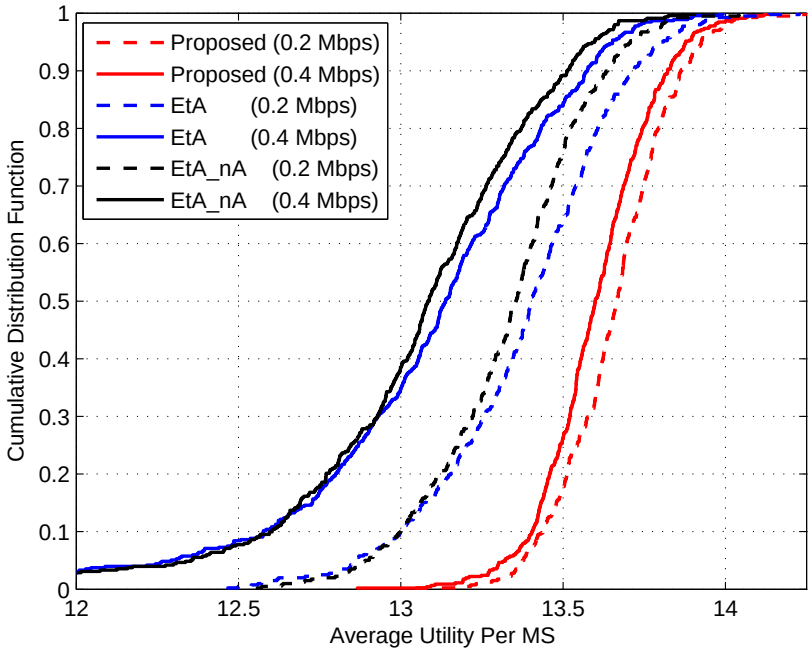

(a) 8 dB CRE bias

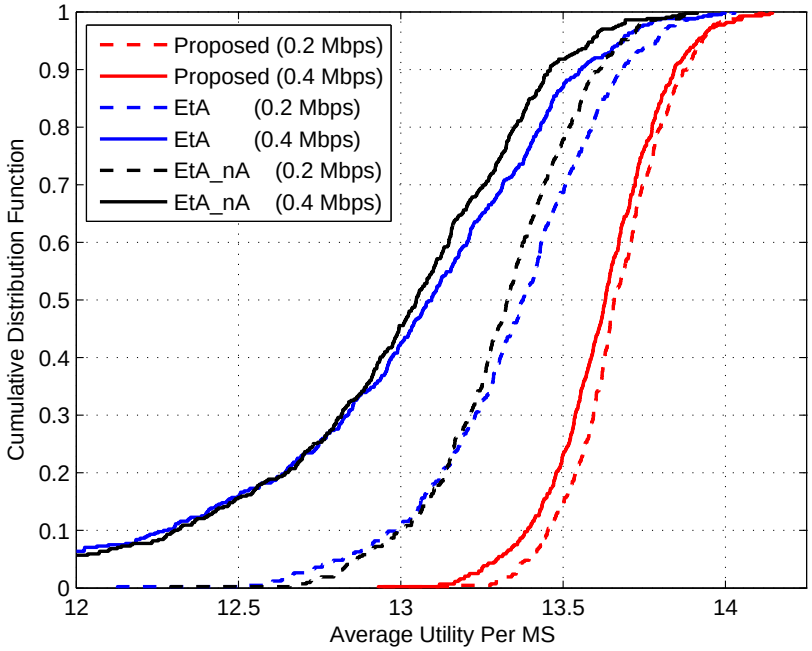

(b) 16 dB CRE bias

Figure 4.4: CDFs of average utility per MS (MMSs+R-PMSs, 4 picocells)

Table 4.4: MS Data Rate (bps/Hz)

MS Type	Case (pico/CRE/target)	Mean			Edge		
		Prop.	EtA	EtA_nA	Prop.	EtA	EtA_nA
MMSs +R-PMSs	2 / 8 / 0.2	0.1061	0.0888	0.0783	0.0147	0.0143	0.0148
	2 / 16 / 0.2	0.1050	0.0842	0.0757	0.0150	0.0139	0.0147
	4 / 8 / 0.2	0.1482	0.1012	0.0875	0.0134	0.0141	0.0146
	4 / 16 / 0.2	0.1468	0.0967	0.0851	0.0140	0.0139	0.0146
	2 / 8 / 0.4	0.1016	0.0755	0.0673	0.0141	0.0110	0.0117
	2 / 16 / 0.4	0.1007	0.0699	0.0625	0.0142	0.0093	0.0101
	4 / 8 / 0.4	0.1421	0.0784	0.0685	0.0124	0.0084	0.0091
	4 / 16 / 0.4	0.1415	0.0725	0.0633	0.0133	0.0065	0.0073
All MSs	2 / 8 / 0.2	0.0959	0.0939	0.0794	0.0156	0.0151	0.0157
	2 / 16 / 0.2	0.0950	0.0916	0.0777	0.0159	0.0147	0.0155
	4 / 8 / 0.2	0.1264	0.1104	0.0895	0.0147	0.0153	0.0158
	4 / 16 / 0.2	0.1252	0.1069	0.0873	0.0153	0.0151	0.0159
	2 / 8 / 0.4	0.0944	0.0969	0.0843	0.0149	0.0118	0.0125
	2 / 16 / 0.4	0.0937	0.0937	0.0823	0.0151	0.0101	0.0109
	4 / 8 / 0.4	0.1249	0.1183	0.1015	0.0136	0.0095	0.0101
	4 / 16 / 0.4	0.1244	0.1130	0.0986	0.0146	0.0075	0.0083

performance gap becomes larger. It is noted that the mean rate of EtA is about 10% higher than that of EtA_nA due to the fact that ER-PMSs in EtA_nA are also scheduled in non-ABSs in a round-robin manner along with R-PMSs. Even if EtA_nA requires a less number of ABSs by allowing ER-PMSs to be scheduled in non-ABSs, this scheduling policy eventually degrades R-PMSs' data rate so that the mean rate of EtA_nA is worse than that of EtA. Since the number of MMSs is about three times of that of R-PMSs in a picocell, the impact of MMSs' throughput gain by having a less number of ABSs is small from the perspective of the mean

rate. However, in the edge rate, EtA_nA shows the higher rate than EtA due to the smaller number of ABSs.

Then, focusing on data rates of all MSs (MMSs+R-PMSs+ER-PMSs), the proposed scheme shows about 2% $\sim$ 40% performance gain over EtA and EtA_nA. Compared to the mean rate, the performance gap reduces due to the fact that ER-PMSs in EtA and EtA_nA achieve much higher data rates than those in the proposed scheme as shown in Figure 4.7 and Figure 4.8. As a result, the mean data rates of all MSs in EtA and EtA_nA are higher than those of MMSs+R-PMSs.

In Figure 4.5 and Figure 4.6, the CDFs of data rates of MMSs+R-PMSs are shown. At a first glance, the performance gap of the proposed scheme by increasing the minimum required data rate from 0.2 Mbps to 0.4 Mbps is marginal, whereas EtA and EtA_nA show -20% $\sim$ -10% degradation. For the 4 picocell case, the proposed scheme provides the large performance gain in the range between 55%-ile and 90%-ile due to higher data rate achieved at R-PMSs in 4 picocells.

4.6 Summary and Future Work

In this chapter, we have discussed a time-domain macrocell transmit power nulling for cross-tier interference mitigation. First, we present a new flexible PMS scheduling policy where ER-PMSs and R-PMSs are basically scheduled to ABSs and non-ABSs, respectively, but they can be also scheduled to non-ABSs and ABSs, respectively, depending on the configured number of ABSs. Then, based on the PMS scheduling policy, the optimization problem is formulated to find the optimal

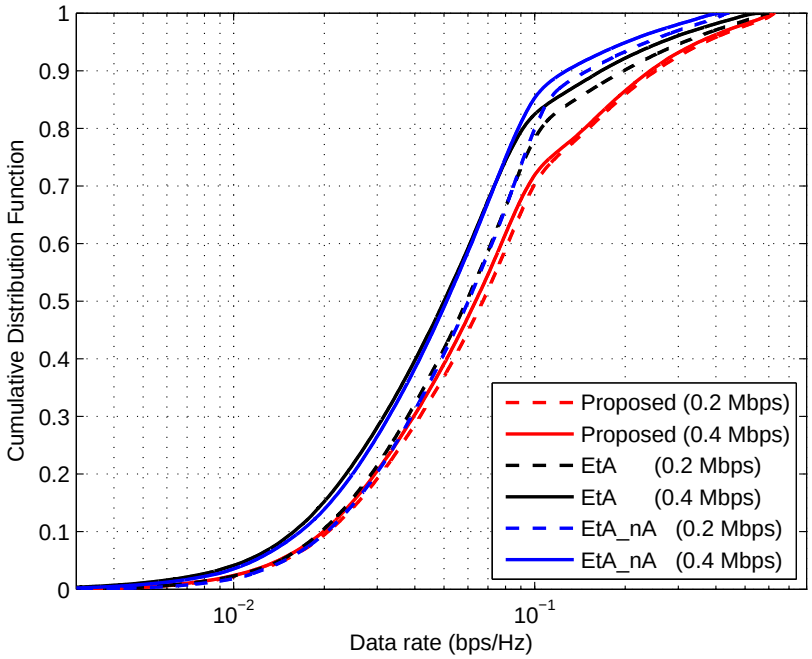

(a) 8 dB CRE bias

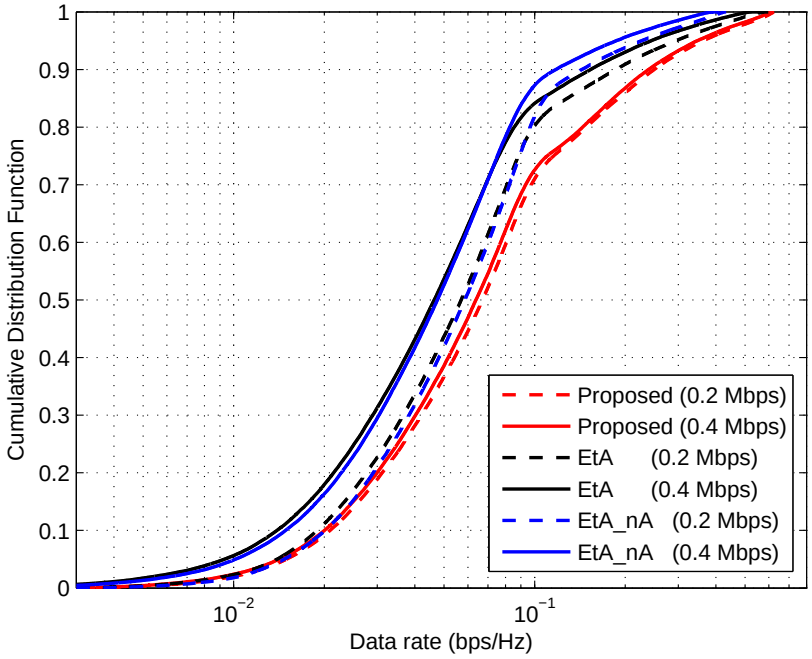

(b) 16 dB CRE bias

Figure 4.5: CDFs of MMSs+R-PMSs' data rate (2 picocells)

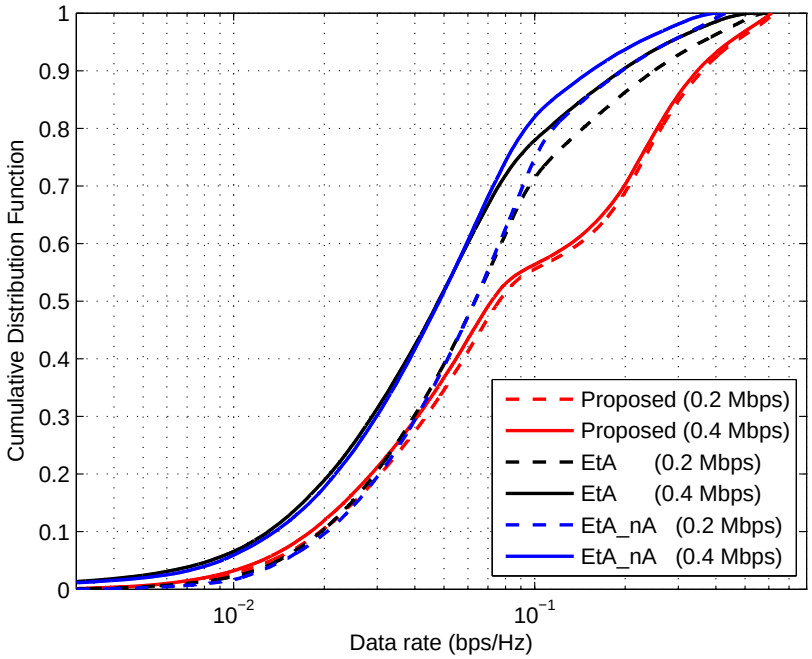

(a) 8 dB CRE bias

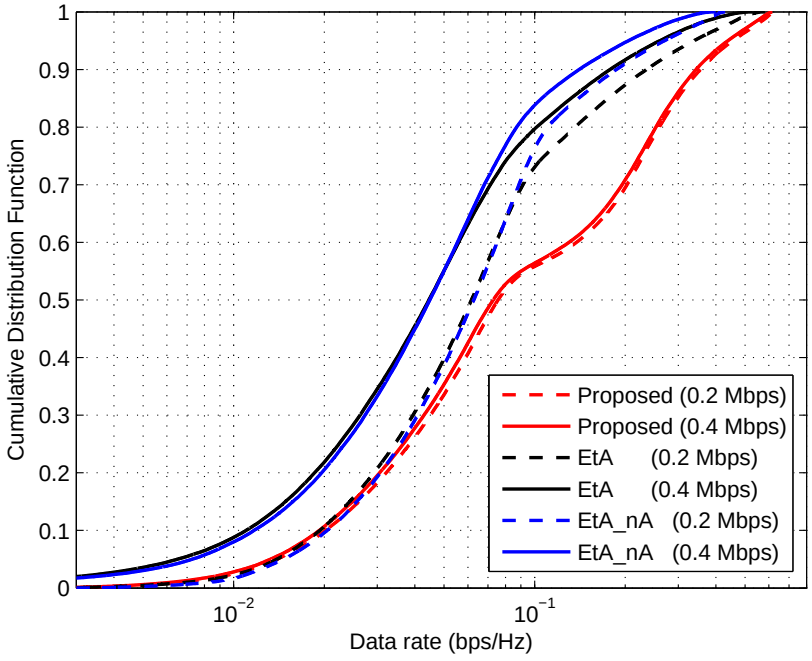

(b) 16 dB CRE bias

Figure 4.6: CDFs of MMSs+R-PMSs' data rate (4 picocells)

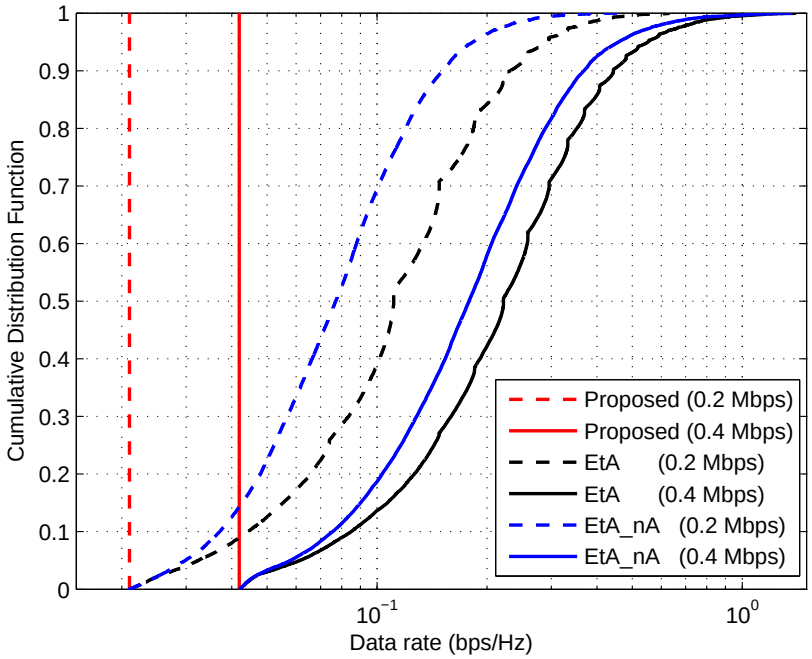

(a) 8 dB CRE bias

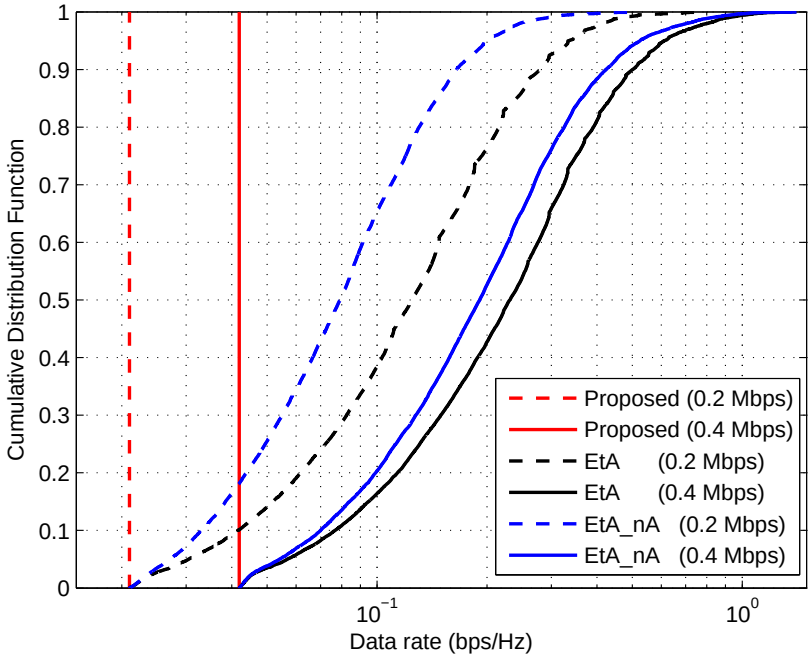

(b) 16 dB CRE bias

Figure 4.7: CDFs of ER-PMSs' data rate (2 picocells)

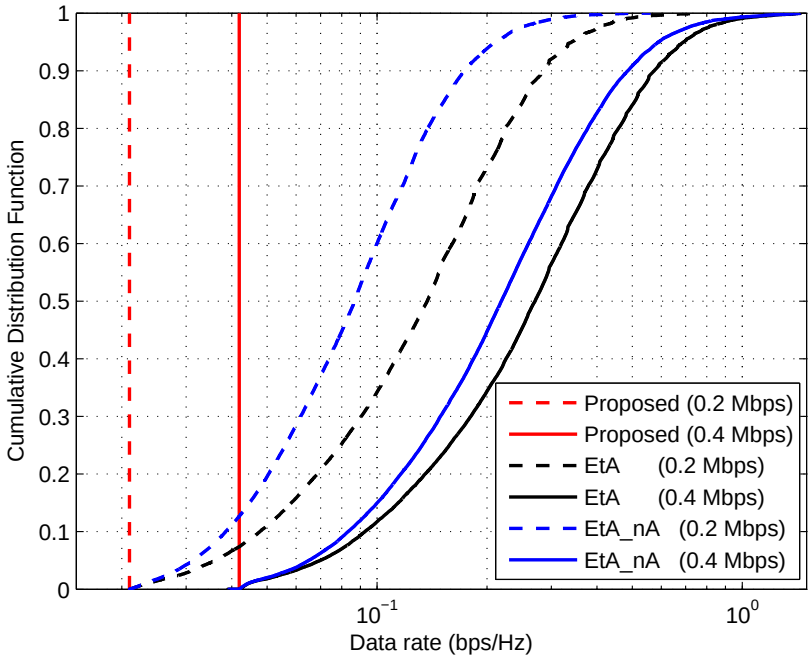

(a) 8 dB CRE bias

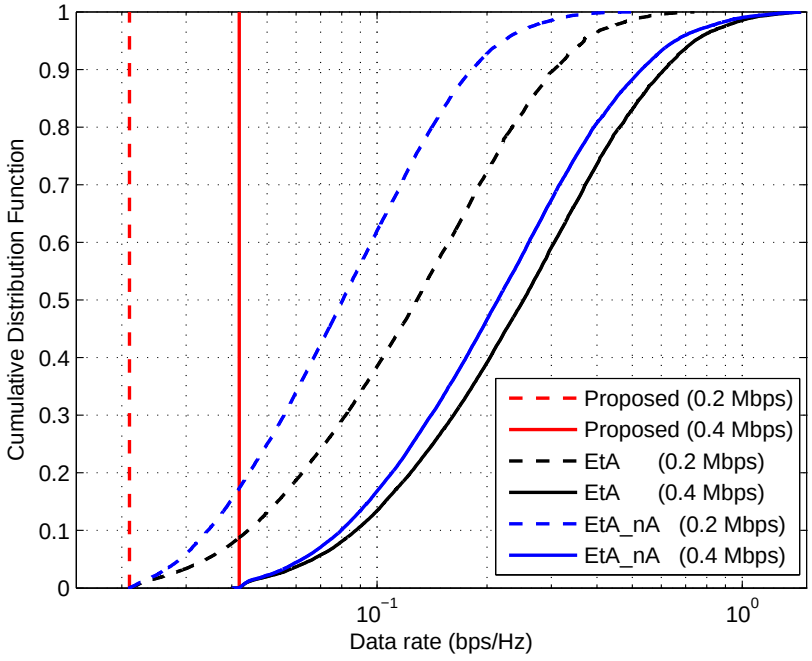

(b) 16 dB CRE bias

Figure 4.8: CDFs of ER-PMSs' data rate (4 picocells)

number of ABSs by which the sum of utilities of MMSs and R-PMSs is maximized subject to ER-PMSs' minimum required data rate.

As future work, the following research item can be further studied.

- *Asynchronous ABS configuration*
  - We can expand the current work based on the synchronous ABS operation to the asynchronous ABS operation case where each macrocell can have a different ABS configuration.
- *Weighted utilities for MMSs and R-PMSs*
  - Due to the relatively small number of PMSs per picocell compared to that of MMSs per maccocell and multiple picocells deployed in a macrocell's coverage, the sum of utilities of R-PMSs could become a dominant factor when the number of ABSs is determined. In other words, a large number of ABSs can be configured for R-PMSs' utility sum which would result in lower data rates of MMSs. To resolve this imbalance, we can apply different weights to MMSs and R-PMSs so that MMSs' possible throughput degradation can be compensated.

Chapter 5: Dynamic Load-aware Cell Association

5.1 Motivation

Although the CRE-based cell association can achieve MMS offloading toward PBSs, MS load balancing is still a challenge in heterogeneous cellular networks as the received signal strength-based cell association basically cannot cope with MS load imbalance in the network. When a cell is heavily loaded, associated MSs' throughput would be degraded due to the small portion of resource allocated to each of MSs even if all MSs observe the strongest received signal strength from the cell (CRE is not assumed).

There have been several research work on MS load balancing for general multi-cell wireless networks [45, 48] and heterogeneous cellular networks [65, 66]. The objective is to find the optimal cell association between MSs and BSs so as to maximize the network-wide utility (i.e. the sum of utilities of MSs).

In heterogeneous cellular networks, when MMSs need to be offloaded to PBSs the challenging issue here is that those offloaded PMSs from macrocells would experience strong cross-tier interference so that the offloading could be limited unless cross-tier interference mitigation is jointly considered.

However, there have been a few studies on a joint optimization of cell associa-

tion and cross-tier interference mitigation. In [67], authors discuss the network-wide utility maximization problem with respect to the cell association and the number of ABSs, and propose an algorithm where the optimal solution with relaxation of integer variables is obtained by non-linear programming and the integer rounding is applied to the relaxed optimal solution. In this work, the MS data rate is not properly modeled as the number of MSs associated with each BS is not taken into account. In [68], authors discuss the network-wide utility maximization problem with respect to the cell association and the number of ABSs, and solve the optimization problem by transforming the combinatorial problem into a convex form by relaxing the binary cell association and the number of ABSs. In this work, the optimal solution requires MSs to be associated with multiple BSs simultaneously, which is not viable in the practical network.

In this chapter, we discuss the network-wide utility maximization problem with respect to the cell association and the number of ABSs. We propose an online algorithm to solve the optimization problem where the cell association and the number of ABSs are jointly optimized. Our proposed algorithm consists of two stages - load balancing and ABS control. In the load balancing stage, each MS's expected data rate by handover given the number of ABSs t is used to determine the best MS's handover to a target BS in a way that the net change of network-wide utility is maximized. In the ABS control stage, MSs to be offloaded are estimated based on MSs' expected data rate with both tier change (macro $\leftrightarrow$ pico) and ABS change ($t \rightarrow t \pm 1$).

Table 5.1: List of parameters and variables

Notation	***Description***
$\mathcal{U}$	Set of MSs
$\mathcal{U}_b$	Set of MSs associated with BS b
$\mathcal{B}$	Set of BSs ($= \mathcal{B}_m \cup \mathcal{B}_p$)
$\mathcal{B}_m$	Set of MBSs
$\mathcal{B}_p$	Set of PBSs
x_{ub}	Association indicator of MS u with BS b
r_u	Expected average throughput of MS u
$r_{ub}(t)$	Long-term average rate of MS u from BS b with ABS t
c_{ub}	Achievable link rate of MS u from BS b in non-ABSs
$\bar{c}_{ub}$	Achievable link rate of MS u from BS b in ABSs
W	System bandwidth
T	ABS periodicity in subframes

5.2 System Model

The network model considered in this paper is a heterogeneous downlink cellular network consisting of two tiers - MBSs and pico BSs overlaid within the MBSs' coverage. Based on Table 5.1, we derive two expressions of average received signal-to-interference plus noise ratio (SINR) in non-ABSs and ABSs as follows. The

average SINR in non-ABSs at MS u from BS b, denoted by Γ_{ub}, is expressed as

$$\Gamma_{ub} = \frac{P_b h_{ub}}{\sum_{b' \in \mathcal{B}, b' \neq b} P_{b'} h_{ub'} + \sigma^2}, \tag{5.1}$$

where P_b, h_{ub}, and σ^2 denote the transmit power of the BS b, the average channel gain of a link between MS u and BS b including path loss, shadowing, and fast fading, and the power of additive white Gaussian noise, respectively. In ABSs, all MBSs' transmit power is set to be zero. Hence, the average SINR in ABSs at MS u from BS b, denoted by $\bar{\Gamma}_{ub}$, is expressed as

$$\bar{\Gamma}_{ub} = \begin{cases} \dfrac{P_b h_{ub}}{\sum_{b' \in \mathcal{B}_p, b' \neq b} P_{b'} h_{ub'} + \sigma^2} & \text{if } b \in \mathcal{B}_p \\ 0 & \text{if } b \in \mathcal{B}_m. \end{cases} \tag{5.2}$$

Given Γ_{ub} and $\bar{\Gamma}_{ub}$, two types of achievable link rates, c_{ub} in non-ABSs and $\bar{c}_{ub}$ in ABSs, are derived using Shannon's formula as

$$\begin{aligned} c_{ub} &= W \log_2 (1 + \Gamma_{ub}) \\ \bar{c}_{ub} &= W \log_2 \left(1 + \bar{\Gamma}_{ub}\right) \end{aligned} \quad \forall u \in \mathcal{U} \;\; \forall b \in \mathcal{B}, \tag{5.3}$$

respectively, where W is the system bandwidth. For any MBS $b \in \mathcal{B}_m$, the average link rate $\bar{c}_{ub}$ in ABSs becomes zero as $\bar{\Gamma}_{ub}$ becomes zero.

$$P_b = 0 \;\rightarrow\; \bar{\Gamma}_{ub} = 0 \;\&\; \bar{c}_{ub} = 0 \quad \forall b \in \mathcal{B}_m \;\; \forall u \in \mathcal{U}_b. \tag{5.4}$$

5.3 Problem Formulation

In this section, we formulate an optimization problem in which the objective is to maximize the network-wide utility by configuring both the user association with

cells in a load-distributed manner and the number of ABSs to improve this load distribution between MBSs and PBSs as follows:

$$\max_{\underline{x},t} \sum_{u\in\mathcal{U}} U(r_u) = \max_{\underline{x},t} \sum_{u\in\mathcal{U}} U\left(\sum_{b\in\mathcal{B}} x_{ub} r_{ub}(t)\right)$$

$$= \max_{\underline{x},t} \sum_{u\in\mathcal{U}}\sum_{b\in\mathcal{B}} x_{ub}\, U\left(r_{ub}(t)\right) \tag{5.5}$$

where $U(\cdot)$ is an increasing, strictly concave, and continuously differentiable utility function, $\underline{x}$ is an association indicator vector $\{x_{ub} : u \in \mathcal{U}, b \in \mathcal{B}\}$ representing whether MS u is associated with BS b $(= 1)$ or not $(= 0)$, and t is the number of ABSs configured at MBSs. We assume synchronous ABS operation where all MBSs follow the same ABS configuration such as the periodicity, the start offset, and the duration.

For the utility function $U(\cdot)$, we utilize the log utility function $U(r) = \log(r)$ as previous work [43] has shown that proportional fairness among users could be achieved when the sum of logarithmic utilities is maximized.

To derive the long-term average rate $r_{ub}(t)$, we assume that the proportional fairness scheduler is used. Following the long-term behavior of the proportional fairness scheduler in [69], $r_{ub}(t)$ can be expressed as

$$r_{ub}(t) = \frac{G(K_b)\left((1-\frac{t}{T})c_{ub} + \frac{t}{T}\bar{c}_{ub}\right)}{K_b}, \tag{5.6}$$

where K_b is the number of MSs associated with BS b which is derived as $K_b = \sum_{u\in\mathcal{U}} x_{ub}$ and $G(\cdot)$ denotes a multi-user diversity gain which can be calculated as $G(k) = \sum_{i=1}^{k} \frac{1}{i}$. Following the configured ABS duration t, $(T-t)$ non-ABSs and t ABSs are basically available for each MS.

By applying the logarithmic utility function and plugging (5.6) to (5.5), we have the formulated optimization problem as follows:

$$\max_{\underline{x},t} \sum_{u\in\mathcal{U}} \sum_{b\in\mathcal{B}} x_{ub} \log\left(\frac{G(K_b)\left((1-\frac{t}{T})c_{ub}+\frac{t}{T}\bar{c}_{ub}\right)}{K_b}\right) \tag{5.7a}$$

$$\text{s.t.} \quad x_{ub} = \{0,1\} \quad \forall u \in \mathcal{U} \;\; \forall b \in \mathcal{B} \tag{5.7b}$$

$$t = \{0,1,\cdots,T-1\}, \tag{5.7c}$$

$$\sum_{b\in\mathcal{B}} x_{ub} = 1 \quad \forall u \in \mathcal{U}, \tag{5.7d}$$

$$K_b = \sum_{u\in\mathcal{U}} x_{ub} \quad \forall b \in \mathcal{B}. \tag{5.7e}$$

As discussed in previous work [45, 48], the cell association problem, i.e., the optimization problem (5.7) with a fixed ABS duration t, is a 0-1 knapsack problem, therefore it is NP-hard. The authors in [45] present an *offline* algorithm which can obtain the optimal cell association in a polynomial time by fixing the number of associated MSs with each BS. For every K_b configuration, the cell association problem is equivalent to the maximum weighted matching problem. This offline algorithm, however, has computational complexity of $O\left(|\mathcal{U}|^{|\mathcal{B}|+3/2}\right)$ which could be too complex in heterogeneous cellular networks as the number of BSs in heterogeneous cellular networks is much larger than that in traditional cellular networks. Moreover, in our problem formulation, the ABS duration t also needs to be jointly optimized along with the cell association. Therefore, we develop an *online* heuristic algorithm inspired by [48] in the next section.

5.4 Proposed Algorithm

The main motivation of load-aware cell association in general is that selecting the serving BS with the strongest received signal strength doesn't necessarily mean that MSs can achieve the highest average rate because the average rate depends on both the received signal strength and the user load shown in (5.6). In the CRE-enabled scenario, the interference would be larger than the desired signal for PMSs which severely degrades their average rate. Thus, the use of ABSs plays an important role as it can change MSs' average rate changes depending on their associated tiers. This could be used to trigger MSs' tier selection between macros and picos. Based on these observations, we develop the following properties which are crucial for our algorithm design.

Proposition 5.1. (Condition for MS handover under ABS t) Assume MS u is associated with BS b with ABS duration t and the number of users in BS b and BS $b^{'}$ are large. Then transferring the MS u from BS b to BS $b^{'}$ improves the network-wide utility if

$$\log \frac{G(K_{b'}+1)e_{ub'}(t)}{K_{b'}+1} - \log \frac{G(K_b)e_{ub}(t)}{K_b} > \delta_{bb'}^{HO} \tag{5.8}$$

where $e_{ub}(t) = (1-\frac{t}{T})c_{ub} + \frac{t}{T}\bar{c}_{ub}$. $\delta_{bb'}^{HO}$ represents the net utility change between BS b and $b^{'}$ which is expressed as

$$\delta_{bb'}^{HO} = \frac{1-\frac{1}{K_b}}{\gamma + \log K_b} - \frac{1}{\gamma + \log K_{b'}} \tag{5.9}$$

where γ is the Euler-Mascheroni constant ($= 0.5772\cdots$).

Proof: Refer to Section 5.7.1.

Proposition 5.2. (Condition for ABS increment from t to t+1) Suppose MBS $i \in \mathcal{B}_m$ selects a subset of its associated MMSs to be offloaded to PBSs, denoted by $\mathcal{U}_i^{OL}$ $\left(|\mathcal{U}_i^{OL}| = n_i,\ n_i \ll K_i\right)$ and PBS $j \in \mathcal{B}_p$ accommodates m_j MMSs out of overall MMSs to be offloaded ($m_j \ll K_j$), i.e., $\sum_{i\in\mathcal{B}_m} n_i = \sum_{j\in\mathcal{B}_p} m_j$. Then ABS increment from t to $t+1$ with offloading MMSs improves the network-wide utility (i.e., the net utility change $\Delta U_+^{ABS}(t+1) > 0$) if the following condition is met:

$$\begin{aligned}
&\sum_{i\in\mathcal{B}_m}\sum_{u\in\mathcal{U}_i^{OL}}\left[\log\frac{G(K_{b_u^p}+m_{b_u^p})e_{ub_u^p}(t+1)}{K_{b_u^p}+m_{b_u^p}} - \log\frac{G(K_i)e_{ui}(t)}{K_i}\right] \\
&- \sum_{i\in\mathcal{B}_m}\left[n_i\left(\frac{1-\frac{n_i}{K_i}}{\gamma+\log K_i} - \frac{1}{T-t}\right) + \frac{K_i}{T-t}\right] \\
&+ \sum_{j\in\mathcal{B}_p}\left[\frac{m_j}{\gamma+\log K_j} + \sum_{u\in\mathcal{U}_j}\frac{a_{uj}-1}{T+t(a_{uj}-1)}\right] \ > \ 0,
\end{aligned} \tag{5.10}$$

where b_u^p is the target PBS to which the MMS u is handed over, $m_{b_u^p}$ is the total number of MMSs that the target PBS b_u^p would accommodate, and a_{uj} is the ratio of the achievable link rate at PMS u with PBS j in ABSs to that in non-ABSs ($= \bar{c}_{uj}/c_{uj}$).

Proof: Refer to Section 5.7.2.

Remark: Three terms in (5.10) can be represented respectively as follows:

$$\Delta U_m^{OL}(t+1) + \Delta U_m(t+1) + \Delta U_p(t+1) > 0, \tag{5.11}$$

where $\Delta U_m^{OL}(t+1)$, $\Delta U_m(t+1)$, and $\Delta U_p(t+1)$ denote the expected net utility change of MMSs to be offloaded to PBSs, MMSs remaining in MBSs, and PMSs by increasing the ABS duration from t to $t+1$, respectively.

Proposition 5.3. (Condition for ABS decrement from t to t-1) Suppose PBS $j \in \mathcal{B}_p$ selects a subset of its associated PMSs to be offloaded to MBSs, denoted

by $\mathcal{U}_j^{OL}$ $\left(|\mathcal{U}_j^{OL}| = m_j,\ m_j \ll K_j\right)$ and MBS $i \in \mathcal{B}_m$ accommodates n_i MMSs out of overall PMSs to be offloaded ($n_i \ll K_i$), i.e., $\sum_{j\in\mathcal{B}_p} m_j = \sum_{i\in\mathcal{B}_m} n_i$. Then ABS decrement from t to $t-1$ with offloading PMSs improves the network-wide utility (i.e., the net utility change $\Delta U_{-}^{ABS}(t-1) > 0$) if the following condition is met:

$$\begin{aligned}
&\sum_{j\in\mathcal{B}_p}\sum_{u\in\mathcal{U}_j^{OL}}\left[\log\frac{G(K_{b_u^m}+n_{b_u^m})e_{ub_u^m}(t-1)}{K_{b_u^m}+n_{b_u^m}} - \log\frac{G(K_j)e_{uj}(t)}{K_j}\right] \\
&-\sum_{j\in\mathcal{B}_p}\left[\frac{m_j\left(1-\frac{m_j}{K_j}\right)}{\gamma+\log K_j} + \sum_{u\in\mathcal{U}_j\setminus\mathcal{U}_j^{OL}}\frac{a_{uj}-1}{T+t(a_{uj}-1)}\right] \\
&+\sum_{i\in\mathcal{B}_m}\left[\frac{n_i}{\gamma+\log K_i} + \frac{K_i}{T-t}\right] \ > \ 0,
\end{aligned} \tag{5.12}$$

where b_u^m is the target MBS to which the PMS u is handed over, $n_{b_u^m}$ is the total number of PMSs that the target MBS b_u^m would accommodate.

Proof: Refer to Section 5.7.2.

Remark: Three terms in (5.12) can be represented respectively as follows:

$$\Delta U_p^{OL}(t-1) + \Delta U_p(t-1) + \Delta U_m(t-1) > 0, \tag{5.13}$$

where $\Delta U_p^{OL}(t-1)$, $\Delta U_p(t-1)$, and $\Delta U_m(t-1)$ denote the expected net utility change of PMSs to be offloaded to MBSs, PMSs remaining in PBSs, and MMSs by decreasing the ABS duration from t to $t-1$, respectively.

From Eq. (5.10), (5.12), we observe that the net utility change of MBSs and PBSs by ABS control, apart from that of MSs to be offloaded, can be represented in a simple form.

Based on the observations discussed above, we describe how the proposed algorithm optimizes the cell association and the ABS duration. Considering the required

procedure and signaling for measurement and reporting, the joint optimization is divided into two stages - the MS load-balancing and the ABS control. In the MS load-balancing stage, MS handovers are performed among BSs in a way that the network-wide utility is increased in a gradient-descent manner under the current ABS duration t. In the ABS control stage, the ABS increment (+1) or decrement (-1) is examined by estimating the possible MSs that can be offloaded based on MSs' measurement reports and corresponding net utility changes $U_{+}^{ABS}(t+1)$ and $U_{-}^{ABS}(t-1)$.

5.4.1 Stage 1: MS Load-balancing under ABS Duration t

By neighbor cell measurement and user load information, every MS u calculates the expected data rates of its neighboring cells by handover, and reports to the serving BS b_u the best target BS $b_u^{'}$ from which it can achieve the largest logarithmic ratio $\phi_u(t)$ by handover as

$$\phi_u(t) = \log \frac{G(K_{b_u^{'}}+1)e_{ub_u^{'}}(t)}{K_{b_u^{'}}+1} \frac{K_{b_u}}{G(K_{b_u})e_{ub_u}(t)} \quad \forall u \in \mathcal{U}. \tag{5.14}$$

Suppose each BS reports their best candidate MS to the central coordinating entity, the central entity chooses the best MS u^* that achieves the largest utility increment by this handover,

$$u^* = \underset{u \in \mathcal{U}^{HO}}{\arg\max} \left(\phi_u(t) - \delta_{b_u b_u^{'}}^{HO}\right), \tag{5.15}$$

where $\mathcal{U}^{HO}$ is the set of candidate MSs selected by each BS and $\delta_{b_u b_u^{'}}^{HO}$ can be calculated based on (5.9). As discussed in (5.8), the handover can be done only if the

selected MS u^* satisfies the following condition with a hysteresis margin $\delta_h^{HO} > 0$ to prevent possible ping-pong effects:

$$\phi_{u^*}(t) - \delta^{HO}_{b_{u^*}b'_{u^*}} > \delta_h^{HO}. \tag{5.16}$$

For a given ABS duration t, the load-balancing operation is performed until there is no MS that satisfies the condition in (5.16) to improve the network-wide utility by handover.

5.4.2 Stage 2: ABS Control from t by +1 or -1

By neighbor cell measurement and user load information, every MS u calculates expected data rates with its neighboring BSs by handover along with ABS change (ABS increment by +1 and ABS decrement by -1). Then, the MS reports the best target BS b'_u and the best ABS value t_u (either +1 or -1) to the serving BS b_u for which it can achieve the highest ratio $\phi_u(t + t_u)$ by handover along with ABS change as

$$\phi_u(t + t_u) \;=\; \log \frac{G(K_{b'_u} + 1)e_{ub'_u}(t + t_u)}{K_{b'_u} + 1} \frac{K_{b_u}}{G(K_{b_u})e_{ub_u}(t)} \quad \forall u \in \mathcal{U}, \tag{5.17}$$

where $\phi_u(t + t_u) > 0$ means that the MS can be considered as a candidate MS for offloading with ABS change t_u.

Unlike load-balancing in stage 1 where a single MS is handed over to a target BS regardless of the BS type, ABS control only considers multiple MSs offloading from MBSs to PBSs, or vice versa. For instance, when the ABS duration increases this leads to MMSs' data rate degradation as the number of non-ABSs decreases.

Hence, a certain number of MMSs should be offloaded to PBSs to compensate the possible MMSs' throughput degradation. When the ABS duration decreases, on the other hand, this leads to PMSs' data rate degradation as the number of ABSs decreases. Therefore, a certain number of PMSs needs to be offloaded to MBSs. As a result, we focus on two cases - ABS increment by +1 with offloading MMSs to PBSs and ABS decrement by -1 with offloading PMSs to MBSs.

After receiving MSs' measurement report messages, every MBS reports to the central coordinating entity the number of currently associated MMSs and information of candidate MMSs for offloading to PBSs such as the target PBS id and $\phi_u(t+1)$. In case of PBSs, each PBS reports the number of currently associated PMSs, the net utility change of them by ABS increment calculated as

$$\sum_{u \in \mathcal{U}_j} \frac{a_{uj} - 1}{T + t(a_{uj} - 1)} \quad \forall j \in \mathcal{B}_p, \tag{5.18}$$

and information of candidate PMSs for offloading to MBSs such as the target MBS id, $\phi_u(t-1)$, and $\frac{a_{uj}-1}{T+t(a_{uj}-1)}$. As observed in (5.10), (5.12), the net utility change by ABS decrement can be obtained by changing the sign of that of ABS increment and subtracting that of PMSs to be offloaded.

The central coordinating entity examines if the current ABS duration t needs to be changed by $+1$ or -1 via the backhaul messages from BSs. To check if the condition in (5.10), (5.12) is satisfied, the central coordinating entity needs to determine the number of offloading MMSs for ABS increment and offloading PMSs for ABS decrement.

Since MSs' reported ratio $\phi_u(t+t_u)$ in (5.17) is calculated based on a single

MS handover, candidate MSs for offloading should be filtered out by adjusting their ratio values. Suppose a candidate MS u has the target BS $b_u^{'}$ with ABS change t_u, and there are k candidate MSs in total which can be offloaded to that target BS. Then, the adjusted ratio $\bar{\phi}_u(t+t_u)$ can be approximated as

$$\begin{aligned}\bar{\phi}_u(t+t_u) &= \log \frac{G(K_{b_u^{'}}+k)e_{ub_u^{'}}(t+t_u)}{K_{b_u^{'}}+k}\frac{K_{b_u}}{G(K_{b_u})e_{ub_u}(t)} \\ &= \log \frac{G(K_{b_u^{'}}+1)e_{ub_u^{'}}(t+t_u)}{K_{b_u^{'}}+1}\frac{K_{b_u}}{G(K_{b_u})e_{ub_u}(t)} + \log \frac{K_{b_u^{'}}+1}{G(K_{b_u^{'}}+1)}\frac{G(K_{b_u^{'}}+k)}{K_{b_u^{'}}+k} \\ &\simeq \phi_u(t+t_u) - \frac{k-1}{K_{b_u^{'}}+1}\left(1-\frac{1}{\gamma+\log(K_{b_u^{'}}+1)}\right), \end{aligned} \tag{5.19}$$

where b_u is the serving BS of MS u. For proof, please refer to Proposition 5.1 and 5.2. When there is only one candidate MS for a target BS (i.e., $k=1$), $\phi_u(t+t_u)$ is equivalent to $\bar{\phi}_u(t+t_u)$. As k increases, $\bar{\phi}_u(t+t_u)$ decreases accordingly. To maximize the MS offloading gain, we only consider MSs satisfying $\bar{\phi}_u(t+t_u)>0$ to determine n_i's and m_j's in (5.10), (5.12).

n_i's and m_j's can be obtained as follows. In the ABS increment case, for a given target PBS $b^{'}$ and ABS change +1, MMSs are sorted in a decreasing order of $\phi_u(t+1)$. From the first row of the list (i.e., $k=1$) to the bottom, k is increased by 1 for each row and it is checked if the following condition for the MMS in kth row is met:

$$\phi_u(t+1) > \frac{k-1}{K_{b'}+1}\left(1-\frac{1}{\gamma+\log(K_{b'}+1)}\right). \tag{5.20}$$

Suppose the MMS in the $k^{'}$th row doesn't satisfy the condition in (5.20), then the number of MMSs offloaded to PBS $b^{'}$, $m_{b'}$, becomes $k^{'}-1$. After determining m_j's for all PBSs using this process, n_i's can be determined by checking the serving MBSs

of those MMSs. In the ABS decrement case, the target BS type for offloading is macro, therefore we find n_i's first and then m_j's can be determined accordingly.

Upon determining n_i's and m_j's, using the conditions in (5.10), (5.12), the number of ABSs can be changed if the following conditions are met:

- ABS increment by +1: $\Delta U_{+}^{ABS}(t+1) > \Delta U_{-}^{ABS}(t-1)$ and $\Delta U_{+}^{ABS}(t+1) > \delta_h^{ABS}$
- ABS decrement by -1: $\Delta U_{-}^{ABS}(t-1) > \Delta U_{+}^{ABS}(t+1)$ and $\Delta U_{-}^{ABS}(t-1) > \delta_h^{ABS}$,

where δ_h^{ABS} is a hysteresis margin to prevent possible ping-pong effects in ABS control.

It should be noted that the proposed method of determining n_i's and m_j's is not optimal for estimating the actual number of MSs that can be offloaded with ABS change. However, from the view point of required report messages from MSs and computations at BSs, the proposed method provides a simple and dynamic way to control the number of ABSs.

5.5 Performance Evaluation

In this section, we demonstrate the performance of the proposed scheme through simulations. The heterogeneous network deployment is constructed as follows. The macro-tier consists of 7 MBSs each of which is three-sectorized (i.e., 21 macrocells), and in each macrocell's coverage outdoor omni-directional picocells and MSs are uniformly distributed. To obtain two achievable link rates c_{ub} and $\bar{c}_{ub}$, instead of

using Shannon's formula, we calculate the bit rates based on channel quality indicators (CQIs) fed back from MSs in the system level simulator developed based on the LTE downlink system level simulator in [61]. The detailed parameters are described in Table 5.2, most of which are adopted from 3GPP's system level simulation parameters in [62], [63], [64].

For the performance evaluation, the following schemes are compared through numerical simulations:

- *Proposed scheme*: Load-aware cell association and ABS control are jointly optimized.
- *Received signal strength-based cell association (RSS)*: The cell association is done by choosing the cell with the strongest received signal strength.
- *Cell range expansion-based cell association (CRE)*: The cell association is done by choosing the cell with the strongest received signal strength plus the CRE bias.

For the proposed scheme, the initial cell association and ABS duration are given as the received signal strength-based BS selection and zero ABSs, respectively. The hysteresis margins for the load-balancing (stage 1) and the ABS control (stage 2) are set to be $\log 1.1$ and $\log(p*1.3)$ where p is the number of picocells per macrocell, respectively. For RSS and CRE, the optimal number of ABSs is found through exhaustive search that maximizes the network-wide utility.

Table 5.3, Figure 5.1, and Figure 5.2 show how many ABSs are configured in three schemes to maximize the network-wide utility. For the CRE (8 dB) and RSS

Table 5.2: Simulation Parameters

Simulation Parameter	***Value***
Number of simulations per scenario	500
Max. iterations per simulation	1500
Carrier frequency	2.0 GHz
System bandwidth	10 MHz
Antenna configuration	SISO
Channel model	Typical Urban (TU)
Inter-site distance	750 m
Noise power spectral density	-174 dBm/Hz
ABS periodicity (T)	40 subframes
Macrocell transmit power	40 W (46 dBm)
Macrocell path loss model	$128.1 + 37.6\log_{10} R$ (R in km)
Macrocell shadowing model	Log normal fading with std. 10 dB
Macrocell antenna gain	15 dBi
Picocell transmit power	1 W (30 dBm)
Picocell path loss model	$140.7 + 36.7\log_{10} R$ (R in km)
Picocell shadowing model	Log normal fading with std. 6 dB
Picocell antenna gain	5 dBi
Min. distance MBS-PBS	75 m
Min. distance PBS-PBS	50 m
Number of macrocells	21 (7 three-sectorized MBSs)
Number of picocells per macrocell	2 / 4
Number of MSs per macrocell	50 (minimum 2 PMSs in picocell without CRE)
CRE bias offset	8 / 16 dB

Table 5.3: Average of Optimal ABSs

Case	**Proposed**	**CRE (16 dB)**	**CRE (8 dB)**	**RSS**
2 picos	20.1	2.27	0.00	0.00
4 picos	32.9	5.82	0.06	0.00

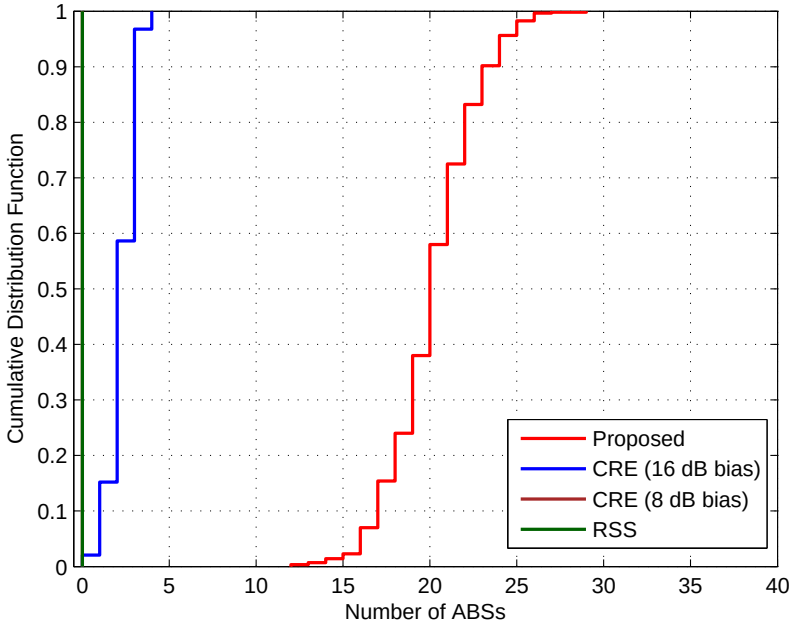

Figure 5.1: CDFs of optimal ABSs (2 picocells)

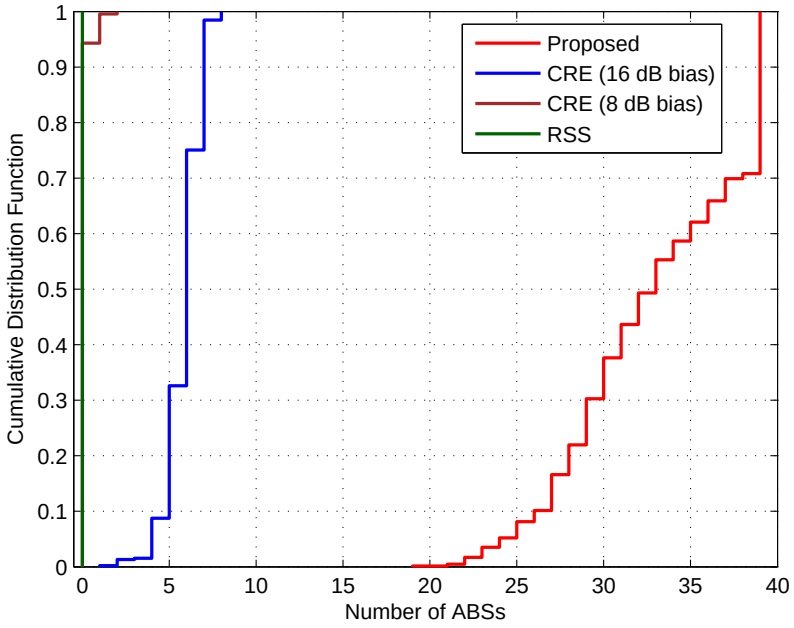

Figure 5.2: CDFs of optimal ABSs (4 picocells)

schemes, the number of configured ABSs is almost zero for both 2 picocell and 4 picocell cases, due to the fact that much more MSs are associated to macrocells even

if the 8 dB of CRE bias offset is applied. Therefore, it is more beneficial to allocate almost zero ABSs for the sake of maximizing the network-wide utility. For the CRE (16 dB) scheme, about $1 \sim 8$ ABSs can be configured to maximize the network-wide utility as shown in Figure 5.1 and Figure 5.2. For the proposed scheme, the number of ABSs configured is about 6 times of that of CRE (16 dB) for both 2 picocell and 4 picocell cases by the joint operation of MS offloading. It is noted that the number of configured ABSs increases about 50% as the number of picocells per macrocell becomes 4 from 2. In Figure 5.1 and Figure 5.2, the CDFs of the number of optimal ABSs are shown. Noticeably, for the 4 picocell case, the maximum number of ABSs (i.e., 39) is configured for about 30% of simulations. This means that almost all MMSs can be offloaded to picocells when picocells are evenly distributed over the macrocells' coverage.

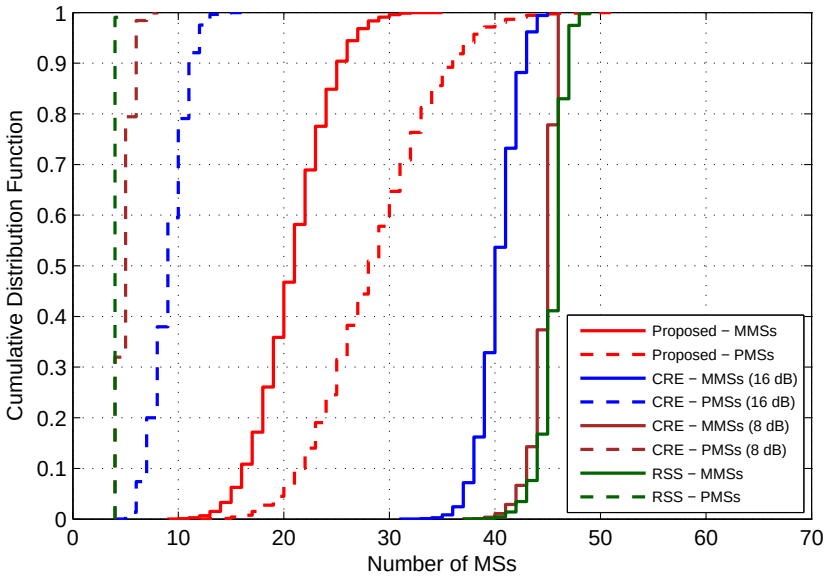

Figure 5.3: CDFs of the number of MSs per macrocell coverage (2 picocells)

In Figure 5.3 and Figure 5.4, the CDFs of the number of MSs per macrocell

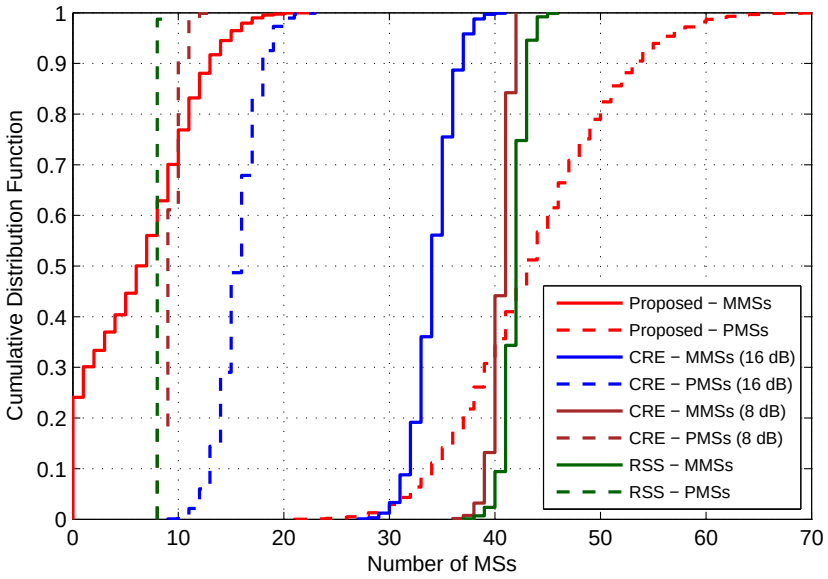

Figure 5.4: CDFs of the number of MSs per macrocell coverage (4 picocells)

coverage are shown. The number of PMSs represents the sum of PMSs in all picocells (2 or 4) located in a macrocell coverage. Therefore, the number of PMSs needs to be divided by the number of picocells in order to check the number of PMSs per picocell. For the 2 picocell case, each marocell accommodates about 30% $\sim$ 50% more MSs than a picocell in their coverage. However, for the 4 picocell case, each picocell accommodates about 30% $\sim$ 50% more MSs than the macrocell which means the better MS load-balancing. Moreover, it is noted that about 25% of macrocells have no MSs associated due to the maximum number of ABSs configured (i.e., 39 ABSs).

Table 5.4: Average Utility per MS

Case	**Proposed**	**CRE (16 dB)**	**CRE (8 dB)**	**RSS**
2 picos	14.39	14.23	14.18	14.15
4 picos	14.82	14.48	14.39	14.35

In Table 5.4, the means of average utility per MS are compared, which is calculated by dividing the sum of utilities by the total number of MSs in the network. Compared to other schemes, the proposed scheme shows about 1% and 3% performance improvement of average utility per MS. As the number of picocells increases, the higher performance improvement is observed as more MSs can be offloaded along with the ABS control. It is also noted that the CRE-based cell association shows the marginal performance improvement (less than 1%) compared to the RSS-based association, i.e., 0 dB of CRE bias offset.

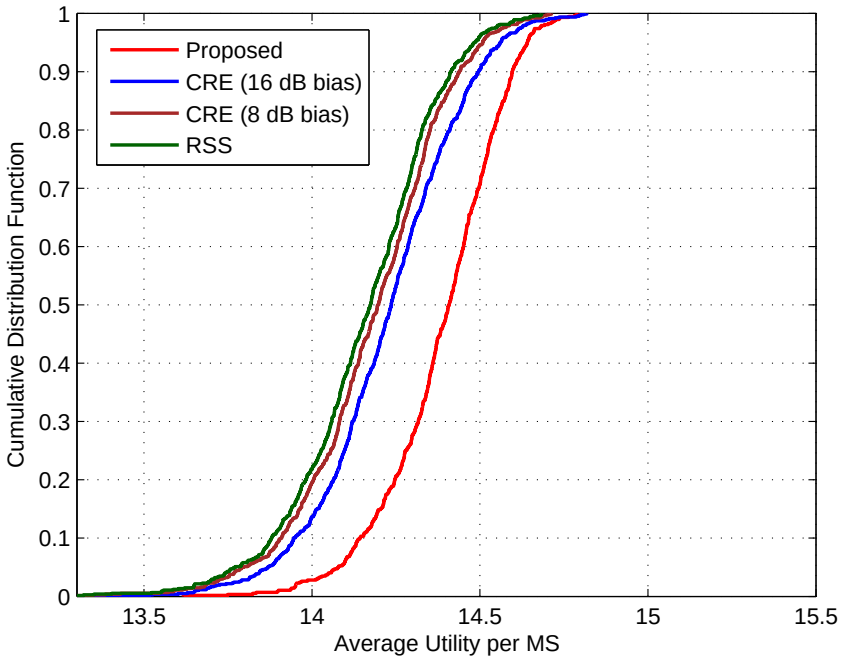

Figure 5.5: CDFs of average utility per MS (2 picocells)

In Figure 5.5 and Figure 5.6, the CDFs of average utility per MS is shown. It is confirmed that the proposed scheme provides much larger performance improvement as the number of picocells increases which results in higher possibility of MS offloading in conjunction with ABS control

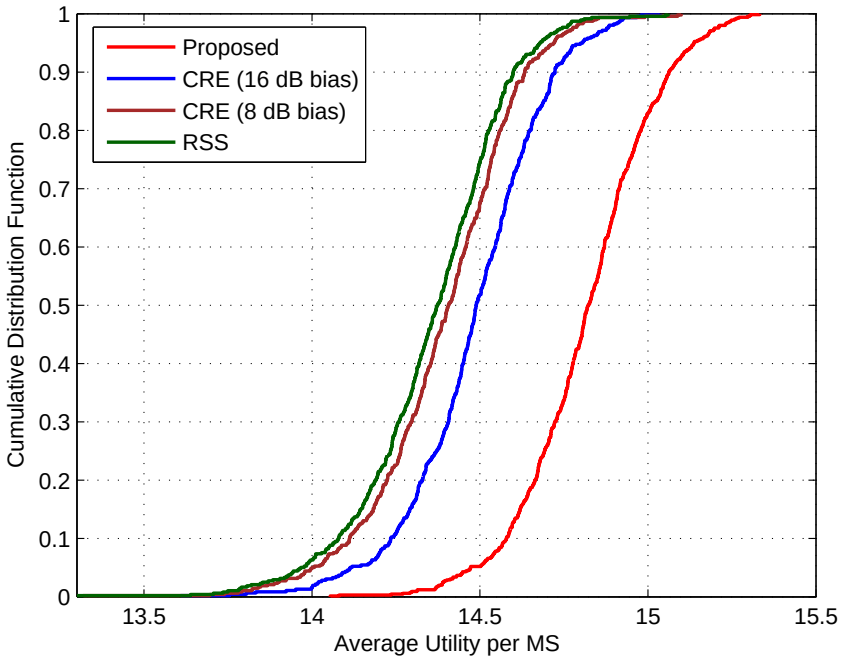

Figure 5.6: CDFs of average utility per MS (4 picocells)

Table 5.5: MS Data Rate (bps/Hz)

Case	**Metric**	**Proposed**	**CRE (16 dB)**	**CRE (8 dB)**	**RSS**
2 picos	Mean	0.226	0.207	0.214	0.216
	Edge	0.060	0.049	0.045	0.043
4 picos	Mean	0.381	0.299	0.290	0.293
	Edge	0.077	0.054	0.050	0.046

In Table 5.5, MS data rates are compared in three schemes. For the 2 picocell case, the proposed scheme shows 5% $\sim$ 10% performance improvement over CRE (8 dB and 16 dB) and RSS schemes in the mean MS data rate. In the edge (5%-ile) data rate, the performance gap becomes about 20% $\sim$ 40%. Although the RSS scheme shows about 3% higher mean data rate than both CRE cases (8 dB and

16 dB) due to the smaller number of PMSs which achieve much higher data rates, the edge data rate is degraded about -7 % by the large number of MMSs. For the 4 picocell case, the performance gap between the proposed scheme and the others becomes much larger than the 2 picocell case. The proposed scheme shows about 30% gain in the mean data rate and about 50% gain in the edge rate. The CRE (16 dB) scheme shows about 2% higher mean data rate than the RSS scheme, which means the cell-splitting gain is enhanced by MS offloading and ABS configuration.

In Figure 5.7 and Figure 5.8, the CDFs of MS data rate are shown. The proposed scheme shows the better fairness among MSs by MS offloading and ABS control. About 90%-ile or above, the CRE and RSS schemes show the higher data rate than the proposed scheme due to the smaller number of PMSs. Since about 5 or less PMSs are accommodated by each picocell, their achievable data rate is much higher than MMSs' in the CRE and RSS schemes as identified in Figure 5.9 and Figure 5.10.

5.6 Summary and Future Work

In this work, we have discussed a joint optimization problem of cell association and cross-tier interference mitigation. The network-wide utility maximization problem is formulated with respect to the cell association and the number of ABSs. In the first stage, MS load balancing is done based on their expected data rate by handover under the current number of ABSs t. When there are no MSs available for handover, the possibility of ABS control is examined for further MS load balancing.

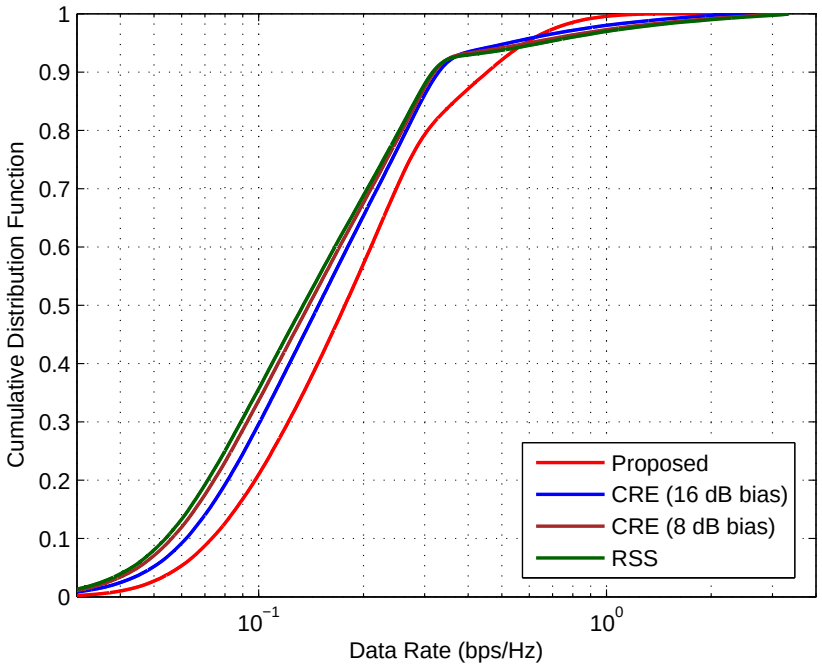

Figure 5.7: CDFs of MSs' data rate (2 picocells)

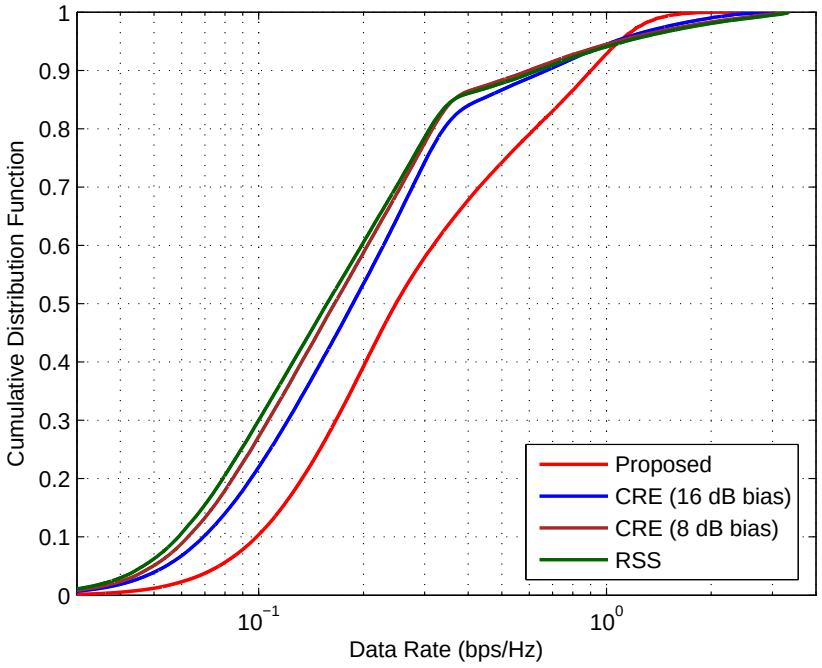

Figure 5.8: CDFs of MSs' data rate (4 picocells)

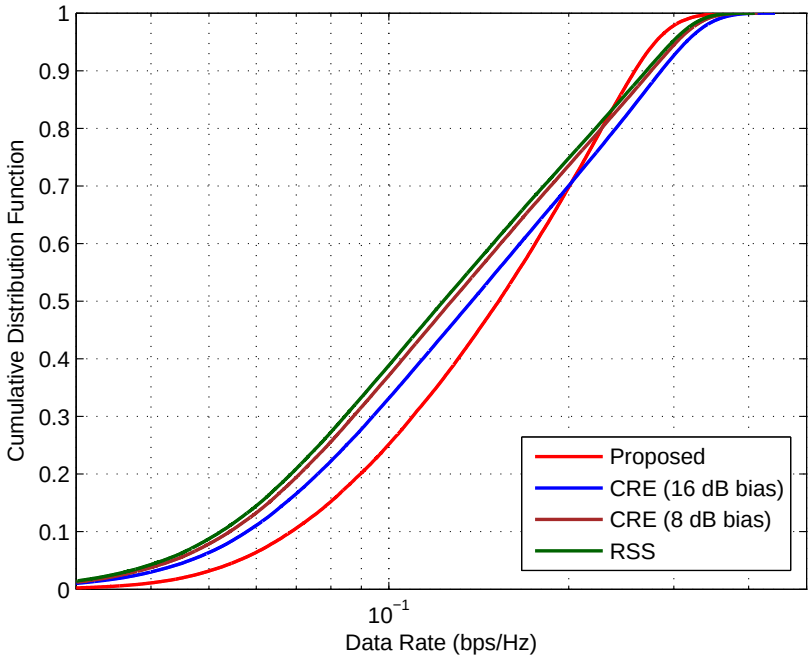

(a) 2 picocells

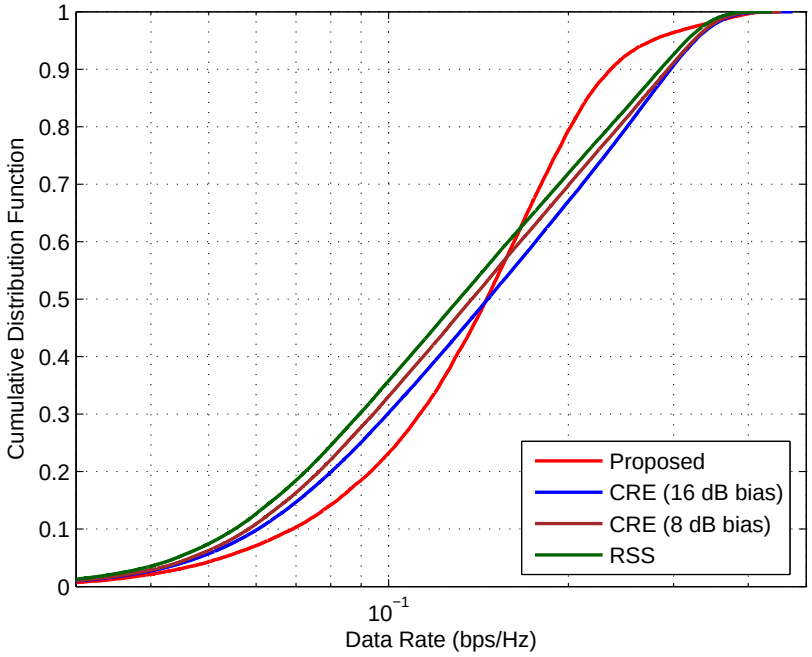

(b) 4 picocells

Figure 5.9: CDFs of MMSs' data rate

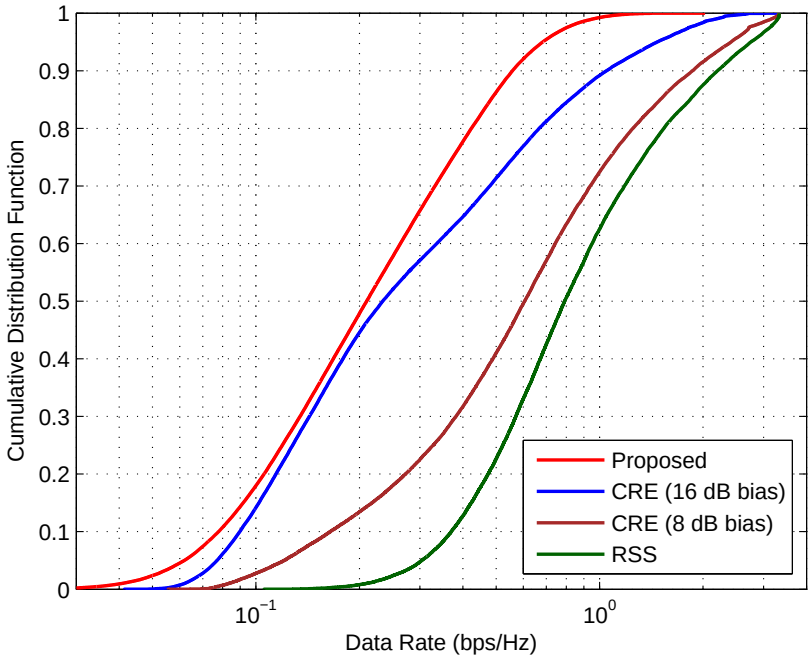

(a) 2 picocells

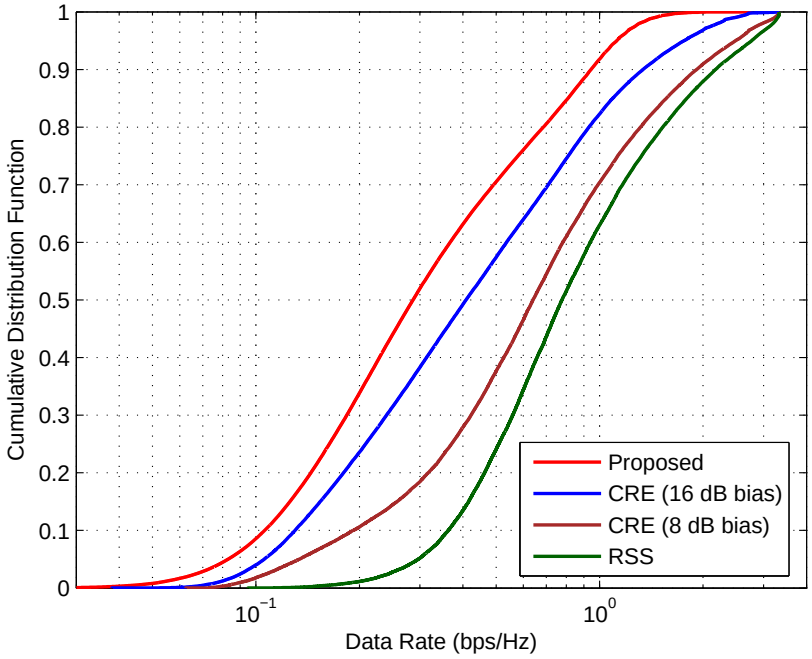

(b) 4 picocells

Figure 5.10: CDFs of PMSs' data rate

In the second stage, the network-wide net utility by increasing (or decreasing) the number of ABSs is estimated from MSs' expected data rate by handover along with the ABS change.

As future work, the following research issues can be further studied.

- *Asynchronous ABS configuration*
  - We can expand the current work based on the synchronous ABS operation to the asynchronous ABS operation case where each macrocell can have a different ABS configuration.
- *Adaptive hysteresis margin for ABS control*
  - Due to the possible inaccuracy in estimating the number of MSs to be offloaded, we can develop an adaptive hysteresis margin to compensate the inaccurate estimation instead of having a fixed hysteresis margin as we have done.

5.7 Appendix

5.7.1 Proof of Proposition 5.1

The net increment of network-wide utility by handing over MS u from BS b to b' can be expressed as

$$\Delta U^{HO} = \left[\log \frac{G(K_{b'}+1)e_{ub'}(t)}{K_{b'}+1} - \log \frac{G(K_b)e_{ub}(t)}{K_b}\right] + \sum_{v \in \mathcal{U}_b \setminus \{u\}} \left[\log \frac{G(K_b-1)e_{bv}(t)}{K_b-1} - \log \frac{G(K_b)e_{bv}(t)}{K_b}\right]$$

$$+\sum_{v\in\mathcal{U}_{b'}}\left[\log\frac{G(K_{b'}+1)e_{vb'}(t)}{K_{b'}+1}-\log\frac{G(K_{b'})e_{vb'}(t)}{K_{b'}}\right], \tag{5.21}$$

where the first, second and last term denote the net utility increment of the MS u, the BS b, and b', respectively. Eq. (5.21) can be further simplified as

$$\begin{aligned}\Delta U^{HO} =& \log\frac{G(K_{b'}+1)e_{ub'}(t)}{K_{b'}+1}\frac{K_b}{G(K_b)e_{ub}(t)}+(K_b-1)\log\frac{G(K_b-1)}{G(K_b)}\frac{K_b}{K_b-1}\\ &+K_{b'}\log\frac{G(K_{b'}+1)}{G(K_{b'})}\frac{K_{b'}}{K_{b'}+1}.\end{aligned} \tag{5.22}$$

Using the log function approximation $\log(1\pm x)\simeq\pm x$ (if $|x|\ll 1$) and the Euler's approximation of the multi-user diversity gain $G(k)=\sum_{i=1}^{k}\frac{1}{i}\simeq\gamma+\log k$, where γ $(=0.5572\cdots)$ is the Euler-Mascheroni constant, we can obtain the following four equations:

$$\cdot\ (K_b-1)\log\frac{K_b}{K_b-1}=(K_b-1)\log\left(1+\frac{1}{K_b-1}\right)\simeq 1 \tag{5.23}$$

$$\cdot\ K_{b'}\log\frac{K_{b'}}{K_{b'}+1}=-K_{b'}\log\left(1+\frac{1}{K_{b'}}\right)\simeq -1 \tag{5.24}$$

$$\begin{aligned}\cdot\,(K_b-1)\log\frac{G(K_b-1)}{G(K_b)} &\simeq (K_b-1)\log\frac{\gamma+\log(K_b-1)}{\gamma+\log K_b}\\ &\simeq (K_b-1)\log\left(1+\frac{\log(K_b-1)-\log(K_b)}{\gamma+\log K_b}\right)\\ &\simeq (K_b-1)\log\left(1+\frac{\log\left(1-\frac{1}{K_b}\right)}{\gamma+\log K_b}\right)\\ &\simeq (K_b-1)\log\left(1-\frac{\frac{1}{K_b}}{\gamma+\log K_b}\right)\\ &\simeq -\frac{K_b-1}{K_b}\frac{1}{\gamma+\log(K_b)}\\ &\simeq \frac{-\left(1-\frac{1}{K_b}\right)}{\gamma+\log K_b}\end{aligned} \tag{5.25}$$

$$
\begin{aligned}
\cdot K_{b'} \log \frac{G(K_{b'}+1)}{G(K_{b'})} &\simeq K_{b'} \log \frac{\gamma + \log(K_{b'}+1)}{\gamma + \log K_{b'}} \\
&\simeq K_{b'} \log \left(1 + \frac{\log(K_{b'}+1) - \log K_{b'}}{\gamma + \log K_{b'}}\right) \\
&\simeq K_{b'} \log \left(1 + \frac{\log\left(1+\frac{1}{K_{b'}}\right)}{\gamma + \log K_{b'}}\right) \\
&\simeq K_{b'} \log \left(1 + \frac{\frac{1}{K_{b'}}}{\gamma + \log K_{b'}}\right) \\
&\simeq \frac{K_{b'}}{K_{b'}} \frac{1}{\gamma + \log K_{b'}} \\
&\simeq \frac{1}{\gamma + \log K_{b'}}. \qquad (5.26)
\end{aligned}
$$

By plugging equations in (5.23)-(5.26) into (5.22), Eq. (5.22) becomes

$$
\Delta U^{HO} = \log \frac{G(K_{b'}+1)e_{ub'}(t)}{K_{b'}+1} \frac{K_b}{G(K_b)e_{ub}(t)} + \frac{1}{\gamma + \log K_{b'}} - \frac{\left(1-\frac{1}{K_b}\right)}{\gamma + \log K_b}. \qquad (5.27)
$$

In order for the user's handover to improve the network-wide utility, $\Delta U^{HO} > 0$ needs to be satisfied, therefore we can derive the condition in (5.8).

5.7.2 Proof of Proposition 5.2 & 5.3

For the ABS increment case, $\Delta U_m(t+1)$ and $\Delta U_p(t+1)$ can be derived as

$$
\begin{aligned}
&\Delta U_m(t+1) \\
&= \sum_{i \in \mathcal{B}_m} \sum_{u \in \mathcal{U}_i \setminus \mathcal{U}_i^{OL}} \left[\log \frac{G(K_i - n_i) e_{ui}(t+1)}{K_i - n_i} - \log \frac{G(K_i) e_{ui}(t)}{K_i} \right] \\
&= \sum_{i \in \mathcal{B}_m} \sum_{u \in \mathcal{U}_i \setminus \mathcal{U}_i^{OL}} \log \frac{G(K_i - n_i)}{G(K_i)} \frac{K_i}{K_i - n_i} \frac{e_{ui}(t+1)}{e_{ui}(t)} \\
&= \sum_{i \in \mathcal{B}_m} \log \left(\frac{G(K_i - n_i)}{G(K_i)} \frac{K_i}{K_i - n_i} \frac{\left(1 - \frac{t+1}{T}\right) c_{ui}}{\left(1 - \frac{t}{T}\right) c_{ui}} \right)^{K_i - n_i}
\end{aligned}
$$

$$= \sum_{i\in\mathcal{B}_m} \left[(K_i - n_i) \log \frac{G(K_i - n_i)}{G(K_i)} + (K_i - n_i) \log \frac{K_i}{K_i - n_i} + (K_i - n_i) \log \frac{T-t-1}{T-t} \right]$$

$$= \sum_{i\in\mathcal{B}_m} \left[(K_i - n_i) \log \frac{G(K_i - n_i)}{G(K_i)} + (K_i - n_i) \log \frac{K_i}{K_i - n_i} + (K_i - n_i) \log \left(1 - \frac{1}{T-t}\right) \right]$$

$$\simeq \sum_{i\in\mathcal{B}_m} \left[-\frac{n_i \left(1 - \frac{n_i}{K_i}\right)}{\gamma + \log(K_i)} + n_i - \frac{K_i - n_i}{T-t} \right], \tag{5.28}$$

$\Delta U_p(t+1)$

$$= \sum_{j\in\mathcal{B}_p} \sum_{u\in\mathcal{U}_j} \left[\log \frac{G(K_j + m_j) e_{uj}(t+1)}{K_j + m_j} - \log \frac{G(K_j) e_{uj}(t)}{K_j} \right]$$

$$= \sum_{j\in\mathcal{B}_p} \sum_{u\in\mathcal{U}_j} \left[\log \frac{G(K_j + m_j)}{G(K_j)} \frac{K_j}{K_j + m_j} \frac{e_{uj}(t+1)}{e_{uj}(t)} \right]$$

$$= \sum_{j\in\mathcal{B}_p} \sum_{u\in\mathcal{U}_j} \left[\log \frac{G(K_j + m_j)}{G(K_j)} \frac{K_j}{K_j + m_j} \frac{(T-t-1)c_{uj} + (t+1)\bar{c}_{uj}}{(T-t)c_{uj} + t\bar{c}_{uj}} \right]$$

$$= \sum_{j\in\mathcal{B}_p} \left[K_j \log \frac{G(K_j + m_j)}{G(K_j)} + K_j \log \frac{K_j}{K_j + m_j} + \sum_{u\in\mathcal{U}_j} \log \left(1 + \frac{a_{uj} - 1}{T + t(a_{uj} - 1)}\right) \right]$$

$$\simeq \sum_{j\in\mathcal{B}_p} \left[\frac{m_j}{\gamma + \log K_j} - m_j + \sum_{u\in\mathcal{U}_j} \frac{a_{uj} - 1}{T + t(a_{uj} - 1)} \right], \tag{5.29}$$

respectively, using the approximations in (5.23)-(5.26). Since $\sum_{i\in\mathcal{B}_m} n_i - \sum_{j\in\mathcal{B}_p} m_j = 0$, the requirement $\Delta U_+^{ABS}(t+1) > 0$ for ABS increment leads us to the condition in (5.10).

Similarly, $\Delta U_m(t-1)$ and $\Delta U_p(t-1)$ for the ABS decrement case can be derived as

$\Delta U_m(t-1)$

$$= \sum_{i\in\mathcal{B}_m} \sum_{u\in\mathcal{U}_i} \left[\log \frac{G(K_i + n_i) e_{ui}(t-1)}{K_i + n_i} - \log \frac{G(K_i) e_{ui}(t)}{K_i} \right]$$

$$
\begin{aligned}
&= \sum_{i\in\mathcal{B}_m}\sum_{u\in\mathcal{U}_i} \log \frac{G(K_i+n_i)}{G(K_i)}\frac{K_i}{K_i+n_i}\frac{e_{ui}(t-1)}{e_{ui}(t)} \\
&= \sum_{i\in\mathcal{B}_m} \log \left(\frac{G(K_i+n_i)}{G(K_i)}\frac{K_i}{K_i+n_i}\frac{\left(1-\frac{t-1}{T}\right)c_{ui}}{\left(1-\frac{t}{T}\right)c_{ui}} \right)^{K_i} \\
&= \sum_{i\in\mathcal{B}_m} \left[K_i \log \frac{G(K_i+n_i)}{G(K_i)} + K_i \log \frac{K_i}{K_i+n_i} + K_i \log \frac{T-t+1}{T-t} \right] \\
&= \sum_{i\in\mathcal{B}_m} \left[K_i \log \frac{G(K_i+n_i)}{G(K_i)} + K_i \log \frac{K_i}{K_i+n_i} + K_i \log \left(1+\frac{1}{T-t}\right) \right] \\
&\simeq \sum_{i\in\mathcal{B}_m} \left[\frac{n_i}{\gamma+\log(K_i)} - n_i + \frac{K_i}{T-t} \right], \qquad (5.30)
\end{aligned}
$$

$$
\begin{aligned}
&\Delta U_p(t-1) \\
&= \sum_{j\in\mathcal{B}_p}\sum_{u\in\mathcal{U}_j\setminus\mathcal{U}_j^{OL}} \left[\log \frac{G(K_j-m_j)e_{uj}(t-1)}{K_j-m_j} - \log \frac{G(K_j)e_{uj}(t)}{K_j} \right] \\
&= \sum_{j\in\mathcal{B}_p}\sum_{u\in\mathcal{U}_j\setminus\mathcal{U}_j^{OL}} \left[\log \frac{G(K_j-m_j)}{G(K_j)}\frac{K_j}{K_j-m_j}\frac{e_{uj}(t-1)}{e_{uj}(t)} \right] \\
&= \sum_{j\in\mathcal{B}_p}\sum_{u\in\mathcal{U}_j\setminus\mathcal{U}_j^{OL}} \left[\log \frac{G(K_j-m_j)}{G(K_j)}\frac{K_j}{K_j-m_j}\frac{(1-\frac{t-1}{T})c_{uj}+\frac{t-1}{T}\bar{c}_{uj}}{(1-\frac{t}{T})c_{uj}+\frac{t}{T}\bar{c}_{uj}} \right] \\
&= \sum_{j\in\mathcal{B}_p} \Bigg[(K_j-m_j)\log \frac{G(K_j-m_j)}{G(K_j)} + (K_j-m_j)\log \frac{K_j}{K_j-m_j} \\
&\qquad\qquad + \sum_{u\in\mathcal{U}_j\setminus\mathcal{U}_j^{OL}} \log\left(1+\frac{a_{uj}-1}{T+t(a_{uj}-1)}\right) \Bigg] \\
&\simeq \sum_{j\in\mathcal{B}_p} \left[-\frac{m_j\left(1-\frac{m_j}{K_j}\right)}{\gamma+\log K_j} + m_j - \sum_{u\in\mathcal{U}_j\setminus\mathcal{U}_j^{OL}} \frac{a_{uj}-1}{T+t(a_{uj}-1)} \right], \qquad (5.31)
\end{aligned}
$$

respectively. Since $\sum_{j\in\mathcal{B}_p} m_j - \sum_{i\in\mathcal{B}_m} n_i = 0$, the requirement $\Delta U_-^{ABS}(t-1) > 0$ leads us to the condition in (5.12).

Chapter 6: Conclusions

In this dissertation, we have investigated two challenges of radio resource management in heterogeneous cellular networks, which are the cross-tier interference mitigation and the load-aware cell association. For the cross-tier interference mitigation, we have focused on a group of pico users located in the expanded range (ER-PMSs) which are associated with picocells by the CRE operation for the purpose of additional user offloading effect even if they observe the stronger received signal strength from macrocells. We present two problems of macrocell transmit power control in frequency- and time-domain such that those ER-PMSs are provided their minimum QoS requirement. For the load-aware cell association, we have focused on a flexible cell association of users in a load-balanced manner, which is different from the traditional policy - the received signal strength-based cell selection. We present a problem of the joint optimization of cell association and cross-tier interference mitigation.

In the first problem, the frequency-domain macrocell transmit power reduction is presented for the cross-tier interference mitigation. From the macrocell's perspective, our interest is to minimize the performance degradation of MMSs by performing macrocell's transmit power reduction for ER-PMSs. A two-step cross-

tier interference mitigation scheme is proposed where the reduced transmit power level is determined in the first stop, and then a group of resource blocks is selected by solving a resource block scheduling problem. Due to the binary nature of resource block scheduling, a greedy-based heuristic algorithm is proposed. Through simulations, we have shown that the heuristic algorithm provides a good trade-off between the complexity and the performance, and the proposed cross-tier interference mitigation efficiently provides minimum required data rates scheme to ER-PMSs with much less transmit power reduction than the compared scheme.

In the second problem, the time-domain macrocell transmit power nulling is presented for the cross-tier interference mitigation. From the view point of the network, our interest turns into maximizing the network-wide utility subject to ER-PMSs' minimum required data rates by controlling the number of ABSs. We first present a new PMS scheduling policy where regular PMSs (R-PMSs) and ER-PMSs can be scheduled onto ABSs and non-ABSs interchangeably. Based on the scheduling policy, we formulate an optimization problem where the sum utility of MMSs & R-PMSs is maximized subject to ER-PMSs' minimum required data rates. For a given number of ABSs, the multi-cell optimization problem can be divided into multiple single cell optimization problems, and then the optimal number of ABSs can be obtained at the central coordinating entity. Through simulations, we have shown that the proposed scheme outperforms other comparing schemes in terms of the sum utility of MMSs & R-PMSs and all MSs.

In the third problem, the dynamic cell association is presented in conjunction with the time-domain macrocell transmit power nulling. From the perspective

of user load balancing in the network, our objective is to achieve better user redistribution to picocells in conjunction with the ABS control in a load-balanced manner than the CRE operation does. To this end, we formulate a network-wide utility maximization problem with respect to the cell association and the number of ABSs. Due to the NP-hardness of the optimization problem, we propose an online heuristic algorithm where a single user handover and an ABS change (+1 or -1) are determined by the expected throughput. In the first stage, for a given number of ABSs the user load balancing is performed by handing over a user in each iteration in a way to improve the network-wide utility. In the second stage, the ABS change by +1 or -1 is examined by estimating the expected number of users offloaded from macros to picos (or vice versa) and the corresponding network-wide utility change.

Bibliography

[1] Cisco. Cisco visual networking index: Global mobile data traffic forecast update, 2013-2018. white paper, Feb. 2014.

[2] S. Parkvall, E. Dahlman, G. Jongren, S. Landstrom, and L. Lindbom. Heterogeneous network deployments in lte. *Ericsson review*, 2011.

[3] 802.16m-2011 - ieee standard for local and metropolitan area networks part 16: Air interface for broadband wireless access systems amendment 3: Advanced air interface, 5 2011.

[4] M. Dohler, R.W. Heath, A. Lozano, C.B. Papadias, and R.A. Valenzuela. Is the phy layer dead? *Communications Magazine, IEEE*, 49(4):159–165, Apr. 2011.

[5] Sara Landstrom, Anders Furuskar, Klas Johansson, Laetitia Falconetti, and Fredric Kronestedt. Heterogeneous networks - increasing cellular capacity. *Ericson Review*, 89:4–9, 2011.

[6] Qualcomm. Lte advanced: Heterogeneous networks. white paper, Jan. 2011.

[7] A. Ghosh, N. Mangalvedhe, R. Ratasuk, B. Mondal, M. Cudak, E. Visotsky, T.A. Thomas, J.G. Andrews, P. Xia, H.S. Jo, H.S. Dhillon, and T.D. Novlan. Heterogeneous cellular networks: From theory to practice. *Communications Magazine, IEEE*, 50(6):54–64, June 2012.

[8] D. Tse and P. Viswanath. *Fundamentals of Wireless Communication*. Wiley series in telecommunications. Cambridge University Press, 2005.

[9] Jiho Jang and Kwang Bok Lee. Transmit power adaptation for multiuser ofdm systems. *Selected Areas in Communications, IEEE Journal on*, 21(2):171–178, Feb. 2003.

[10] Cheong Yui Wong, R.S. Cheng, K.B. Lataief, and R.D. Murch. Multiuser ofdm with adaptive subcarrier, bit, and power allocation. *Selected Areas in Communications, IEEE Journal on*, 17(10):1747 –1758, Oct. 1999.

[11] D. Kivanc, Guoqing Li, and Hui Liu. Computationally efficient bandwidth allocation and power control for ofdma. *Wireless Communications, IEEE Transactions on*, 2(6):1150–1158, Nov. 2003.

[12] Wonjong Rhee and John M. Cioffi. Increase in capacity of multiuser ofdm system using dynamic subchannel allocation. In *Vehicular Technology Conference Proceedings, 2000. VTC 2000-Spring Tokyo. 2000 IEEE 51st*, volume 2, pages 1085–1089, 2000.

[13] I.C. Wong, Zukang Shen, B.L. Evans, and J.G. Andrews. A low complexity algorithm for proportional resource allocation in ofdma systems. In *Signal Processing Systems, 2004. SIPS 2004. IEEE Workshop on*, pages 1–6, oct. 2004.

[14] I. Koutsopoulos and L. Tassiulas. Cross-layer adaptive techniques for throughput enhancement in wireless ofdm-based networks. *Networking, IEEE/ACM Transactions on*, 14(5):1056–1066, Oct. 2006.

[15] Guoqing Li and Hui Liu. Downlink radio resource allocation for multi-cell ofdma system. *Wireless Communications, IEEE Transactions on*, 5(12):3451 –3459, Dec. 2006.

[16] T. Thanabalasingham, S.V. Hanly, L.L.H. Andrew, and J. Papandriopoulos. Joint allocation of subcarriers and transmit powers in a multiuser ofdm cellular network. In *Communications, 2006. ICC '06. IEEE International Conference on*, volume 1, pages 269 –274, Jun. 2006.

[17] M. Sternad, T. Ottosson, A. Ahlen, and A. Svensson. Attaining both coverage and high spectral efficiency with adaptive ofdm downlinks. In *Vehicular Technology Conference, 2003. VTC 2003-Fall. 2003 IEEE 58th*, volume 4, pages 2486–2490 Vol.4, Oct 2003.

[18] Huawei. Soft frequency reuse scheme for UTRAN LTE. In *3GPP TSG RAN WG1 41 R1-050507*. May 2005.

[19] S. Sesia, I. Toufik, and M. Baker. *LTE, The UMTS Long Term Evolution: From Theory to Practice*. Wiley InterScience online books. Wiley, 2009.

[20] S-E Elayoubi and B. Fourestie? On frequency allocation in 3g lte systems. In *Personal, Indoor and Mobile Radio Communications, 2006 IEEE 17th International Symposium on*, pages 1–5, Sept 2006.

[21] S-E Elayoubi, O. Ben Haddada, and B. Fourestie? Performance evaluation of frequency planning schemes in ofdma-based networks. *Wireless Communications, IEEE Transactions on*, 7(5):1623–1633, May 2008.

[22] S.H. Ali and V.C.M. Leung. Dynamic frequency allocation in fractional frequency reused ofdma networks. *Wireless Communications, IEEE Transactions on*, 8(8):4286–4295, Aug. 2009.

[23] M. Rahman and H. Yanikomeroglu. Enhancing cell-edge performance: a downlink dynamic interference avoidance scheme with inter-cell coordination. *Wireless Communications, IEEE Transactions on*, 9(4):1414–1425, Apr. 2010.

[24] M. Rahman and H. Yanikomeroglu. Inter-cell interference coordination in ofdma networks: A novel approach based on integer programming. In *Vehicular Technology Conference (VTC 2010-Spring), 2010 IEEE 71st*, pages 1 –5, May 2010.

[25] M. Rahman, H. Yanikomeroglu, and W. Wong. Interference avoidance with dynamic inter-cell coordination for downlink lte system. In *Wireless Communications and Networking Conference, 2009. WCNC 2009. IEEE*, pages 1–6, Apr. 2009.

[26] R.Y. Chang, Zhifeng Tao, Jinyun Zhang, and C.-C.J. Kuo. A graph approach to dynamic fractional frequency reuse (ffr) in multi-cell ofdma networks. In *Communications, 2009. ICC '09. IEEE International Conference on*, pages 1–6, June 2009.

[27] D. Lopez-Perez, A. Valcarce, G. de la Roche, and Jie Zhang. Ofdma femtocells: A roadmap on interference avoidance. *Communications Magazine, IEEE*, 47(9):41–48, September 2009.

[28] Qinliang Su, Aiping Huang, Zhouyun Wu, Guanding Yu, Zhaoyang Zhang, Kai Xu, and Jin Yang. A distributed dynamic spectrum access and power allocation algorithm for femtocell networks. In *Wireless Communications Signal Processing, 2009. WCSP 2009. International Conference on*, pages 1–5, Nov 2009.

[29] V. Chandrasekhar and J.G. Andrews. Spectrum allocation in tiered cellular networks. *Communications, IEEE Transactions on*, 57(10):3059–3068, October 2009.

[30] J. Ling, D. Chizhik, and R. Valenzuela. On resource allocation in dense femtodeployments. In *Microwaves, Communications, Antennas and Electronics Systems, 2009. COMCAS 2009. IEEE International Conference on*, pages 1–6, Nov 2009.

[31] M.I. Kamel and K.M.F. Elsayed. Absf offsetting and optimal resource partitioning for eicic in lte-advanced: Proposal and analysis using a nash bargaining approach. In *Communications (ICC), 2013 IEEE International Conference on*, pages 6240–6244, June 2013.

[32] D. Lopez-Perez and Xiaoli Chu. Inter-cell interference coordination for expanded region picocells in heterogeneous networks. In *Computer Communications and Networks (ICCCN), 2011 Proceedings of 20th International Conference on*, pages 1–6, Aug. 2011.

[33] D. Lopez-Perez, Xiaoli Chu, and I. Guvenc. On the expanded region of picocells in heterogeneous networks. *Selected Topics in Signal Processing, IEEE Journal of*, 6(3):281 –294, Jun. 2012.

[34] G.B. Dantzig. *Linear Programming and Extensions*. Princeton landmarks in mathematics and physics. Princeton University Press, 1963.

[35] Qian Li, R.Q. Hu, Yiran Xu, and Yi Qian. Optimal fractional frequency reuse and power control in the heterogeneous wireless networks. *Wireless Communications, IEEE Transactions on*, 12(6):2658–2668, June 2013.

[36] Jiyong Pang, Jun Wang, Dongyao Wang, Gang Shen, Qi Jiang, and Jianguo Liu. Optimized time-domain resource partitioning for enhanced inter-cell interference coordination in heterogeneous networks. In *Wireless Communications and Networking Conference (WCNC), 2012 IEEE*, pages 1613–1617, Apr.

[37] Michal Cierny, Haining Wang, Risto Wichman, Zhi Ding, and Carl Wijting. On number of almost blank subframes in heterogeneous cellular networks. *CoRR*, abs/1304.2269, 2013.

[38] S. Das, H. Viswanathan, and G. Rittenhouse. Dynamic load balancing through coordinated scheduling in packet data systems. In *INFOCOM 2003. Twenty-Second Annual Joint Conference of the IEEE Computer and Communications. IEEE Societies*, volume 1, pages 786–796 vol.1, March 2003.

[39] Lin Du, J. Biaham, and L. Cuthbert. A bubble oscillation algorithm for distributed geographic load balancing in mobile networks. In *INFOCOM 2004. Twenty-third AnnualJoint Conference of the IEEE Computer and Communications Societies*, volume 1, pages –338, March 2004.

[40] J.X. Qiu and Jon W. Mark. A dynamic load sharing algorithm through power control in cellular cdma. In *Personal, Indoor and Mobile Radio Communications, 1998. The Ninth IEEE International Symposium on*, volume 3, pages 1280–1284 vol.3, Sep 1998.

[41] Y. Bejerano and Seung jae Han. Cell breathing techniques for load balancing in wireless lans. *Mobile Computing, IEEE Transactions on*, 8(6):735–749, June 2009.

[42] P. Bahl, M.T. Hajiaghayi, K. Jain, S.V. Mirrokni, Lili Qiu, and A. Saberi. Cell breathing in wireless lans: Algorithms and evaluation. *Mobile Computing, IEEE Transactions on*, 6(2):164–178, Feb 2007.

[43] Frank Kelly. Charging and rate control for elastic traffic. *European Transactions on Telecommunications*, 1997.

[44] S. Borst. User-level performance of channel-aware scheduling algorithms in wireless data networks. *Networking, IEEE/ACM Transactions on*, 13(3):636–647, June 2005.

[45] T. Bu, Li Li, and R. Ramjee. Generalized proportional fair scheduling in third generation wireless data networks. In *INFOCOM 2006. 25th IEEE International Conference on Computer Communications. Proceedings*, pages 1–12, April 2006.

[46] Y. Bejerano, Seung jae Han, and Li Li. Fairness and load balancing in wireless lans using association control. *Networking, IEEE/ACM Transactions on*, 15(3):560–573, June 2007.

[47] Hongseok Kim, G. de Veciana, Xiangying Yang, and M. Venkatachalam. Distributed alpha-optimal user association and cell load balancing in wireless networks. *Networking, IEEE/ACM Transactions on*, 20(1):177–190, Feb 2012.

[48] Kyuho Son, Song Chong, and G. Veciana. Dynamic association for load balancing and interference avoidance in multi-cell networks. *Wireless Communications, IEEE Transactions on*, 8(7):3566–3576, July 2009.

[49] Yi Yu, Qingyang Hu, C.S. Bontu, and Z. Cai. Mobile association and load balancing in a cooperative relay cellular network. *Communications Magazine, IEEE*, 49(5):83–89, May 2011.

[50] Yi Yu, R.Q. Hu, and Z. Cai. Optimal load balancing and its heuristic implementation in a heterogeneous relay network. In *Global Telecommunications Conference (GLOBECOM 2011), 2011 IEEE*, pages 1–6, Dec 2011.

[51] Qian Li, R.Q. Hu, Geng Wu, and Yi Qian. On the optimal mobile association in heterogeneous wireless relay networks. In *INFOCOM, 2012 Proceedings IEEE*, pages 1359–1367, March 2012.

[52] Qian Li, R.Q. Hu, Yi Qian, and Geng Wu. A proportional fair radio resource allocation for heterogeneous cellular networks with relays. In *Global Communications Conference (GLOBECOM), 2012 IEEE*, pages 5457–5463, Dec 2012.

[53] H.S. Dhillon, R.K. Ganti, and J.G. Andrews. A tractable framework for coverage and outage in heterogeneous cellular networks. In *Information Theory and Applications Workshop (ITA), 2011*, pages 1–6, Feb 2011.

[54] H.S. Dhillon, R.K. Ganti, F. Baccelli, and J.G. Andrews. Modeling and analysis of k-tier downlink heterogeneous cellular networks. *Selected Areas in Communications, IEEE Journal on*, 30(3):550–560, April 2012.

[55] Jinyoung Oh and Youngnam Han. Cell selection for range expansion with almost blank subframe in heterogeneous networks. In *Personal Indoor and Mobile Radio Communications (PIMRC), 2012 IEEE 23rd International Symposium on*, pages 653–657, Sept 2012.

[56] Qingyang Hu, Yi Yu, Z. Cai, J.E. Womack, and Yi Song. Mobile association in a heterogeneous network. In *Communications (ICC), 2010 IEEE International Conference on*, pages 1–6, May 2010.

[57] K. Okino, T. Nakayama, C. Yamazaki, H. Sato, and Y. Kusano. Pico cell range expansion with interference mitigation toward lte-advanced heterogeneous networks. In *Communications Workshops (ICC), 2011 IEEE International Conference on*, pages 1–5, June 2011.

[58] A. Bou Saleh, O. Bulakci, S. Redana, B. Raaf, and J. Ha?ma?la?inen. Enhancing lte-advanced relay deployments via biasing in cell selection and handover decision. In *Personal Indoor and Mobile Radio Communications (PIMRC), 2010 IEEE 21st International Symposium on*, pages 2277–2281, Sept 2010.

[59] Wonjong Noh, Wonjae Shin, Changyong Shin, Kyunghun Jang, and Hyun-Ho Choi. Distributed frequency resource control for intercell interference control in heterogeneous networks. In *Wireless Communications and Networking Conference (WCNC), 2012 IEEE*, pages 1794–1799, Apr. 2012.

[60] Beatriz Soret and Klaus I. Pedersen. Macro transmission power reduction for hetnet co-channel deployments. In *Global Telecommunications Conference (GLOBECOM 2012), 2012 IEEE*, pages 4342–4346, Dec. 2012.

[61] Josep Colom Ikuno, Martin Wrulich, and Markus Rupp. System level simulation of LTE networks. In *Proc. 2010 IEEE 71st Vehicular Technology Conference*, Taipei, Taiwan, May 2010.

[62] 3rd Generation Partnership Project. 3GPP TR 36.912 V11.0.0 - Feasibility study for Further Advancements for E-UTRA (LTE-Advanced) (Release 11). Technical report, Sep. 2012.

[63] 3rd Generation Partnership Project. 3GPP TR 36.814 V9.0.0 - Evolved Universal Terrestrial Radio Access (E-UTRA); Further advancements for E-UTRA physical layer aspects. Technical report, Mar. 2010.

[64] 3rd Generation Partnership Project. 3GPP TR 36.931 V11.0.0 - Evolved Universal Terrestrial Radio Access (E-UTRA); Radio Frequency (RF) requirements for LTE Pico Node B. Technical report, Sep. 2012.

[65] Qiaoyang Ye, Beiyu Rong, Yudong Chen, M. Al-Shalash, C. Caramanis, and J.G. Andrews. User association for load balancing in heterogeneous cellular networks. *Wireless Communications, IEEE Transactions on*, 12(6):2706–2716, June 2013.

[66] S. Corroy, L. Falconetti, and R. Mathar. Dynamic cell association for downlink sum rate maximization in multi-cell heterogeneous networks. In *Communications (ICC), 2012 IEEE International Conference on*, pages 2457–2461, June 2012.

[67] S. Deb, P. Monogioudis, J. Miernik, and J.P. Seymour. Algorithms for enhanced inter-cell interference coordination (eicic) in lte hetnets. *Networking, IEEE/ACM Transactions on*, 22(1):137–150, Feb 2014.

[68] Qiaoyang Ye, Mazin Al-Shalash, Constantine Caramanis, and J.G. Andrews. On/off macrocells and load balancing in heterogeneous cellular networks. In *Global Telecommunications Conference (GLOBECOM 2013), 2013 IEEE*, pages 3919–3924, Dec. 2013.

[69] H.J. Kushner and P.A. Whiting. Convergence of proportional-fair sharing algorithms under general conditions. *Wireless Communications, IEEE Transactions on*, 3(4):1250–1259, July 2004.